Sulfur oxidation in moderately thermophilic leaching bacteria

Dissertation

zur Erlangung des akademischen Grades eines
Doktors der Naturwissenschaften
– Dr. rer. nat. –

vorgelegt von

Claudia Janosch
geboren in Düsseldorf

Institut für Chemie
der
Universität Duisburg-Essen

2013

Die vorliegende Arbeit wurde im Zeitraum von April 2008 bis Juli 2011 im Arbeitskreis von Prof. Dr. Wolfgng Sand am Institut für Chemie der Universität Duisburg-Essen durchgeführt.

Tag der Disputation: 19.09.2013

Gutachter:	Prof. Dr. W. Sand
	Prof. Dr. B. Siebers
Vorsitzender:	Prof. Dr. O. Schmitz

To My Father

- Almost all aspects of life are engineered at the molecular level, and without understanding molecules we can only have a very sketchy understanding of life itself. All approaches at higher levels are suspect until confirmed at the molecular level. - (Francis Crick)

Acknowledgements

First and foremost I would like to thank my supervisor **Prof. Dr. Wolfgang Sand** for giving me the opportunity to step as a newcomer in his working group into the fascinating world of molecular biology and to do my PhD in this area.

Furthermore, I would like to thank **Prof. Dr. Bettina Siebers** for the co-revision of this work and discussions about genes, which “don’t want to be cloned”.

Special thanks go to **Dr. Mario Vera** for taking the position as a co-advisor and for his extensive support throughout my work. I was in the lucky position to receive great encouragement and to find a door that was always open for questions and discussions.

This work was carried out in the frame of IGF project 263ZN under the auspices of AIF and funded through the programme for Industrial Collective Research (IGF) of the German Federal Ministry of Economy and Technology by decision of the German Bundestag.

Great thanks to **Dr. Ansgar Poetsch** and **Tanja Bojarzyn** from the Ruhr Universität Bochum for their scientific support and their analysis of the proteins by Tandem Mass Spectrometry.

I would like to thank **Shelly M. Deane** and **Dr. Douglas E. Rawlings** (University of Cape Town, South Africa) for providing *At. caldus*- like strains MNG, f and #6. Furthermore, I like to thank **H.- B. Zhou** (Central South University Changsha, China) for providing *At. caldus*-like strains S1 and S2.

I would like to give the biggest, biggest thanks to the **all collegues of Prof. Dr. Sand lab**, especially to **Nanni Noël**, **Dr. Bianca Florian** and **Andrzej Kuklinski** for a great PhD time from the very beginning till the end. Thanks Nanni, that you have sent me all the missing papers and data when I’ve been already left the universitiy.

Great thanks to **Dr. Felipe Leon Morales** for doing scientific work and „handicraft work“ till late evenings with me and of course all the interesting scientific discussions.

I would like to acknowledge **Sören Bellenberg** for providing Scripts for COG and proteomic analysis. This has made my work much easier.

I would also like to thank **Christian Thyssen** for helping hands in managing the sometimes bullish Ion chromatography and HPLC.

Great thanks to **Beate Krok** and **Agata Wikiel**, who have given me so often an accommodation after the moving to Essen and of course all the social and scientific discussions till midnight.

I would also like to thank all present and former colleagues from the **AG Siebers**. **Sabine Dietl** is especially acknowledged for her great help all these years.

Thanks go to **Dr. Andreas Veith** and **PD Dr. Arnulf Kletzin** for finding some time to discuss new facts about the tiny and sometimes quite complicated SOR.

I would like to acknowledge **Cindy Jade Africa** for the english corrections of parts of this thesis.

Great thanks goes to **Cornelia Roßmann** and **Fam. Potas** for moralic support, especially at the end of this thesis.

And more than thousand thanks to my mother and my boyfriend for their special support and their surpassing patience!

Publications

C. Janosch, C. Thyssen, M. Vera, V. Bonnefoy, T. Rohwerder & W. Sand (2009): **Sulfur oxygenase reductase in different *Acidithiobacillus caldus*-like strains**. *Adv Materials Res* **71-73**: 239-242.

R. Stadler, M. Fürbeth, M. Grooters, C. Janosch, A. Kuklinski & W. Sand (2010): **Studies on the Application of Microbially Produced Polymeric Substances As Protecting Layers Against Microbially Influenced Corrosion of Iron And Steel**. Paper no. 10209, Proceedings of CORROSION 2010, San Antonio, Texas.

C. Thyssen, M. Vera, C. Janosch, C. Spröer & W. Sand (2011): **A novel acidophilic γ- prote-obacterium for bioleaching.** In: Biohydrometallurgy: Biotech key to unlock mineral resources value, Vol 2, Q. Guanzhou, J. Tao, Q. Wenqing, L. Xueduan, Y. Yu, W. Haidong (eds.), Proceedings of the 19th International Biohydrometallurgy Symposium, pp 979-891, Changsha, China.

C. Janosch, S. Bellenberg, W. Sand, A. Poetsch & M. Vera. **Comparison of metabolic pathways of *Acidithiobacillus caldus* grown on elemental sulfur versus thiosulfate;** in preparation.

C. Janosch, M. Vera & W. Sand: **Elemental sulfur oxidatation in acidophilic moderatly leaching bacteria**; in preparation.

Summary

Control of sulfur compound oxidation in the moderately and extremely thermophilic range is of importance in bioleaching operations for the industrial winning of heavy metals. Consequently, knowledge of the biochemistry of sulfur oxidation is required for inhibition as well as enhancement in bioleaching operations. In this work, the sulfur oxidation pathways of the leaching strains *Acidithiobacillus caldus* and the *Sulfobacillus thermosulfidooxidans* were investigated.

Several energy sources for *At. caldus* were used. It grew best on elemental sulfur (S^0) compared to thiosulfate and tetrathionate at 45 °C.

Several genes have been proposed to be involved in sulfur oxidation in *At. caldus*. The expression levels of six of them, *sor* (ACA_0302), *soxB* (ACA_2394), *soxX* (ACA_2389), *sqr_I* (ACA_0303), *sqr_II* (ACA_2485) and *tth* (ACA_1633), were measured under different growth conditions in order to find out whether there is a differential regulation depending on the substrate and temperature. Additionally, the *sox_I* cluster (ACA_2389-ACA_2394) of *At. caldus* was analyzed for cotranscription in order to demonstrate its potential gene organization in an operon.

A big part of this thesis included a high throughput proteomic analysis of elemental sulfur (S^0) and thiosulfate grown cells of *At. caldus*. A total number of 1292 proteins (45.8 %) was identified from 2821 protein encoding genes annotated in the genome of At. caldus type strain DSM 8584^T. 1215 proteins were detected in S^0 grown bacteria and 1120 proteins were detected in thiosulfate grown bacteria. 85 proteins were found to be induced in S^0, while 13 proteins were found to be induced in thiosulfate grown bacteria. All proteins were classified according to COG categories. The proteins involved in the sulfur and carbon metabolism, respiratory complexes, EPS production and cell mobilization (pili) were deeply analyzed. Apart from sulfur oxygenase reductase (Sor) all proteins involved in sulfur metabolism were found in the proteomes. The rhodanese (ACA_2397) in one heterodisulofide reductase (Hdr) cluster was up-regulated on S^0, and the tetrathionate hydrolase (Tth) was up-regulated on thiosulfate grown *At. caldus* cells.

The *sor* gene was screened via PCR in different *At. caldus* strains with degenerated primers designed for the bacterial *sor* branch. *Sor* genes were found to be present in almost all *At. caldus* strains. Furthermore, the enzymatic activity of Sor and a putative sulfur dioxygenase (Sdo) were analysed in crude extracts for the strains *At. caldus* DSM 8584^T, *At. caldus* C-SH12 (DSM 9466), the *At. caldus*-like isolates MNG, f, and

Sb. thermosulfidooxidans DSM 9293^T. Here, the comparison of enzymatic assays with (Sdo) and without (Sor) addition of an external thiol groups (provided by GSH) were performed. The sulfide formation was quantified as indicator for Sor activity, which could not be measured in any of the *At. caldus* strains analyzed. However, the type strain of *Sb. thermosulfidooxidans* Sor showed an oxygenase activity of 1.2 U/mg and a reductase activity of 77 mU/mg at 75 °C at the optimum pH 7.5.

Recently, the whole genome of *Sb. thermosulfidooxidans* DSM 9293^T was sequenced. The *At. caldus* aa sequences were used for searching homologues proteins probably involved in sulfur oxidation. Interestingly, two genes encoding Sor and one HDR cluster (Sulth_1021-Sulth_1026) were found. *DoxD* and 3 putative *tth* genes could also be identified. Contrary to *At. caldus, doxD* and *tth* were not found clustered together in *Sb. thermosulfidooxidans.* Furthermore, one putative cluster of anaerobic dimethyl sulfoxide reductase *dsrABC* and *dsrEFH*-like (Sulth_2366-Sulth_2369) was identified. Interestingly, no genes encoding Sox proteins were found.

Table of contents

Table of abbreviations

aa	amino acids
ACA_xxxx	locus tag of *At. caldus* type strain genes
ADP	Adenosine-diphosphate
AMD	Acid Mine Drainage
AMP	Adenosine-mono-phosphate
Amp	Ampiciline
ATP	Adenosine-tri-phosphate
APS	Adenylylphosphosulfate
ARD	Acid Rock Drainage
Atc_xxxx	locus tag of *At. caldus* SM-1
bp	base pairs
BLAST	Basic Local Alignment Search Tool
BSA	Bovine Serum Albumin
CBB	Calvin- Benson- Bassham (cycle)
CODEHOP	COnsensus-DEgenerate Hybrid Oligonucleotide Primers
COG	Clusters of Orthologous Groups of proteins
C_T	cycle treshold
CPS	capsular polysaccharides
CQ	Caldariella Quinone
Da	Dalton
DNA	Deoxyribonucleic acid
dNTP	Deoxynucleotide Triphosphate
DQ	decyl ubiquione
DSR	Dimethylsulfoxide reductase
EC number	Enzyme Commision number
EDTA	Ethylenediaminetetraacetic acid
e.g.	*exempli gratiā* (for example)
EMP	Embden-Meyerhof-Parnas (pathway)
EPS	Extracellular Polymeric Substances
et al.	*et alii* (and others)
gi	gene identity (no.)
GSH	glutathione
HDR	Heterodisulfide reductase
IC	Ion chromatography
ISC	inorganic sulfur compound
kb	kilo bases
MeS	Metal sulfide
n.a.	not analyzed
NAD^+	Nicotinamide adenine dinucleotide (oxidized form)
NADH	Nicotinamide adenine dinucleotide (reduced form)

$NADP^+$	Nicotinamide adenine dinucleotide phosphate (oxidized form)
NADPH	Nicotinamide adenine dinucleotide phosphate (reduced form)
n.r.	not reported
nt	nucleotides
MS	Mass spectrometry
IPTG	Isopropyl-β-D-thiogalactopyranoside
PAGE	Polyacrylamide gel electrophoresis
OMP	Outer membrane protein
PCR	Polymerase Chain Reaction
Pfam	Protein family
PPP	Pentose phosphate pathway
PIPES	Piperazin-1,4-bis(2-ethansulfonic acid)
qPCR	Quantitative Polymerase Chain Reaction
Rhd	Rhodanase
RISC	reduced inorganic sulfur compounds
RNA	Ribonucleic acid
rpm	rounds per minute
RT	Reverse Transcription
RuBisCO	ribulose-1,5-bisphosphate carboxylase/ oxygenase
S^0	elemental sulfur
Sar	Sulfite:Acceptor Oxidoreductase
Sat	Sulfate adenylyltransferase
Sdo	Sulfur Dioxygenase
SDS	Sodium dodecyl sulfate
Sor	Sulfur Oxygenase Reductase
Sox	Sulfur Oxidizing System
Sqr	Sulfide:Quinone Oxidoreductase
Sth_xxxx	locus tag of *Sb. thermosulfidooxidans* type strain genes
TCA	Tricarboxylic acid (cycle)
TCC	Total cell count
T4SS	Type IV secretion system
Tris	2-Amino-2-hydroxymethyl-propane-1,3-diol
Tqo	Thiosulfate:Quinone Oxidoreducatase
Tth	Tetrathionate Hydrolase
U	Unit of enzyme activity
X-gal	5-bromine-4-chloro-3-indoxyl-β-D-galactopyranoside

List of figures

List of tables

1 INTRODUCTION

1.1 Bioleaching mechanisms

Bioleaching is the biological conversion of an insoluble metal compound into a water-soluble form. In metal sulfide (MeS) bioleaching, MeS are oxidized to metal ions and sulfate by aerobic acidophilic ferrous iron and/or sulfur oxidizing bacteria and archaea (Schippers and Sand 1999). The MeS oxidation itself is a chemical process, where ferric iron is the relevant oxidizing/attacking agent for the MeS being reduced to ferrous iron. The sulfur moiety of the MeS is oxidized to sulfate and various intermediate reduced inorganic sulfur compounds (RISCs), e.g. elemental sulfur (S^0), polysulfide and thiosulfate. The role of microorganisms is to oxidize the products of this MeS oxidation in order to regenerate ferric iron and protons closing this cyclic process.

$$2\ Fe^{2+} + 1/2\ O_2 + 2H^+ \rightarrow 2\ Fe^{3+} + H_2O \quad \text{(Eq. 1)}$$

$$1/8\ S_8 + 3/2\ O_2 + H_2O \rightarrow SO_4^{2-} + 2\ H^+ \quad \text{(Eq. 2)}$$

During this oxidation process the residual sulfur can form a layer on the MeS; termed the sulfur passivation layer. Sulfur oxidizing bacteria degrade these sulfur passivation layers on the mineral surface allowing metal sulfide dissolution (Rohwerder *et al.* 2003).

S^0 and RISC oxidation is essential in the bioleaching process as proton generation during this process keeps the pH low and thus the ferrous iron in solution. The microbial oxidation of ferrous to ferric iron is 10^5 to 10^6 times faster than the chemical oxidation of ferric iron at pH 2-3 (Lacey and Lawson 1970).

Two different mechanisms have been proposed to explain the role of microorganisms in the relevant redox reactions and RISC speciation involved in MeS oxidation. These are the indirect and the direct leaching mechanisms. The latter one, i.e. a direct enzymatic oxidation of the sulfur moiety of MeS (reviewed by Ehrich 2002 and Sand *et al.* 1995) lost any justification. In the indirect mechanism (explained above) the MeS is oxidized by ferric ions, which are then re-oxidized by the bacteria. This comprises two sub-mechanisms: the “contact” and the “non-contact mechanism” (Rawlings 2002). Both postulated the oxidation of ferrous iron by bacteria. In the non-contact mechanism, planktonic cells oxidize ferrous iron in the bulk solution and thus regenerate the oxidizing agent (Sand *et al.* 1995). In contrast, the contact mechanism requires the cells to be in direct contact, attached, to the MeS surface. Leaching

bacteria have been demonstrated to exhibit a strong affinity for attachment to MeS (Rawlings 2002). These bacteria subsequently become embedded in a matrix of extracellular polymeric substances (EPS) (Fig. 1) in the formation of biofilms (Kinzler *et al.* 2003).

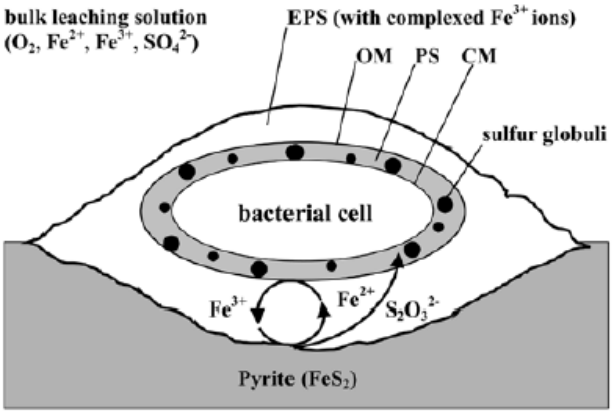

Fig.1: Model for the contact leaching mechanism catalyzed by a cell of *At. ferrooxidans* (from Rohwerder *et al.* 2003).
Production of EPS in presence of pyrite (FeS_2) allows attachment. Ferrous iron is oxidized within the EPS layer of the cell; the released sulfur moiety of pyrite is converted to thiosulfate (S_2O_3), which could be (in case of *At. ferrooxidans*) directly oxidized to sulfate or stored in form of S^0 globules within the periplasmic space; Abbreviations: CM cytoplasmic membrane, PS periplasmic space, OM outer membrane.

Two different reaction mechanisms, the thiosulfate and the polysulfide pathway have been proposed to explain MeS dissolution (Schippers *et al.* 1996; Schippers and Sand 1999). Generally, leaching is achieved by a combination of proton attack and oxidation processes. However, the pathway controlling the dissolution is mineral specific and dependent on its acid solubility, which is determined by its electronic configuration (Schippers and Sand 1999; Sand *et al.* 2001; Schippers 2004; Edelbro *et al.* 2003). Acid-insoluble metal sulfides e.g. pyrite (FeS_2), molybdenite (MoS_2) or tungstenite (WS_2), require an oxidation process to dissolve and the degradation follows the “thiosulfate pathway”. Chemical bonds between the sulfur atom and metal atoms do not break until a total of 6 successive single-electron oxidation steps have been conducted and thiosulfate is liberated (Luther *et al.* 1987; Schippers *et al.* 1996). In contrast, in the “polysulfide pathway”, spalerite (ZnS), galena (PbS), arsenopyrite (FeAsS) or chalcopyrite ($CuFeS_2$) are dissolved by a combination of electron extraction by ferric iron and proton attack (acid-soluble). Here the sulfide moiety should be oxidized in a single-electron transfer step. The first free sulfur

compound most likely is a sulfide cation (H_2S^+), can spontaneously dimerize to a free disulfide (H_2S_2) and is further oxidized via higher polysulfides and polysulfide radicals to elemental sulfur (Steudel 1996; Schippers and Sand 1999). In both pathways, apart from sulfate, S^0 is formed, but in different concentrations. The thiosulfate pathway releases approx. 10% of the S^0, while the polysulfide pathway is responsible for more than 90% of S^0 release.

These mechanisms explain the simplicity and low operating costs due to the basic equipment of bioleaching in comparison with conventional mining processes (Brierley and Brierley 2001; Dold 2008; Rubio 2012). In bioleaching no sulfur dioxide emissions occur and the process is adaptable for recovering metals from low grade ores and waste materials (Watling 2006).

Bioleaching is frequently observed in nature, too. The Rio Tinto in Spain is a good example of a natural bioleaching habitat. It is a very acidic river containing high heavy metal concentrations due to bioleaching processes dissolving pyrite and other MeS from the Iberian Pyrite Belt (González-Toril *et al.* 2003). A negative effect of bioleaching can be observed in shut-down or ill-managed metal or coal mines. Here strongly acidic run-offs also referred to as Acid Mine/ Rock Drainage (AMD/ARD) can arise (Johnson 2003) causing serious environmental pollution, if not properly controlled (Johnson and Hallberg 2003).

1.2 Leaching microorganisms

There is a big interest for finding suitable microbial populations to be used in commercial operations for processing different minerals (Rawlings and Johnson 2007). In mesophilic leaching processes mainly the Gram-negative genera *Leptospirillum* and *Acidithiobacillus* with *At. ferrooxidans* and *At. thiooxidans* are present. *At. ferrooxidans* is one of the most studied mesophilic leaching bacteria for its iron and sulfur oxidation pathways (Bonnefoy and Homes 2011; Quatrini *et al.* 2009; Ramírez *et al.* 2004). The complete genome sequences of two *At. ferrooxidans* strains are available (ATCC 23270 = NC_011761.1; ATCC 53993 = NC_011206.1). However, due to its higher tolerance towards acidity and ferric iron, *L. ferrooxidans* is by far more often found as the dominant iron-oxidizer in industrial operation (Vásquez and Espejo 1997; Rawlings *et al.* 1999a).

Most industrial heap and tank bioleaching operations run in the mesophilic range, but operations at increased temperature promise higher reaction rates (Olson *et al.* 2003; Batty and Rorke 2006). Under these temperature regimes, the most present bacteria

genera are the Gram-positive *Acidimicrobium, Ferrimicrobium* and *Sulfobacillus*, as well the Gram-negative *Acidithiobacillus caldus*. Archaeal species of *Ferroplasma* are present, too. A big interest has been focused on thermophilic and extreme thermophilic microorganisms, where apart from the bacterium *Aquiflex aeolicus,* just Archaea are dominant. Some members of the *Sulfolobales* are known to be involved in bioleaching with genera like *Acidianus, Sulfolobus* and *Metallosphaera* (Rohwerder *et al.* 2003; Gericke *et al.* 2001). *Acidianus brierleyi* was the first isolated archaeon in connection with bioleaching (Brierley 1978). It is able to grow on sulfur or ferrous iron as well as heterotrophically utilizing complex organic compounds, like beef extract or trypton (Segerer *et al.* 1986). The application of *A. brierleyi* leads to higher recovery rates of gold by oxidation of pyrite than achieved with mesophilic microorganisms (Brierley 1990). *Sulfolobus metallicus* is an obligate chemolithoautotrophic archaeon oxidizing ferrous iron, RISCs and/or MeS (Huber and Stetter 1991; Jordan *et al.* 2006). Only little is known about its iron and sulfur metabolism. Another prominent achaeon is *Metallosphaera sedula*, an aerobic iron- and sulfur- oxidizing chemolithotrophic archaeon that also grows with complex organics (Huber *et al.* 1989).

There is also evidence for heterotrophic bacteria and fungi contributing to bioleaching by metal mobilisation due to enzymatic reactions, production of organic acids or by compounds with hydrophilic reactive groups. Bacteria of the genus *Acidiphilium*, *Bacillus* and fungi of the genus *Aspergillus* and *Penicillium* are among them (Bosecker 1997).

This work is focused on moderately thermophilic sulfur oxidizers *Sulfobacillus* spp. and *At. caldus.*

1.2.1 ***Acidithiobacillus caldus***

At. caldus is a Gram-negative bacterium forming extremely short rod-shaped cells, each with a single polar flagellum (Hallberg and Lindstrom 1994). Its optimal growth conditions are within the pH range 1 - 3.5 at 45 °C. It is the only species of the genus *Acidithiobacillus,* which can grow mixotrophically using S^0, tetrathionate or thiosulfate with yeast extract or glucose (Hallberg and Lindstrom 1994; Qiu *et al.* 2007). Although, it cannot oxidize iron or pyrite, it can grow on sulfur and RISCs from pyrite in combination with iron oxidizers like *L. ferrooxidans* (Kelly and Wood 2000). Furthermore, it has been shown to oxidize arsenopyrite (Dopson and Lindström

2004). Three strains are validated: *At. caldus* C-SH12, the type strain *At. caldus* KU (ATCC 51756) and *At. caldus* SM-1 and complete genome sequences exist for the latter two (Valdes *et al.* 2009, NCBI; You *et al.* 2011).

1.2.2 *Sulfobacillus* spp.

Sulfobacillus spp are thermotolerant, Gram-positive, aerobic, endospore-forming, acidophilic bacteria from the phylum Firmicutes, which have a low G+C mol % content in their DNA. Their temperature range for growth is between 20 to 60 °C and their pH is between 2–5. On ferrous iron medium the pH is in a lower range due to iron precipitation. This genus grows autotrophically and mixotrophically with ferrous iron, with RISCs in the presence of yeast extract, and heterotrophically with yeast extract only. Species known in the genus *Sulfobacillus* are: *Sb. acidophilus* (Norris *et al.* 1996), *Sb. benefaciens* (formally *Sulfobacillus* strain BRGM 2), *Sb. montserratensis* (formerly *Sulfobacillus* strain L15), *Sb. sibiricus* (Melamud *et al.* 2003), *Sb. thermosulfidooxidans* (Golovacheva and Karavaiko 1978) and *Sb. thermotolerans* (Bogdanova *et al.* 2006). Complete genome sequences are available for *Sb. acidophilus* DSM 10332^T (NCBI: CP003179.1), *Sb. acidophilus* TPY (NCBI: CP002901.1) and for *Sb. thermosulfidooxidans* DSM 9293^T (NCBI Project ID:61271).

Sulfobacillus thermosulfidooxidans

Two strains are available of *Sb. thermosulfidooxidans* (type strain DSM 9293 and strain DSM 11920). The type strain was isolated from a copper-zinc deposit in Kasakhastan (Golovacheva and Karavaiko 1978). Both strains metabolize glucose primarily via the Entner-Doudoroff pathway, but after enrichment of the medium with 5 % CO_2 glucose is metabolized via the Embden-Meyerhof pathway (Krasil'nikova *et al.* 2001). These strains grow poorly organotrophically, but are capable of growth under oxygen limitation or anaerobic conditions with ferric iron as terminal electron acceptor and glycerol (or S^0 + yeast) as electron donor (Bridge and Johnson 1998). Best growth conditions are 50-55 °C, pH 1.9-2.4, 2.0-2.5 g/L ferrous iron, 1-2 mM sodium thiosulfate, 0.02 % glucose and 0.02 % yeast (Zhuravleva *et al.* 2006).

1.3 Microbial sulfur oxidation

As mentioned before, RISCs are sulfide (H_2S as well as MeS), polysulfides, elemental sulfur (S_8), sulfite (SO_3^{2-}), thiosulfate ($S_2O_3^{2-}$) and polythionates ($S_nO_6^{2-}$, $n \geq 3$), such as tri-, tetra- and pentathionates. Their use as electron donors is the

predominant energy-yielding process in acidic natural sulfur-rich biotopes, including mining sites containing sulfidic ores. Consequently, the activity of acidophilic sulfur compound-oxidizing prokaryotes has both an important environmental impact as well as an emergent biotechnological use. Sulfur compounds have the tendency to form homoatomic chains and rings reacting with each other easily. Several RISC oxidizing microorganisms belong to archaeal orders e.g. *Sulfolobales*, and bacterial domains e.g. *Acidithiobacillus, Aquaspirillum, Aquifex or Beggiatoa*. Apart from these lithotrophic prokaryotes, many phototrophic microorganisms are able to utilize RISCs as electron donors for anoxygenic photosynthesis (Friedrich *et al.* 2005), e.g. *Allochromatium*, *Chlorobium* and *Rhodobacter*. RISC oxidation is also performed by chemotrophic bacterial endosymbionts in worms or mussels (Nelsen and Fischer 1995, Minic and Hervé 2004). Chemolithotrophic Bacteria and Archaea use RISCs for feeding electrons into the respiratory chain, while phototrophic bacteria mainly use RISCs to transfer electrons for the non-cyclic photoreaction, which provides $NADPH_2$ needed for CO_2 fixation.

1.3.1 **Elemental sulfur**

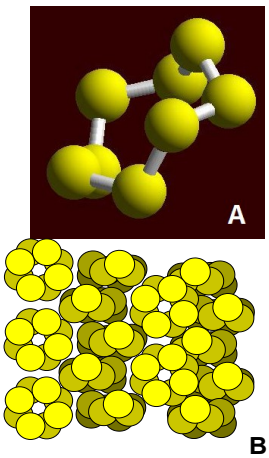

Fig.2: A) Cyclic crown-shaped S_8 molecule (www.webelements.com); **B)** Scheme of rhombic sulfur crystals; α-S_8

Elemental sulfur (S^0) is a non-metallic chemical element. In pure form, at temperatures below 95.6 °C, it exists in yellow rhombic crystals (α-sulfur) as S_8-ring (Fig. 2). These S_8-rings consist of 8 covalently single bound sulfur atoms (Fig. 2A). This form of elemental sulfur is the most thermodynamically stable and the most commonly occuring in nature. S^0 is practically insoluble in water at room temperature (5 µg/L H_2O; Boulegue 1978). Consequently, S^0 needs to be activated by S^0-oxidizing organisms prior to oxidation (Rohwerder and Sand 2003). S^0 can either be activated through S8-ring opening by nucleophilic attack, thereby forming polysulfanes, or by its reduction to polysulfide. It is believed that highly reactive linear sulfur molecules like polysulfide are the initial substrates for

sulfur-oxidizing enzymes rather than the octameric S^0 (Steudel 2000; Rohwerder and Sand 2007; Franz *et al.* 2009).

1.3.2 **Bacterial sulfur oxidation pathways**

The enzymatic oxidation of S^0 proceeds via at least two steps: *i*) S^0 is oxidized to sulfite by enzyme reactions and *ii*) sulfite is further oxidized to sulfate by a sulfite:acceptor oxidoreductase (Sar; Zimmerman *et al.* 1999) or dehydrogenases. Many intermediates may be formed, such as thiosulfate and tetrathionate. However, two major pathways of sulfur compound oxidation are described in detail in Gram-negative bacteria. The most studied is the Sox (sulfur-oxidizing) pathway present in mesophilic bacteria growing at neutral pH, such as *Paracoccus pantotrophus* and *Starkeya novella* (Friedrich *et al.* 2001). Here a set of dehydrogenases and other proteins catalyze the oxidation of sulfide, S^0, thiosulfate and sulfite to sulfate accompanied at an electron transfer to cytochrome C. In *P. pantotrophus* the *sox* gene cluster comprises 15 genes organized in three transcriptional units, *soxRS*; *soxVW and soxXYZABCDEFG*. The essential proteins for an active SOX system are the periplasmic proteins SoxYZ, SoxB, SoxCD and SoxXA which interact with each other (Friedrich *et al.* 2001; Welte *et al.* 2009; Friedrich *et al.* 2008). SoxXA catalyzes the oxidative transfer of thiosulfate and/or other inorganic sulfur compounds (ISCs) to the thiol group of a conserved cysteine in SoxYZ forming a cysteine S-thiosulfonate (thiocysteine sulfate) derivative. This is oxidized while covalently attached to SoxYZ and the sulfone sulfur (containing R-SO_2-R) is cleaved off by the hydrolase SoxB, yielding sulfate. The outer sulfur atom of the cysteine persulfide in SoxYZ is then oxidized to cysteine-S-sulfate by $Sox(CD)_2$ and is finally hydrolyzed to sulfate and SoxB to regenerate SoxYZ (Fig. 3A).

SoxCD is a $\alpha_2ß_2$ heterotetramer, where SoxC is the molybdenum cofactor-containing subunit and SoxD is a diheme c-type cytochrome, and works as sulfur dehydrogenase. In *P. pantotrophus* it has been shown that without $Sox(CD)_2$ 2 mol of electrons are produced per mol of thiosulfate, and addition of $Sox(CD)_2$ increases the yield to eight electrons (Bardischewsky *et al.* 2005). Consequently a Sox system without $Sox(CD)_2$ will exhibit low activity. The yield of two electrons from thiosulfate by the Sox system lacking $Sox(CD)_2$ suggests that S^0 or polysulfide is the product of this reaction. Indeed, it is known that in the purple sulfur bacterium *Allochromatium vinosum sox* genes were identified to be present in two gene clusters without

containing *soxCD* and these Sox proteins are able to oxidize thiosulfate while forming S^0 globules as intermediates (Fig. 3B; Hensen *et al.* 2006). The same phenomenon has been observed in green sulfur bacteria, e.g. *Chlorobaculum tepidum* (Sakurai *et al.* 2010). During the oxidation of thiosulfate to sulfate, the sulfane sulfur from SoxY cannot be directly oxidized and is most likely transferred to internal S^0 globules. These are in turn degraded and oxidized by a reversely working dissimilatory sulfite reductase (DsrAB), which is encoded by the first two genes of a 15 gene *dsr* cluster (Pott and Dahl 1998; Dahl *et al.* 2005; Frigaard and Dahl 2009). Clusters of *sox* and *dsr* genes have also been identified in other S^0-storing bacteria, suggesting that these mechanisms of S^0 oxidation are evolutionary conserved. Interestingly, sulfite oxidation does not necessarily need SoxCD in *P. pantotrophus* (Friedrich *et al.* 2000).

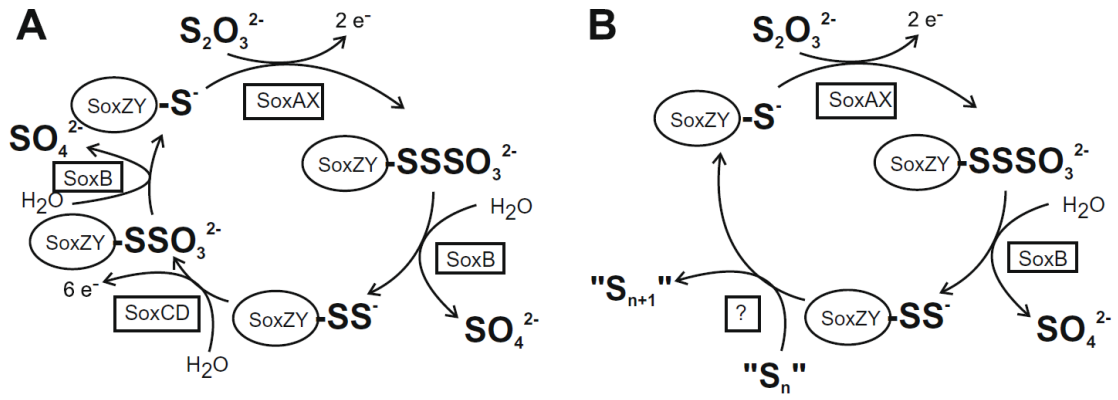

Fig.3: A) Model of Sox-mediated thiosulfate oxidation in *P. pantothrophus* and B) in *Al. vinosum* (from Welte *et al.* 2009)
A) In *Pa. pantotrophus* the sulfane dehydrogenase Sox$(CD)_2$ oxidizes the sulfane sulfur of the SoxY-persulfide to SoxY-thiosulfonate with the concomitant release of six electrons, SoxB hydrolytically cleaves off the terminal sulfone moiety as sulfate and releases SoxYZ for a new reaction cycle. **B)** In *Al. vinosum,* Sox$(CD)_2$ is not present but SoxY still has to be regenerated for the next cycle of thiosulfate binding. Therefore, the sulfane moiety was proposed to be transferred by an unknown factor to finally form S^0 globules.

The Sox multienzyme-complex is absent in some acidophilic leaching bacteria such as *At. ferrooxidans, At. thiooxidans* or *Acidiphilium spp*.. Instead, a sulfur dioxygenase (Sdo) (EC 1.13.11.18) has been proposed to be responsible for the initial S^0 oxidation step. Here, the first reaction is an opening of the elemental S_8-ring. This proceeds mainly on the assumption that this reaction is an activation by thiol groups (R-SH-groups) (Vishniac and Santer 1957, Pronk *et al.* 1990), which is a non-enzymatic reaction; a nucleophilic attack from the thiol group on the S_8-ring. Thus S^0 can be reduced to a nonasulfane derivate (Eq. 3), which can be subsequently

oxidized by the postulated Sdo to a sulfinate group. It has been shown that only these thiol-bound sulfane sulfur atoms ($R\text{-}SS_nH$) are reactive enough to be oxidized by Sdo (Rohwerder 2002). Afterwards, the sulfite is hydrolytically separated (Eq. 5) and hence the thiol group recovered.

$$S_8 + RSH \rightarrow RS_9H \qquad \text{(Eq. 3)}$$

$$RS_nH + O_2 \rightarrow RS_{n-1}SO_2^- + H^+ \qquad \text{(Eq. 4)}$$

$$RS_{n-1}SO_2^- + H_2O \rightarrow RS_{n-1}H + SO_3^{2-} + H^+ \qquad \text{(Eq. 5)}$$

Mesoacidophilic bacteria are especially dependent on the low molecular thiol groups, which can be replaced *in vitro* by glutathione (GSH) (Suzuki 1974, 1994). The following equation summarizes the reaction of Sdo:

$$1/8\ S_8 + O_2 + H_2O \rightarrow HSO_3^- + H^+ \qquad \text{(Eq. 6)}$$

The activity of this enzyme was demonstrated in several studies (Suzuki 1994, Rohwerder and Sand 2003) and partial purification was achieved (Chahal 1986). Furthermore, the incorporation of molecular oxygen was proven by ^{18}O labeling experiments (Suzuki 1965). The product of Sdo is sulfite (Eq. 5, 6), which is mainly oxidized further to sulfate by Sar, most likely reducing soluble cytochromes. In *At. ferrooxidans* strain R1, the electrons are transferred to the terminal cytochrome oxidase systems of the aa_3 or ba_3-type (Rohwerder and Sand 2003).

Recently, bioinformatic analysis has shown that the gene cluster *hdrABC* (Heterodisulfide reductase) has been found in *At. caldus*, *At. ferrooxidans*, *Aquifex aeolicus*, *M. sedula*, *S. acidocaldarius*, *S. tokodaii* and *S. solfataricus* (Quatrini *et al.* 2009), and it has been be postulated to catalyze a similar sulfur oxidation reaction as Sdo, despite the lack of biochemical evidence to support this. Sdo was firstly postulated to be located in the periplasmic space of Gram-negative bacteria (Rohwerder *et al.* 2003). More recently, it is suggested to be cytoplasmic, which is in agreement with the fact that the predicted localization of the heterodisulfide reductase catalytic site is in the cytoplasm (Quatrini *et al.* 2009). Sdo is glutathione dependent and HdrABC catalyzes the reversible reduction of the disulfide bound X-S-S-X with energy conservation in methanogenic Archaea (Hamann *et al.* 2007) and sulfate reducing Archaea and Bacteria (Mander *et al.* 2004). In both cases, HdrA

receives the electrons from the hydrogenase and transfers them through HdrC to the heterodisulfide reductase catalytic site located in HdrB. Accompanying the reduction of heterodisulfide, protons are extruded across the membrane creating a proton motive force. It is hypothesized that for the sulfur oxidizers referred above, HDR could be working in reverse oxidizing disulfide intermediates (from sulfur oxidation) to sulfite and delivering the collected electrons to the membrane quinone pool. It is still not known whether the Sdo pathway is valid for all acidophilic Gram-negative bacteria, but it is likely that more than one enzymatic system is present in most species (Rohwerder and Sand 2007).

In addition to the sulfur oxidation pathway in *At. ferrooxidans*, the oxidation of sulfide by sulfide:quinone oxidoreductase (Sqr; Wakai *et al.* 2004, Brasseur *et al.* 2004) and thiosulfate by thiosulfate:quinone oxidoreductase (Tqo; Müller *et al.* 2004) has been elucidated. The latter oxidizes thiosulfate *in vitro* with tetrathionate as product and ferricyanide or decyl ubiquinone (DQ) as electron acceptors. Tetrathionate can be degraded to thiosulfate by a tetrathionate hydrolase (Tth). This enzyme has been characterized for *At. ferrooxidans* (Kanao *et al.* 2007; Beard *et al.* 2011) and *At. caldus* (Bugaytsova and Lindstrom 2004; Rzhepishevska *et al.* 2007). The involvement of electron transfer via quinones to oxygen is also supported by the finding that bd-type and bo_3-type quinone oxidases (Brasseur *et al.* 2004; Wakai *et al.* 2004) as well as a downhill electron transport via a bc1 complex (Brasseur *et al.* 2004) are present during sulfur oxidation in *At. ferrooxidans* (Fig. 4).

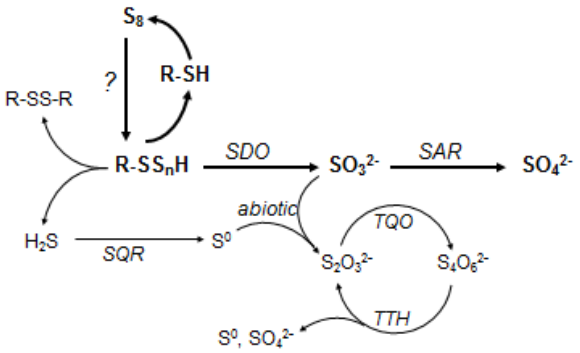

Fig.4: Hypothetical model of sulfur oxidation in acidophilic proteobacteria (from Rohwerder and Sand 2007).

Abbreviations: sulfur dioxygenase (Sdo), sulfite:acceptor oxidoreductase (Sar), periplasmic cytochrome (Cyt.), terminal oxidases (ba_3, aa_3), sulfide:quinone oxidoreductase (Sqr), thiosulfate:quinone oxidoreductase (Tqo) and tetrathionate hydrolase (Tth). For more details see text.

1.3.3 **Sulfur oxidation in Archaea**

The unique combination of dissimilatory aerobic sulfur oxidation and anaerobic sulfate respiration is exclusively found in the order *Sulfolobales* within the archaeal kingdom Crenarchaeota (Segerer *et al.* 1985). -*Acidianus ambivalens* (*A. ambivalens*)-, a member of the *Sulfolobales*, has developed into one of the model organisms for sulfur oxidation studies in archaea.

Archaea possess no outer membrane and consequently no periplasmic space. Hence, most enzymatic reactions are proposed to occur in the cytoplasm. Sulfur needs to be transported from the outside to the cytoplasm through the cytoplasmic membrane. However, the process of mobilization is still unclear.

The RISC oxidation pathways are similar between acidophilic archaea and bacteria, because they possess homologues enzymes. However, the hydrogen sulfide (H_2S) production of sulfur oxygenase reductase (Sor) is a distinctive feature of the archaeal pathways (Kletzin 1989).

Sor reactions are detailed as followed: 1. S^0 oxygenation and 2. S^0 disproportionation. In the latter 3 moles of S^0 are converted into 1 mole sulfite and 2 moles H_2S (Kletzin 1989, 1992, Urich *et al.* 2006) (Eq. 7 and 8). However, it is difficult to determine the stoichiometry of the enzymatic reaction, measured as H_2S and $S_2O_3^{2-}$ production, because H_2S is highly volatile and is quickly lost from the liquid phase. The use of H_2S-complexing zinc ions in the assay has allowed the determination of the stoichiometry of 1 between reduced and oxidized products (Kletzin 1989), (Eq. 9). In Eq. 10, the non-enzymatic formation of thiosulfate formed from sulfite and sulfur is given, which is consequently not the primary product of the enzymatic catalysis.

Sulfur oxygenation: $S^0 + O_2 + H_2O \rightarrow \mathbf{HSO_3^-} + H^+$ (Eq. 7)

Sulfur disproportionation: $3\ S^0 + 3\ H_2O \rightarrow \mathbf{HSO_3^-} + \mathbf{2\ H_2S} + H^+$ (Eq. 8)

Sum: $4\ S^0 + O_2 + 4\ H_2O \rightarrow \mathbf{2\ HSO_3^-} + \mathbf{2\ H_2S} + 2\ H^+$ (Eq. 9)

Side reaction: $S^0 + \mathbf{HSO_3^-} \rightarrow S_2O_3^{2-} + H^+$ (Eq. 10)

Inhibitors of the enzymatic reaction are thiol-binding reagents such iodoacetic acid and zinc ions (Kletzin 1989; Urich 2005).

No energy conservation occurs during Sor catalysis, but the reaction products are substrates for downstream enzymes. Sulfite can react abiotically with an excess of S^0 to thiosulfate. Sulfite and thiosulfate are substrates for the membrane bound enzymes Sar, which catalyze the oxidation of sulfite to sulfate, and thiosulfate:quinone oxidoreductase (Tqo; Müller *et al.* 2004), catalyzing the generation of tetrathionate from thiosulfate and feeding the electrons into the quinone pool in the cytoplasmic membrane. Apart from the Sar pathway, adenylylsulfate (Aps) reductase and adenylyltransferase (Apat) are involved in the generation of ATP from sulfite by substrate level phosphorylation (Zimmermann *et al.* 1999). The third product, hydrogen sulfide, is oxidized back to S^0 by the membrane bound sulfide:quinone oxidoreductase (Sqr). All electrons made available from sulfur oxidation in the course of Sqr, Sar and Tqo activities reduce Caldariella quinones (CQ) but not cytochromes (Brito *et al.* 2009; Müller *et al.* 2004).

Apart from the abiotic reaction of S^0 with sulfite, another soluble enzyme could be identified (Kletzin 2006) to generate thiosulfate (see Fig. 5). This enzyme is called tetrathionate hydrolase (Tth) and is the acceptor enzyme to Tqo (Kletzin 2006). Hence, these two enzymes catalyze the thiosulfate/tetrathionate cycle. Furthermore, tetrathionate is decomposed to sulfate, thiosulfate and S^0 by an extracellular tetrathionate hydrolase in tetrathionate-grown *A. ambivalens* cells (Protze *et al.* 2011). It is probably attached to the cytoplasmic membrane or to the proteinaceous surface layer, the sole cell wall component of *A. ambivalens* (Veith *et al.* 2009). The *Acidianus* Tth is biochemically and phylogenetically similar to the *Acidithiobacillus* Tth (Bugaytsova and Lindström 2004). Both enzymes are located outside the cell and have optimal activities at acidic pH (Protze *et al.* 2011).

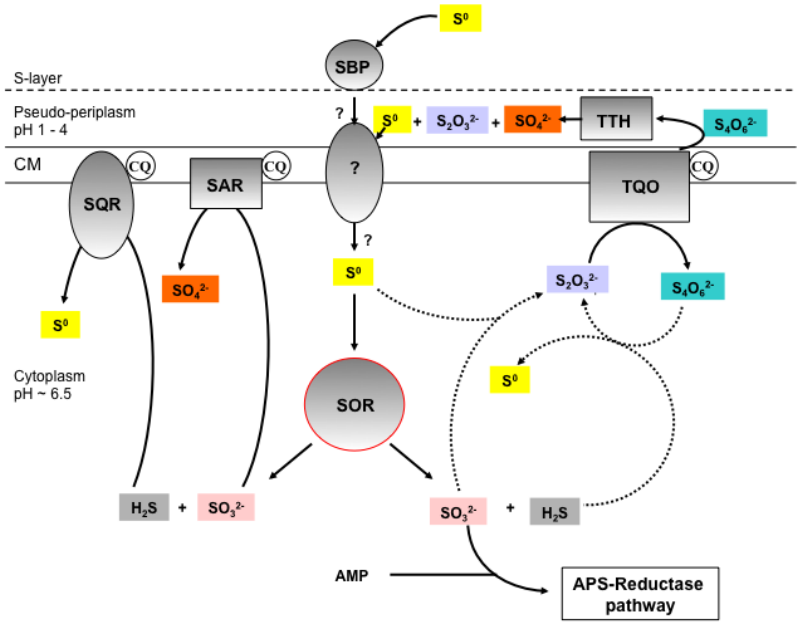

Fig.5: Hypothetical model of the sulfur oxidation pathways in *A. ambivalens* (adapted from Kletzin 2008 and modified after Protze *et al.* 2011).
Abbreviations: CM, cytoplasmic membrane; SAR, sulfite:acceptor oxidoreductase; SQR, sulfide:quinone oxidoreductase; SBP, sulfur binding protein; SOR, sulfur oxygenase reductase; TQO, thiosulfate:quinone oxidoreductase; TTH, tetrathionate hydrolase; CQ, caldariella quinone; AMP, adenosine-mono-phosphate; APS, adenylylphosphate: ?, indicate processes which are not clear until now. See text for details.

1.4 Focus: sulfur oxygenase reductase

As mentioned before, Sor simultaneously oxidizes and disproportionates S^0 (Kletzin 1989; He *et al*. 2000). Only in 1968, Tano and Imai have reported a similar enzyme activity from the mesophilic bacterium *At. thiooxidans* ON 106 (formerly *Thiobacillus thiooxidans*), where in cell-free extracts the production of thiosulfate and hydrogen sulfide from S^0 has been detected. Until now, neither the responsible enzyme has been isolated, nor has this result been confirmed independently. The Sor and the sulfur oxygenase in *A. brierleyi* were very similar with respect to the sizes of the holoenzymes and of the single subunits. In addition, the reaction products sulfite, thiosulfate and other properties, but not the formation of sulfide was reported (Emmel *et al*. 1986). However, it could be concluded that both catalyze the same reaction and that the sulfide formation of the *A. brierleyi* enzyme had been overlooked (Kletzin 1992). The same coupled oxygenase and disproportionation reaction has been found for a third enzyme, the Sor from *Acidianus tengchongensis* (formerly *Acidianus* strain sp.5) (He *et al.* 2000, 2004; Sun *et al.* 2003). Comparison between its Sor and the *A. ambivalens* one revealed several differences between these two Sors, see Table 2. In addition, a gene encoding Sor was identified as the source of the

dominant transcript in S^0-grown cells of the type strain of *S. metallicus* (gb:EF040586), with its predicted protein showing high identities to the previously described Sor from *S. tokodaii* and species of *Acidianus* (Bathe and Norris 2007).
In 2007, Chen and coworkers reported a bacterial Sor activity from cells of a bioreactor treating gold-bearing concentrates. They analyzed Sor activity from *At. caldus* SM-1. This was the first time Sor activity was determined for acidophilic moderately thermophilic bacteria and the documentation of a *sor* gene in *At. caldus*. Furthermore, two *sor* genes are encoded in the genomes of the type strains *Sb. thermosulfidooxidans*, one in *Sb. acidophilus* (gb: AEW03939) and another one in *Sb. acidophilus* TPY (gb: AEJ38607). Recently, the recombinant Sor of *Halothiobacillus neapolitanus* was investigated in greater detail in order to determine its structural and biochemical properties. This Sor has a temperature range of activity of 10-99 °C with an optimum at 80 °C (42 U/mg protein) (Veith *et. al.* 2011b).

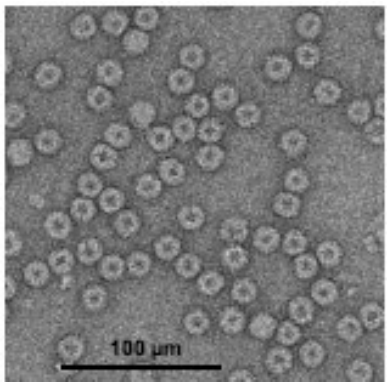

Fig.6: **Electron micrograph of the Sor holoenzyme of *A. ambivalens*.**
Globular particles with a diameter of ~15.5 nm are visible (Kletzin 1989).

To date, a total number of 17 *sor* genes (+6 sequences of uncharacterized archaea) and putative Sor protein sequences have been identified. 10 of these belong to bacterial and 7 belong to archaeal species. X-ray crystallographic structures have been determined for three Sor enzymes, from *A. ambivalens* (Urich 2005), from *A. tengchongensis* (Li *et al.* 2008) and from *Halothiobacillus neapolitanus* (Veith *et al.* 2011b). All showed that the spherical, hollow oligomers are composed of 24 identical subunits arranged in a 432 point-group symmetry (Janner 2008a; Janner 2008b) and an external diameter of approx. 15 nm (Fig. 6). In *A. ambivalens* the homo-icosatetrameric holoenzyme has a molecular mass of 840 kDa. Each monomer contains one mononuclear non-heme iron site within the ligands H85, H89, E113 (positions in the protein sequence) and two water molecules in an octahedral arrangement. The cysteines C31, C100 and C103 are in the vicinity of the iron site and located along the same cavity within the interior of the subunit, therefore defining the enzyme´s active site. Mutations of the iron ligands and of C31 resulted in an inactive enzyme, whereas mutations of C100 and C103 resulted in a reduced activity. Thus, C31, H86, H90 and E114 are essential for the

enzymatic reaction of Sor and most probably from the sulfur binding residue which aligns the substrate for the initial oxygenation catalyzed by the iron site. From the structural point of view, it is postulated for Sor the cyclic α-S_8 is not the substrate, but linear polysulfides (Urich *et al.* 2006), which have been very recently shown (Veith 2011a). Consequently, the Sor reaction most likely starts with a hydrolytic release of hydrogen sulfide from the sulfur chain, forming a highly reactive sulfenic acid intermediate (R-S_n-SOH).

A summary of biochemical properties of the Sor enzymes and the sulfur oxygenase, is given in Table 2.

Table 1: Biochemical properties of the SOR enzymes and the sulfur oxygenase

Species	*A. ambivalens*	*A. ambivalens*	*A. tengchongensis*	*A. brierleyi*	uncult. bact. SB	*At. caldus*-like strains S1/S2	*Aq. aeolicus*	*Hn. neapolitanus*
Source	native	*E. coli*	*E. coli*	native	*E. coli*	native	*E. coli*	*E. coli*
Molecular mass subunits	35.187 kDa[a]	36.311 kDa[a]	35.172 kDa[a]	35.00 kDa[b]	34.077 kDa[a]	34.829 kDa[a]	37.674 kDa[a]	34.965 kDa[a]
pH_{opt} / pH_{range}	7.0 - 7.4 / 4 -8	n.r.	5 / 3.5 - 9.0	7.0 / n.r.	7.5 / n.r.	n.r.	n.r. / 5.5 - 8.0	8.4 / 5.4 - 11
T_{opt} / T_{range}	85°C / 50°C - 100°C	n.r.	70°C / 50°C - >90°C	65°C / 50°C - >80°C	75 - 80°C / n.r.	65°C / 30°C - 65°C	80°C / 20°C - 90°C	80°C / 10°C - 99°C
Specific oxygenase activity	10.6 U/mg	2.8 U/mg	753 U/mg	0.9 U/mg	3.76 U/mg	n.r.	78.8 U/mg	42.38 U/mg
Specific reductase activity	2.6 U/mg	0.66 U/mg	42.2 U/mg	n.r.	n.r.	n.r.	3.05 U/mg	4.11 U/mg
reference	Kletzin 1989	Urich *et al*. 2004	Sun *et al*. 2003	Emmel *et al*. 1986	Chen *et al*. 2007	Janosch *et al*. 2009	Pelletier *et al*. 2008	Veith *et al*. 2011b

[a]calculated from sequence; [b]apparent mass in SDS gel; n.r. = not reported

1.5 Sulfur metabolism in *Acidithiobacillus caldus*

As mentioned, *At. caldus* is able to oxidize RISCs. Thiosulfate oxidation takes place in the periplasm, in contrast to the oxidation of tetrathionate, sulfide, sulfite and S^0, is believed to be located in the cytoplasmn (Hallberg *et al.* 1996). Several intermediates have been found in these oxidation processes; thiosulfate is oxidized to tetrathionate, elemental sulfur is formed during the oxidation of tetrathionate and the oxidation of sulfide; sulfite is an intermediate of tetrathionate and sulfur metabolism. Most of these results were confirmed in recent experiments. Tth has been purified with an optimum pH of 3 for its activity. The periplasmic localization of the enzyme has been determined by differential fractionation of *At. caldus* cells, testing activity in the different cell fractions: cell pellet, membrane fraction and supernatant. Detectable products of the Tth reaction are thiosulfate and pentathionate (Bugaytsova and Lindström 2004). The gene *tth* is located in a putative operon (in the following order) *IsaC1* (transposase), *rsrR*, *rsrS* (two component transcriptional regulator system), *tth*, *doxD* (quinol oxidase subunit) and *IsaC2* (transposase) (gi:255022205-255022210). Western blotting has shown up-regulation of Tth in thiosulfate or tetrathionate grown cells in comparison with S^0 grown ones (Rzhepishevska *et al.* 2007). In 2009, after the release of the complete genome sequence of the *At. caldus* type strain (Valdes *et al.* 2009), two putative Sox systems were found to be encoded (Mangold *et al.* 2011). Another interesting finding is that $Sox(CD)_2$ is missing in this organism allowing one to hypothesize that the Sox system in *At. caldus* may catalyze sulfite oxidation, or thiosulfate oxidation in low activity or when forming S^0 globules. The latter has not been reported in *At. caldus* until now. No gene encoding direct sulfite oxidation like SAR has been found in either the type strain or in the genome of *At. caldus* SM-1 (Valdes *et al.* 2009; You *et al.* 2011). Also, no candidate for the enzyme APS-reductase could be found (Mangold *et al.* 2011). However, the presence of genes like *sat* and *dsrABC* could indicate indirect sulfite oxidation.

The genome of *At caldus* ATCC 51756 possesses a *sor* gene and two putative orthologs of *hdr* and two orthologs of *sqr*. During growth on S^0 in comparison to tetrathionate, *sox* and *hdr* genes were up-regulated suggesting their involvement in sulfur utilization, whereas both *sox* clusters were up-regulated on tetrathionate (Mangold *et al.* 2011). In 2007, Chen and coworkers found bacterial Sor in a bioreactor treating gold-bearing concentrates. They analyzed Sor activity from an *At. caldus*-like isolate (*At. caldus* SM-1). Its *sor*-like gene, called sor_{SB}, was cloned

and expressed in *E. coli* and the Sor activity was determined (Chen *et al.* 2007). However, this result has not been confirmed independently. Furthermore, the genome sequence of *At. caldus* SM-1 does not contain a *sor* gene. It seems to have been deleted by the activity of a transposition element, since at a location in the genome of the SM-1 strain a transposase is present in its encoding locus, compared to the type strain (You *et al.* 2011). We also measured Sor activity in two *At. caldus*-like isolates S1 and S2 (Janosch *et al.* 2009), however the enzyme measurements were afterwards not reproducible.

The potential use of Sdo and/or Sor in the *At. caldus* sulfur oxidation pathway remains to be resolved. It has been speculated that they might be used under different growth conditions or for different RISC substrates. It is on the aforementioned opened questions that this work is focused. *At. caldus* strains, *At. caldus*-like isolates and the type strain of *Sb. thermosulfidooxidans* have been analyzed for Sor activity. Furthermore, the proteomes of the type strain grown on S^0 vs the one grown on thiosulfate are compared. The data reported here shall contribute to a deeper insight in sulfur metabolism of these leaching bacteria.

2 AIMS OF THIS STUDY

In the moderately thermophilic range *At. caldus* and *Sulfobacillus* spp. are the most abundant sulfur oxidizers and they have been the subject of this study. Until now the Sor enzyme has been intensively analysed in extremely thermophilic sulfur-oxidizing Archaea, but very little is known about its occurrence in moderately thermophilic sulfur-oxidizing Bacteria. Genomic analyses indicate that the *sor* gene is encoded in the genomes of the type strains of *At. caldus*, *Sb. acidophilus*, *Sb. thermosulfidooxidans* and *Sb. acidophilus* TPY. The present work aimed at screening for the presence of the *sor* gene in several *At. caldus* strains and isolates as well as to quantify enzymatic activities of Sor and Sdo in these strains and in *Sb. thermosulfidooxidans* DSM 9293^T. Transcriptomic studies of several genes encoding enzymes involved in sulfur metabolism in *At. caldus* were also considered. The genes *sor*, *tth*, *soxX* and *soxB* of one gene cluster and both homolog *sqr* genes were analyzed with RT-qPCR in cells grown on either S^0, thiosulfate or tetrathionate at two different temperatures. Furthermore, one of the *sox* clusters was investigated for cotranscription to analyze whether these genes share a possible regulation system.

For better understanding of sulfur metabolism in *At. caldus* a high troughput proteomic study of cells grown on S^0 compared with cells grown on thiosulfate was done. This semi-quantitative analysis revealed proteins/ enzymes of *At. caldus* expressed under one or both conditions. A detailed analysis was done considering proteins involved the sulfur and carbon metabolism, respiratory complexes, EPS production and cell motility.

Additionally, an *in silico* comparison of the so far known *At. caldus* sulfur metabolism pathways with the ones in *Sb. thermosulfidooxidans* genome has been done. Taken together, all the results presented in this thesis will contribute to a better knowledge of RISC metabolism in moderately thermophilic leaching bacteria.

3 MATERIAL AND METHODS

3.1 Microorganisms

The following Table 2 shows the bacterial and archaeal strains used in this thesis.

Table 2: Bacteria and Archaea used in this study

Species	Strain	Isolation/ References
Acidithiobacillus caldus	DSM 8584^T (KU^T/ ATCC 51756)	Tetrathionate enrichment culture K from P. Norris, Univ. of Warwick, UK ;Hallberg and Lindström 1994, Kelly and Wood 2000.
Acidithiobacillus caldus	DSM 9466	Continuous bioleaching reactor, Australia; alternative name C-SH12; Goebel and Stackebrandt 1994.
Acidithiobacillus caldus-like	S1	Provided by Zhou, Central South Univ. Changsha; coal heap drainage in Changsha Hunan Province, China; Zhou *et al.* 2007.
Acidithiobacillus caldus-like	S2	Provided by Zhou Central South Univ. Changsha; coal heap drainage in Changsha Hunan Province, China; Qiu *et al.* 2006, Zhou *et al.* 2007.
Acidithiobacillus caldus-like	MNG	Provided by Shelly M. Deane and Doug Rawlings, University of Cape Town, South Africa, Rawlings *et al*. 1999b.
Acidithiobacillus caldus-like	f	Provided by Shelly M. Deane and Doug Rawlings, University of Cape Town, South Africa, Rawlings *et al*. 1999b.
Acidithiobacillus caldus-like	#6	Provided by Shelly M. Deane and Doug Rawlings, University of Cape Town, South Africa, Rawlings *et al*. 1999b.
Sulfobacillus acidophilus	DSM 10332^T	Coal spoil, UK; Norris *et al.* 1996.
Sulfobacillus thermotolerans	DSM 17362 (VKM B-2339)	Sulfidic gold-containing concentrate, Russia: Eastern Siberia; Bogdanova 2002, Tsaplina *et al.* 2006
Sulfobacillus thermosulfidooxidans	DSM 9232^T	Spontaneously heated ore deposit, Eastern Kazakhstan; Golovacheva and Karavaiko 1991.
Sulfolobus metallicus	DSM 6482^T	Solfataric field, Iceland; Huber and Stetter 1991.

3.2 Media and growth conditions

3.2.1 Standard S^0 medium for *Acidithiobacillus caldus*

All *At. caldus* strains and all *At. caldus*-like isolates were cultivated in modified Mackintosh medium (Mackintosh 1978), as substrate with 5 g/L S^0. Ferric sulfate has only been added in trace concentrations (~1 mg/L). The standard starting pH was adjusted to pH 2.5 and cells were grown at 45°C. For some specific experiments (details see chapter 3.3.2; 3.3.7 and 3.3.12), the starting pH was shifted to 4.8 or growth was additionally tested at 30°C and 50°C.

3.2.2 Thiosulfate medium for *Acidithiobacillus caldus*

Thiosulfate cultures of *At. caldus* were grown in DSM 71 basal solution at pH 4.8. After autoclaving, sterile filtered sodium thiosulfate solution 5 g/L was added to the basal solution. Before inoculation, cells were washed twice with sterile DSM 71 basal solution.

3.2.3 Tetrathionate medium for *Acidithiobacillus caldus*

Tetrathionate cultures were grown according to Zhou *et al.* 2007. Start pH was adjusted to pH 3. After autoclaving, sterile filtered 3 g/L potassium tetrathionate solution was added. Before inoculation, cells were washed twice with sterile basal solution of this medium.

3.2.4 Growth curves of *Acidithiobacillus caldus*

At. caldus DSM 8584^T was grown in 500 mL cultures in triplicates in standard elemental S^0, in thiosulfate or in tetrathionate medium. Cultures were incubated at 30°C or 45 °C with shaking at 180 rpm. During growth, samples were taken daily for determination of total cell count (TCC) via microscopy (LEICA microscop model DMLS) using a Thoma chamber. Also pH, S^0, thiosulfate, tetrathionate and sulfate concentration in the medium were determined. Sulfate start concentrations (coming from the medium) were subtracted from all sulfate concentrations.

3.2.5 **Medium for *Sulfobacillus* spp.**

All *Sulfobacillus* spp. were grown in modified Mackintosh medium plus S^0 like *At. caldus* at 45 °C with 180 rpm shaking and a start pH of 2.5. Furthermore, 0.2 g/L yeast extract were added after autoclaving, prepared in 100 x stock solution.

3.2.6 **Iron medium for *Sulfobacillus thermosulfidooxidans***

Sb. thermosulfidooxidans DSM 9392^T was also grown in basal salt solution as described by Mackintosh 1978 with 2 g/L ferrous iron supplied as $FeSO_4$ x 7 H_20. Iron stock solution (100 x) and basal solution were autoclaved separately and combined before inoculation. Also here, 0.2 g/L yeast extract was added after autoclaving.
This medium was chosen for Sor enzyme control assays.

3.2.7 **Medium for *Sulfolobus metallicus***

The type strain of *S. metallicus* DSM 6482^T was cultivated in modified Mackintosh medium with the addition of 0.2 g/L yeast extract (like Sulfobacilli). Cultures were incubated at 65 °C without shaking and a starting pH of 2.5. In this study this strain was further investigated for the Sor reactions and a proposed Sdo presence.

All strains were grown in 50 mL medium for DNA isolation, in 500 mL medium for RNA isolation and in 5- 10L medium for enzyme assays. All basal solutions were autoclaved at 121°C for 20 min. Medium containing S^0 were autoclaved at 110 °C for 30 min. Bigger bottles for enzyme assays were autoclaved for 90 min and these cultivations were aerated and stirred at 300 rpm. However, *S. metallicus* was cultivated in 10 x 500 mL medium at 65 °C without shaking.

3.3 Molecular biology techniques

3.3.1 **DNA extraction**

If necessary, S^0 was removed by low speed centrifugation, 120 x g for 5 min with a Heraeus Sepatech centrifuge type Biofuge 28RS; Rotor HFA 13.50 #3746. Then, the supernatant was transferred to new sterile centrifuge tubes and this procedure was repeated twice. Afterwards, the samples were centrifuged at 11,180 x g for 10 min. The supernatant was discarded and the cells were washed with 1 mL 1 M sodium chloride.

Then, DNA was extracted according to the protocol of Aljanabi and Martinez (1997). DNA quality was analyzed using agarose gel electrophoresis and absorbance measurements at 230 nm, 260 nm, 280 nm and 340 nm were done with BioPhotometer plus (Eppendorf). DNA was stored at -20 °C.

3.3.2 **RNA extraction**

For transcriptomic analyses *At. caldus* was grown on S^0, thiosulfate and tetrathionate media at 30 °C, 45 °C and with S^0 also at 50 °C. Cells were harvested in late exponential growth phase. Cell pellets were resuspended in 1-2 mL "RNA-Later" (25 mM sodium citrate, 10 mM EDTA, 70 g ammonium sulfate/100 mL solution, pH 5.2) and incubated over night at room temperature and afterwards stored in this solution for no longer than 2 months at 4 °C.

After removal of RNA-Later, cells were washed twice in diluted sterile sulfuric acid solution pH 3. Total RNA extraction was performed with a hot-phenol method (Guiliani *et al.* 1997; Vera *et al.* 2008) with some modifications. Instead of ethanol, RNA was precipitated by 100 % isopropanol at -20 °C overnight. After resuspension in water approx. 100 µg RNA were cleaned with RNAeasy Mini Kit (Qiagen). DNA was eliminated by the addition of 30 U RNase-free Turbo DNase I (Ambion). Afterwards, RNA was additionally cleaned with High Pure RNA Isolation Kit (Roche) including a second on-column DNase-Step. RNA purity was tested by measuring specific absorption at 230, 260 and 280 nm using BioPhotometer plus (Eppendorf). Integrity of RNA was tested by agarose gel electrophoresis using 1 µg RNA. Successful DNA digestion was tested by PCR using GoTaq® polymerase (Promega®).

3.3.3 **Reverse-Transcription (RT)**

1 µg of RNA was reverse transcribed using 200 U of MMLV-RT, 300 ng random (hexamer) primers, 10 mM dNTPs in 25 µL final reaction volume. All reagents were used from Promega®. RT reactions were done at 42 °C for 1h. Control assays without RT were run in parallel. Reverse transcription was stopped by incubation at 65 °C for 10 min. The samples were stored at -20 °C. PCR amplifications were done with 1:20 cDNA dilutions as template.

3.3.4 **Preparation of polymerase chain reactions (PCR)**

All PCRs of DNA fragments were performed in a final reaction volume of 25 µL using 20-50 ng of genomic DNA template, 5 x Green Flexi buffer, 2.5 mM $MgCl_2$, 1 mM dNTPs, 10 pmol of each single primer and 1 U GoTaq®DNA, all from Promega®. Reactions were performed in Eppendorf Mastercyler personal and MiniCycler™: MJ Research PTC-150. Gradient PCR for determining the best annealing temperature for quantitative real- time PCR BioRad® C1000™ ThermalCycler was applied.

The following temperature program was used: 5 min initial denaturation at 95 ºC followed by 30 to 40 cycles of denaturation for 30 s at 95 ºC, primer annealing for 30 to 45 s at X ºC (see Table 3A) and 0.5 to 1.5 min of extension at 72 ºC, depending on the size of the expected amplicons, amplicons<1 kb 0.5 min; amplicons >1 kb 1 min and amplicons >1.5 kb 1.5 min. The final extension step lasted 3 min at 72 ºC.

3.3.5 **Primer design for analyzing bacterial *sor***

Degenerated primers for analyzing the *sor* gene were designed using the CODEHOP program (http://bioinformatics.weizmann.ac.il/blocks/codehop.html). First the primer pair PCJ2_for-PCJ3_rev was designed on *sor* sequences of *A. ambivalens* (gi:6065813:3998-4927), *Picrophilus torridus* DSM 9790 (gi:48477072), uncultured bacterium SB (gi:94470460), *Ferroplasma acidarmanus* fer1 (gi:126007703:169179-170102), *S. metallicus* (gi:124298242), and *S. tokodaii* str. 7 (gi:24473558:1121037-1121972). With these primers, it was possible to get the *sor* sequence of *At. caldus*-like S1/ S2.

At the time, when designing degenerated primers bsor_f1-bsor_r2 for bacterial *sor*, only sequences of *At. caldus* type strain (gi:255021290:37049-37984), uncultured bacterium BSB (gi:94470458), *H. neapolitanus* C2 (gi:261854630:1323758-1324702) and *Desulfomicrobium baculatum* DSM 4028 (gi:256827818:1284547-1285479) were available.

Primers for cotranscription and real-time PCR were designed with the *At. caldus* gene sequences using the Primer3Plus®software available at www.bioinformatics.nl.

3.3.6 **Cotranscription of putative *sox I* operon**

For testing cotranscription of the putative *sox I* operon, PCRs were performed using 1 µL 1/20 diluted cDNA from S^0 grown cells at 45 °C. All PCR reactions were

performed in 40 cycles of: 30 s 95°C, 30 s at X °C (see Table 3B) and 45 s at 72 °C. Control assays were performed with 20 ng of *At. caldus* genomic DNA.

3.3.7 **Quantitative real-time RT-PCR**

Sor, *tth*, *soxX* and *soxB* of one gene cluster and both *sqr* genes were analyzed with quantitative real-time RT-PCR (RT-qPCR) in cells grown on either S^0, thiosulfate or tetrathionate at 30°C and 45°C. Because *sor* is postulated to be optimally active in the thermophilic range, this gene was additionally analyzed in cells grown on S^0 at 50°C, which is the maximum growth temperature of *At. caldus*.

RT-qPCR was performed using the Biorad® IQ5 system with the Biorad® IQ SybrGreen Supermix. PCR reactions were done following provider instructions in 25 µL final volume using 1 µL of 1/20 diluted cDNA sample as template and the primers listed in Table 2. The program included: 3 min at 95 °C; 40 cycles of 10 s at 95 °C, 15 s at X °C (Table 4C), 20 s at 72 °C, with fluorescence measurement at the end of this step; 2 min at 72 °C. Melting curves were done in a ramp from 60 °C to 95 °C in 0.5 °C steps. Calibration curves were done using serial tenfold genomic DNA dilutions ranging from 20 ng to 200 fg. As reference, rrs (16S rDNA encoding gene) was used. Data analysis and calculation of normalized N-fold induction values from cycle amplification threshold (C_t) values were done as described by Kubista *et al.* 2006.

The mathematical model according to Pfaffl (2001) and Ståhlberg *et al*. (2005) was used to determine the expression ratio of two genes in three biological samples and two technical replicates. This quantification is also called comparative quantification (Pfaffl *et al*. 2002). One gene is the reporter whose expression is expected to be affected by the condition studied, (e.g. these six *At. caldus* genes mentioned above), and the other is a reference gene whose expression should be constant, here the 16S rDNA of *At. caldus*.

The relative expression of two genes in a same sample is given by Ståhlberg *et al.* (2005):

$$\frac{N_{\mathrm{x}}}{N_{\mathrm{y}}} = K_{RS}\,\frac{\eta_{\mathrm{y}}(1+E_{\mathrm{y}})^{\mathrm{CTy}-1}}{\eta_{\mathrm{x}}(1+E_{\mathrm{x}})^{\mathrm{CTx}-1}} \qquad \text{(Eq. 11)}$$

N_x and N_y are the numbers of mRNA molecules of the reference gene x (16S rRNA gene) and gene y (reporter gene e.g. *sor*), respectively, in the sample. K_{RS} is the relative sensitivity of the detection chemistries of the two assays (Ståhlberg *et al.*

2003), and η_A and η_B are the cDNA synthesis yields of gene x and gene y, respectively, defined as the fractions of mRNA molecules that are transcribed to cDNA in the RT reaction (Ståhlberg *et al.* 2004). The exponent C_T-1 accounts for the production of double stranded DNA in the first PCR cycle from the single stranded cDNA template generated by the reverse transcription reaction. η is assumed to be independent of both the total RNA and target mRNA concentrations. *E* is the PCR efficiency, which is calculated from the slope (k), estimated from a standard curve, as:

$$E = 10^{-\frac{1}{k}} - 1 \qquad \text{(Eq. 12)}$$

Assuming the same RT yields in the samples K_{RS} and η cancel and the comparative expression ratio of the two samples is given by:

$$\frac{\text{Sample A}}{\text{Sample B}} = \frac{\left[\frac{N_x}{N_y}\right]_{\text{Sample A}}}{\left[\frac{N_x}{N_y}\right]_{\text{Sample B}}} = \frac{\left[\frac{(1+E_y)^{CTy-1}}{(1+E_x)^{CTx-1}}\right]\text{Sample A}}{\left[\frac{(1+E_y)^{CTy-1}}{(1+E_x)^{CTx-1}}\right]\text{Sample B}} \qquad \text{(Eq. 13)}$$

Further assuming that the PCR efficiencies in the two samples are the same, the expression ratio simplifies to:

$$\frac{N_x}{N_y} = K_{RS}\,\frac{\eta_y(1+E_y)^{CTy-1}}{\eta_x(1+E_x)^{CTx-1}} \qquad \text{(Eq.14)}$$

3.3.8 **Purity test of bacterial strains and isolates**

To ensure that all strains and isolates were pure cultures, a PCR-mediated detection method (de Wulf-Durand *et al.* 1997) was applied. In brief, this is a PCR-based method with primers derived from 16S rRNA sequences for sensitive and specific detection of six groups (in this thesis only five groups were used) of microorganisms involved in the commercial bioleaching of mineral ores. Small-subunit rRNA genes were amplified by two-stage nested PCR. The annealing T° was modified (see Table 3A) and a PCR touch-down program was used, starting with 10°C above the actual annealing T° with a decrease of 1°C per cycle to this annealing temperature for further 20 cycles.

Furthermore, *At. caldus*-like isolates S1 and S2 were tested for archaeal contamination with a primer set according to Achenbach and Woese (1995).

Table 3: Primers used in this study

A: Primers with several usages

primer name	primer sequence 5'→ 3'	target gene	product size	annealing temp.	reference
16s_27fw	agagtttgatcctggctcag	16 S rDNA	~ 1.5 kb	58 °C	Brosius *et al.* 1978, Lane 1991
16s_1492rv	gcctaccttgttacgactt	Bacteria			
Arch25F	cyggttgatcctgccrg	16 S rDNA	~ 1.5 kb	52 °C	Achenbach and Woese 1995
Arch1492R	tacggytaccttgttacgactt	Archeae			
sorC1-F	gtiggiccnaargtntgy	*sor*	~ 230 bp	31 °C	Chen *et al.* 2007
sorH1-R	rtgcatntcytcrtgrtc				
bsor_1F	gtccttcgagaccatgatgmargtnggncc	bacterial *sor*	~ 800 bp	52 °C	this study
bsor_2R	ccgccactgggcctsytccatcatng				
PCJ2_for	caggcctcccagcaggtnggnccnaa	*sor*	840 bp	50 °C	this study
PCJ3_rev	ctcccgccatgaggtgtcctccatnayngg				
SULFO170F	caatcccgcatacgttcc	16 S rDNA	436 bp	52 °C	de Wulf-Durand *et al.* 1997
SULFO606R	aaaccgctacgtatcgcac	*Sulfobacillus* spp.			
CALD460F	atccgaatacggtctgcta	16 S rDNA	~ 1 kb	52 °C	de Wulf-Durand *et al.* 1997
CALD1475R	tataccgtggtcgtcgcc	*At. caldus*			
THIO458F	gggtgctaatawcgcctgctg	16 S rDNA	~ 1 kb	54 °C	de Wulf-Durand *et al.* 1997
THIO1473R	taccgtggtcatcgccct	*At. thiooxidans*			
LEPTO176F	cgaatagtatccggttccg	16 S rDNA	503 bp	52 °C	de Wulf-Durand *et al.* 1997
LEPTO679R	aaattccgcttccctctcc	*Leptospirillum* spp.			
FERRO458F	gggttctaatacaatctgct	16 S rDNA	~ 1 kb	50 °C	de Wulf-Durand *et al.* 1997
FERRO1473	taccgtggtaaccgccct	*At. ferrooxidans*			
T7	taatacgactcactataggg	promoter regions	x[1)]+ 158 bp	50 °C	Promega: pGEM®-T vector
SP6	atttaggtgacactatagaa	in pGEM®-T vector			

[1)]depending on amplicon size which should be cloned

B: Cotranscription primers

primer name	primer sequence 5'→ 3'	target region	product size	annealing temp.	reference
soxX_F	tattgcctttgatcgggaaa	1	474 bp	52°C	this study
soxYRv_cot	atacggggacgttgttcttg				
soxYFw_cot	gtgcctgtcaccatcgaaat	2	389 bp	54°C	this study
soxZRv_cot	ggagcggacttccaccat				
cotSoxZfor	cctacctggccttcaaga	3	485 bp	52°C	this study
cotSoxArev	ccagagctccttacccgta				
cotSOXAf	aggcgagacggcacatttc	4	546 bp	52 °C	this study
cotDUFr	cagcacgagattgcacactt				
DufFw_cot	cgagcaagagtccctacgtc	5	420 bp	54 °C	this study
SoxBRv_cot	aaggtcacgttgccatagtc				

C: Real-time PCR primers

primer name	primer sequence 5'→ 3'	target gene	product size	annealing temp.	reference
ACA_0303_F	ctacctggctcaaggagcac	*sqr_I*	173 bp	58 °C	this study
ACA_0303_R	ggtgatgcgggtaatgtctt	ACA_0303			
ACA_2845_F	tacttgccgtaggccatt	*sqr_II*	218 bp	58 °C	this study
ACA_2845_R	cgcaagggtatccacttcat	ACA_2845			
SoxB_F	gtataccggggagcagatca	*soxB_I*	198 bp	58 °C	this study
soxB_R	tatttcttcgtggcggaaac	ACA_2394			
SoxX_F	tattgcctttgatcgggaaa	*soxX_I*	236 bp	58 °C	this study
soxX_R	cctgctgcaattcttttggt	ACA_2389			
AcTS_Fw1	gtcaaatcgcacgaggaaat	*sor*	150 bp	59 °C	this study
AcTS_Rv1	gtccgtcatacccatgatcc	ACA_0302			
TTHf	tacgatgccatcaatctgga	*tth*	250 bp	61 °C	this study
TTHr	cccacgagttcccaagataa	ACA_1633			
Ac16S-fw	aggccttcgggttgtaaagt	16 S rDNA	196 bp	59 °C	this study
Ac16S-rv	atttcacggcagacgtaacc	ACA_1796			

3.3.9 **Cotranscription of putative *sox I* operon**

For testing cotranscription of the putative *sox I* operon, PCR was performed using 1 µL of 1:20 diluted cDNA from cells grown on S^0 at 45 °C. All PCR reactions were

performed in 40 cycles of: 30 s 95°C, 30 sat X °C (see Table 3B) and 45 s 72 °C. Control assays were performed with 20 ng of *At. caldus* genomic DNA.

3.3.10 **Electrophoresis**

PCR products were analyzed by agarose gelelectrophoresis in 1- 1.7% agarose gels in TAE buffer (20 mM Tris-acetate pH 8,0; 0,5 mM EDTA) at 100 V for 30-45 min (Amersham Biosciences, Electrophoresis power supply 301), depending on the expected size of the PCR product. Small fragments (<500 bp) need increased agarose concentrations and prolonged running times. The gels were stained for 20 min by incubation in 0.2 µg/mL ethidium bromide in TAE, washed in water and photographed using a Biorad® GelDoc™ station.

3.3.11 **Cloning**

Positive *sor* gene amplicons and amplicons of the purity test were cloned in *E. coli* before being sent for sequencing. Amplicons were cut out from the gel after electrophoresis and cleaned up using Wizard® SV Gel and PCR Clean-Up System (Promega®) following manufacture's protocol. Concentration and purity of cleaned amplicons were estimated using BioPhotometer plus (Eppendorf). Afterwards, PCR products were cloned using the pGEM®-T vector system from (Promega®) following the ligation protocol of the manufacturer in 10 µL reactions.

Heat-shock transformation

An overnight culture of *E. coli* DH5α in LB medium was prepared and 100 µL were transferred in 6 mL new LB medium and were grown at 37 °C to OD_{600} = 0.4. Cells were incubated 10 min on ice, then centrifuged at 2,655 x g for 7 min at 4 °C, resuspended in 250 µL ice cold $CaCl_2$- solution and afterwards centrifuged again at 2,655 x g for 5 min. Cells were resuspended in 100 µL $CaCl_2$-solution and incubated 30 min on ice for competence induction. Afterwards, the whole (10 µL) ligation mix was added to *E. coli* cells. One tube got 100 µL without ligation mix (negative control). After the incubation at 4 °C for 30 min, cells were heat shocked 2 min at 42 °C. After addition of 0.8 mL SOC medium, cells were grown for 1 h at 37 °C with 150 rpm shaking and afterwards plated on LB with Amp/ X-gal/ IPTG twin plates, which were incubated for 14-16 h at 37 °C.

Confirming positive clones

Plasmids containing an insert were isolated using Roti®-Prep Plasmid MINI (Carl Roth). Concentrations of plasmids were analyzed using a BioPhotometer plus (Eppendorf). The presence of an insert cloned on pGEM-T vector was confirmed by PCR using T7 and SP6 primers, adjacent to its cloning site.

Sequencing positive clones

Plasmids with a cloned insert were sent for sequencing to the "Zentraler DNA-Sequenzierservice" of the Medical Faculty of the Institute for Human Genetics, Universitätsklinikum Essen. For analysis of received sequences the BioEdit software (version 7.1.3) was applied.

3.3.12 **Protein extraction for proteome analysis**

For proteomic experiments, growth was done in DSM 71 medium with S^0 and thiosulfate as described with both media at pH 4.8 to avoid differences due to different starting pH. Pre-treatment of cells for inoculation of cultures was the same as for growth curves. Cultures were incubated at 45 °C with shaking at 180 rpm.
For each growth condition, cells were harvested, when a cell density of approx. 10^8 cells/mL was reached. After short spins to remove S^0 powder, cells were centrifuged at 10,000 x g for 10 min at 20 °C, resuspended and washed in diluted sterile sulfuric acid at pH 3. Cell pellets were finally resuspended in 1 mL RNA-Later. After lysis and first acid phenol (Sigma) extraction, proteins were recovered from the phenolic phase. They were washed with one volume of nanopure water and incubated at 70 °C for 10 min with vortexing each 2 min. Afterwards, samples were cooled 10 min on ice and centrifuged at 2,655 x g for 10 min at 4 °C. The aqueous phase was discarded. Proteins were precipitated from the phenol phase by adding 1.5 volumes of ice-cold acetone. Samples were mixed and incubated at -20 °C overnight. Afterwards, protein pellets were collected by centrifugation at 2,655 x g for 10 min at 4 °C and washed twice with acetone. Again samples were centrifuged at 2,655 x g for 10 min, acetone was discarded and pellets were dried for 20 min at 25°C. Dry protein pellets were stored at -20 °C.

3.3.13 **SDS-PAGE**

SDS-PAGE was done according to Laemmli (1970). Briefly, proteins were dissolved in sample buffer (Tris-HCl 187 mM pH 6.8; SDS 6 % p/v; glycerine 30 % v/v; 2-

mercaptoethanol 15 % v/v; bromophenol blue 0.06 % p/v) and boiled for 10 min. Electrophoresis was performed in 12.5 % polyacrylamide gels with the BioRad® Mini PROTEAN® Tetra System at a constant voltage of 200 V for 45 min. To determine the protein amount to be loaded, a test gel was run with different amounts of sample for a short time and evaluated. Gels were stained for 15 min in staining solution containing 10 % Brilliant Blue R (Sigma-Aldrich), 50 % methanol, 7 % glacial acetic acid and 43 % nanopure water and afterwards they were destained in a solution containing 25 % methanol, 7.5 % glacial acetic acid and 67.5 % nanopure water.

3.3.14 **High throughput proteomic analyses**

MS analyses were done in the laboratory of Dr. Ansgar Poetsch, Ruhr University Bochum. Preparation of gel lanes and the high throughput analyses were done according to Vera *et al.* 2013. All database searches were performed using SEQUEST algorithm, embedded in BioworksTM (Rev. 3.3.1, Thermo Electron © 1998-2006), with an *At. caldus* DSM 8584^T database containing 2878 sequences. For protein identification, a threshold for both protein and peptide probability was set to 0.001 and at least two different peptides per protein were required.

3.3.15 **Protein quantification**

The protein quantifications were analysed according to Vera *et al*. 2013 with the following modifications: When a certain protein was found to be present in only 3 out of the 4 samples, the missing fourth value was replaced by the mean of log2 values from these 3 samples. Proteins identified in less than 3 samples were excluded from further quantitative analysis. A Student's t-test (n = 4) was performed and proteins had to fulfill the following criteria to be regarded as differentially expressed: if log2 (normalized spectral count) ratio was greater than 1,5 for a protein, this protein was considered to be induced in sulfur. When log2 ratio was less than −1.5, the protein was considered to be induced in thiosulfate. Additionally, *p*-values were accepted to be < 0.05. In addition, strong expression changes (absolute log2 ratio of ≥ 1.5) were included in tables with *p*-values between 0.05 and 0.1. Tables were constructed with *At. caldus* gene annotation (www.ncbi.nlm.nih.gov).

3.3.16 **Bioinformatic analyses**

Gene sequences were analyzed using database from National Center for Biotechnology Information (NCBI) (www.ncbi.nlm.nih.gov), the Kyoto Encyclopedia of

Genes and Genomes (KEGG) (www.genome.jp/kegg/) and the BLAST server on DOE joint genome institute (JGI) (www.jgi.doe.gov/). The searches for homologues genes and proteins were done with BLASTn (nucleotide blast) and BLASTp (protein blast) programs within those three databases. To compare gene or protein sequences, multiple sequence alignments with ClustalW (www.ebi.ac.uk/Tools/msa/clustalw2/) were done (Higgins *et al.* 1994). For phylogentical classification, the COGnitor (Cluster of Orthologpus Groups of proteins) software was used. This software also allows prediction of some protein functions by homology comparison. (e.g. www.ncbi.nlm.nih.gov/COG/old/xognitor.html) (Tatusov *et al.* 2000). For further protein analyses the data base of European Bioinformatics Institute (www.ebi.ac.uk) was used.

3.3.17 **Cell harvest and preparation of cell-free extract**

The cultures were analyzed under the microscope for high cell density (≥ 2 x 10^8 cells/mL). In addition the pH was measured. A pH around 1 indicates S^0 oxidation (production of sulfuric acid). Cell harvest was done at 8,671 x g (Thermo scientific sorvall RC 6+ cetrifuge equipped with rotor F10S-6x500y Fiber Lite®) (Pirmoon Technologies Inc.). The volume was reduced to 300 mL. Afterwards, S^0 was removed by short spin centrifugation at 1,500 x g and finally cells were pelleted again at 11,270 x g. Cells were washed twice with washing solution (pH 3) according to Rohwerder and Sand (2003). According to pellet weight (pellet yield between 2 g and 7 g), cells were resuspended 1/10 (w/v) in Tris-HCl (100 mM) pH (6.5 - 8.5) according to the pH of the following enzyme assay. Cells were broken using a French®Press (Thermo electron corporation; French Pressure cell Press) in 4 passages of 10-15 mL units. Crude extracts were then divided in 2 mL units and centrifuged at 20,817 x g for 20 min at 4 °C. Supernatants were combined and protein concentrations were measured.

3.3.18 **Protein determination according to Bradford**

For determining the protein concentration of the crude cell-free extract, the photometric determination after Bradford (1976) was applied. Calibration was prepared with BSA solutions (0, 20, 50, 80 and 100 g/L).

3.3.19 **Enzyme assays**

Previous analyses of Sor showed no dependency on external thiol groups. Consequently, enzyme activity without glutathione (GSH) should indicate Sor reactions. Cell-free extracts of the moderately thermophilic sulfur-oxidizing bacteria and the thermophilic archaeon *S. metallicus* were tested for Sdo activity according to the assay by Suzuki (1965) modified by Rohwerder and Sand (2003). All assays were performed aerobically at 30 °C, 45 °C and 65°C for the *At. caldus* strains and the type strain of *S. metallicus,* and at 45 °C and 65 °C-80 °C in 5 °C steps for *Sb. thermosulfidooxidans*. If the enzyme activity is only detected after GSH addition, this might indicate Sdo presence.

The reaction mixtures contained protein at approx. 1 mg protein in 5 mL of 100 mM Tris-HCl buffer at several pH, 20 mL dispersed S^0 in water according to Rohwerder and Sand (2003) and 0.4 mM GSH-solution, the latter is applied for Sdo enzyme assays. Consequently, Sor was tested always with approx. 40 mg/L protein reacting with approx. 16-17 mM S^0 in the reaction mixture. For Sdo approx. 38 mg/L protein reacted with 16 mM S^0 and 0.4 mM GSH (Fig. 7).

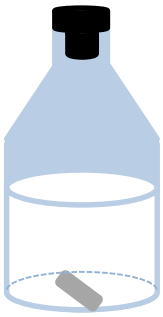

Sor

5 mL protein (~1 mg)/ Tris-HCl
20 mL dispered S^0 in water (20 mM)

25 mL total volume

Sdo

5 mL protein (~1 mg)/ Tris-HCl
20 mL dispered S^0 in water (20 mM)
1.25 mL GSH (10 mM)

26.25 mL total volume

Fig.7: Preparation of Sor and Sdo enzyme assays
S^0 has been diluted in aceton and afterwards dialyzed in water over night. The S^0/ protein mixture was added in serum flasks and heated to several assay temperatures. Finally approx. 40 mg/L protein reacts with approx. 16 mM dialysed S^0 (plus 400 µM GSH for Sdo).

At first, 20 mL dispersed S^0 was added to a 50 mL serum flask (Supelco Vials, crimp top, serum bottle; O.D. × H 43 mm × 73 mm; Sigma-Aldrich), then protein/ buffer mix was added and finally for Sdo activity tests GSH was added. Air was flushed through flasks, which were then closed with rubber lids (Butyl septum for neck N2; Ochs GmbH) to avoid H_2S loss. Bottles were heated in a water bath to several temperatures (see Table 4) and stirred at 180 rpm. 1.5 mL samples were taken after 1 min, 5 to 30 min (in 5 min intervals) and 40 min with a syringe. Samples were

filtered with Nylon Filters (Rotilabo®-Spritzenfilter 0.45 µm, Nylon, unsterile; Roth) prior to process them for ion-exchange chromatography.

For the determination of sulfide, 200 µL samples were fixed in 200 µL 2 % Zn-acetate at the same collection times.

Table 4: Sor and Sdo enzyme activity tests

A) Sor enzyme activity test

strain	Enzyme assay T°
At. caldus strains and isolates	30 °C, 45 °C, 65 °C
S. metallicus DSM 6482^T	30 °C, 45 °C, 65 °C
Sb. thermosulfidooxidans DSM 9232^T	45 °C, 65 °C – 80 °C in 5 °C steps

B) Sdo enzyme activity test

strain	Enzyme assay T°
At. caldus strains and isolates	30 °C, 45 °C, 65 °C
S. metallicus DSM 6482^T	30 °C, 45 °C, 65 °C
Sb. thermosulfidooxidans DSM 9232^T	45 °C, 65 °C, 70 °C

The pH-optimum values for *Sb. thermosulfidooxidans* Sor activity were determined in a range between pH 6.5 – 8.5 (in 0.5 pH steps) at 75°C.

The sum of sulfite, sulfate and thiosulfate as equivalent for enzyme activity was quantified by ion-exchange chromatography according to Weiß (1991). The specific activities were calculated from the linear increase of the reaction products. One Unit (U) of enzyme activity was defined as 1 µmol of formed sulfite, sulfate and thiosulfate (oxygenase) or hydrogen sulfide (reductase) per minute.

To determine non-enzymatic reactions, assays with 40 mg/L BSA at all temperatures were performed.

3.3.20 **Determination of S^0 and tetrathionate**

S^0 was extracted in three steps from a 1 mL culture. Samples were centrifuged at 10,000 x g for 8 min. Cell pellets were resuspended in 96% ethanol and sonified for 10 min (Bandelin Sonorex digitec). Afterwards, samples were vortexted for 15 min and centrifuged again, as described above. This supernatant is the first S^0 extraction of a sample. The sum of 3 extractions gives the concentration of S^0 in the culture. To determine tetrathionate, 1 mL samples were centrifuged at 10,000 x g for 5 min and supernatants were diluted 1:100 for measurements.

A HPLC system from Kontron/BIO-TEK Instruments was used, consisting of a pump (422), a gradient former (425), an autosampler (465), a diode array detector (440) and software 450-MT2/DAD. To determine S^0 a guard column cartridge (VA 5/3

Nucleogel RP and a separation column (EC 125/4 Nucleodur 100-5 C18 EC) with a mobile phase of methanol 1.2 mL/min were used. Data were logged for each measurement for a period of 5 min. Chromatograms were recorded at 254 nm per time.

For tetrathionate determination the same guard column cartridge and a separation column (VA 150/4.6 Nucleogel RP 100-8) were used. The mobile phase consisted of a 25 % acetonitrile-water mixture (v/v) including 2 mM Tetrabutylammonium at pH 7.7. Flowrate was 1 mL/ min, data were logged for each measurement for a period of 10 min. Chromatograms were recorded at 215 nm per time.

3.3.21 **Determination of thiosulfate, sulfite and sulfate**

Thiosulfate, sulfite and sulfate were quantified by ion-exchange chromatography and conductivity detection as described by Schippers and Jørgensen (2002). The DIONEX system DX 500 with an AS3500 autosampler, ASRD ULTRA II 2 mm surpressor, conductivity detector CD20, gradient generator EG 50 in combination with the EluGen cartridge EGC II KOH, guard column AG17C 2 x 50 mm and separation column AS17C 2 x 250 mm were used. The chromatogram was processed with Chromeleon 6.70 Build 1820 software. A KOH gradient was applied starting with 10 mM for 1 min following a linear increase over 4.5 min to 50 mM. Afterwards, the concentration declined over 1 min to 10 mM and retained for an additional minute before the next measurement. Flowrate was 0.36 mL/ min. Standards of thiosulfate, sulfite and sulfate were prepared as aqueous stock solutions of potassium or sodium salts.

3.3.22 **Determination of sulfide**

Dissolved sulfide was determined using the methylene-blue-method of Deutsche Einheitsverfahren (DEV) DIN 38 405 Teil 26 (DEV 1989), direct determination, with Dimethylene-p-phenylendiamine solution: 0.2 % dimethylene-p-phenylendiamine in 3.6 M sulfuric acid and ferric iron solution: 1 % solution of ammoniumiron(III)sulfate in 0.36 M sulfuric acid. The determination is based on the reaction of sulfide with dimethylene-p-phenylendiamine to leucomethylene-blue, which oxidizes in the presence of ferric iron ions to methylene-blue. After 10 min incubation, the determination was done photometrically with LKB Biochrom Novaspec 4049 Spectro-

photometer at 670 nm. Calibration was done with sodium sulfide in 2 % zinc-acetate from 0 up to 25 µM (in 5 µM steps).

4 RESULTS

4.1 Growth of *At. caldus* with several RISCs at different temperatures

4.1.1 *At. caldus* growth at 30 °C

The following figures (Fig. 8-12) show the growth behavior, pH evolution and the concentration of tetrathionate, thiosulfate, sulfate and S^0 in the *At. caldus* cultures at 30 °C.

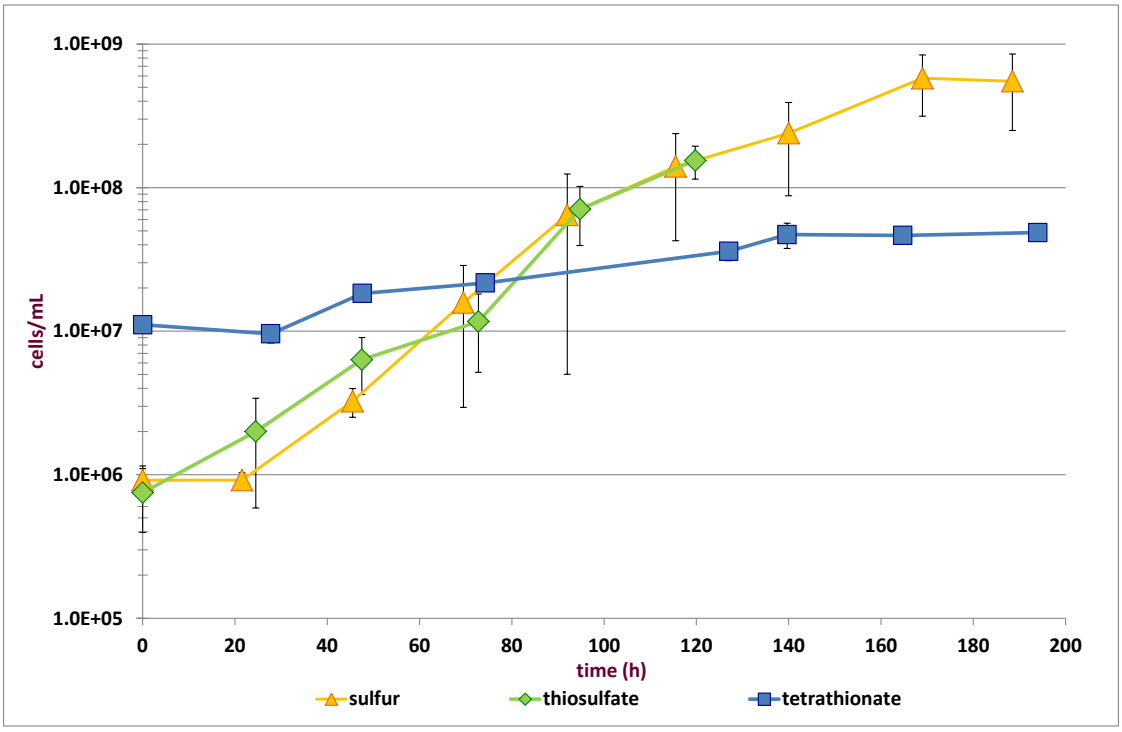

Fig. 8: *At. caldus* growth on different RISC's at 30°C
At. caldus cultures were grown at 30°C in standard S^0, thiosulfate or in tetrathionate medium. TCC were measured daily. Standard deviations are given from triplicates.

The best RISC sources for growing *At. caldus* at 30 °C were S^0 and thiosulfate. No significant differences were observed between them in the growth behavior. Both started with an inoculum of approx. $1x10^6$ cells/mL and grew over 120 h (5 days) to a concentration of $2x10^8$ cells/mL. This means, after inoculation the cells divided approx. 8 times. In contrast to this, tetrathionate grown cells showed only slight growth. After a lag phase of approx. one day, they started slowly to grow. The cell inoculum of these cultures were $1x10^7$ cells/mL and after 140 h (~ 6 days), the cell concentration reached only $4.7x10^7$, meaning these cells only divided twice.

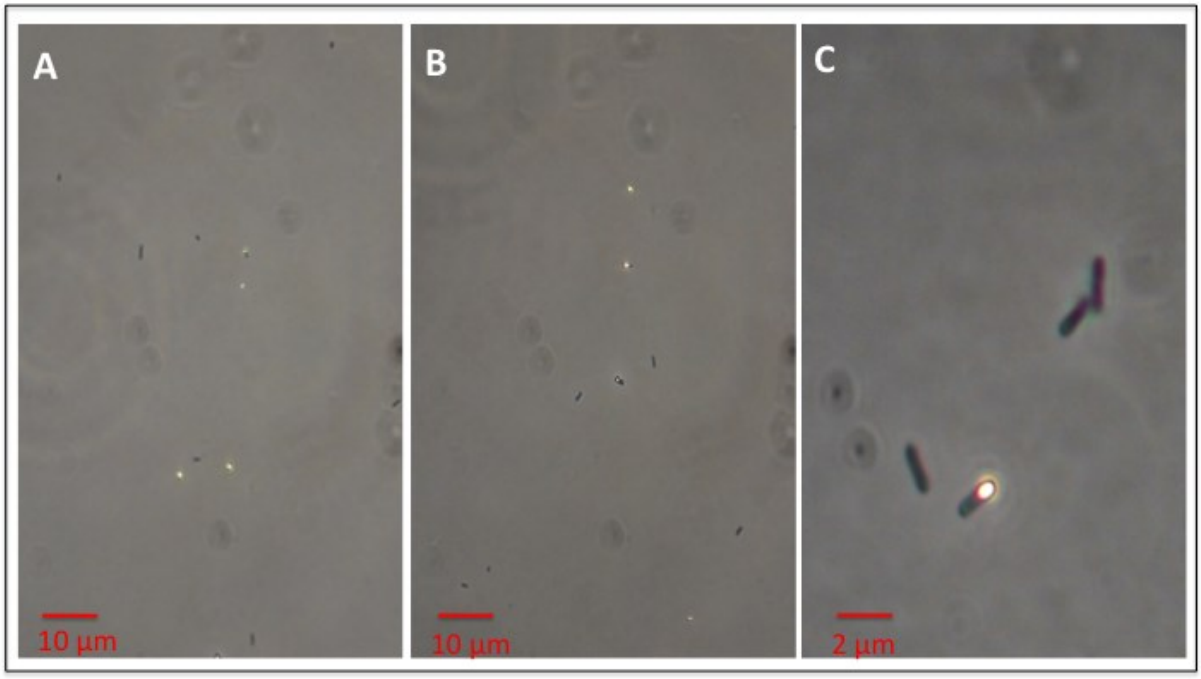

Fig. 9. Light-microscopy of *At. caldus* grown on tetrathionate medium at 30 °C, day 6.
A) and **B)** are representative fields at 400x magnification, showing *At. caldus* cells with S^0 globules (bright body), spread in the whole culture. **C)** *At. caldus* cells at 400x magnification + 5x digital zoom.

In thiosulfate grown cultures at 30 °C between day 3 and 4, approx. 10 % of *At. caldus* cells showed S^0 globules. The culture media were milky turbid. Between day 5 and 6, S^0 globules disappeared. The same was observed in tetrathionate grown cultures, however S^0 globules appeared between day 5 and 6. Also here S^0 globules disappeared two days later.

In thiosulfate cultures grown at 45 °C the presence of S^0 globules was observed at day 2. At day 4 they disappeared. In tetrathionate cultures at 45 °C no S^0 globules were observed at any time.

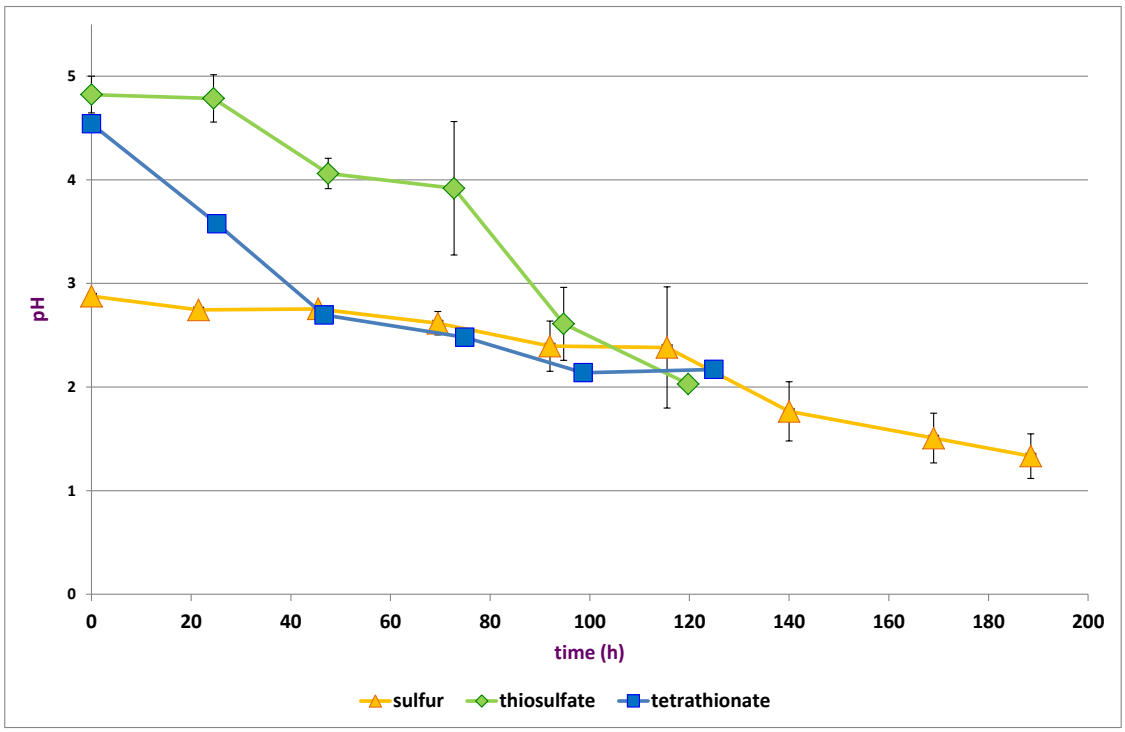

Fig. 10: pH during *At. caldus* growth at 30 °C on different RISC's.
At. caldus cultures were grown at 30°C in standard S^0, thiosulfate or tetrathionate supplemented medium and pH values were measured daily. Standard deviations are given from these triplicates.

The starting pH of S^0 cultures was approx. 3. It decreased constantly over 188 h (~ 8 days). This is in agreement with the growth curve of S^0 cultures. The pH in thiosulfate cultures decreased fast and reached after 5 days a pH of 2, while the tetrathionate cultures started at pH 4.5 and decreased within 2 days to pH 2.7. Afterwards, pH decreased slowly and reached 1.9 after 8 days.

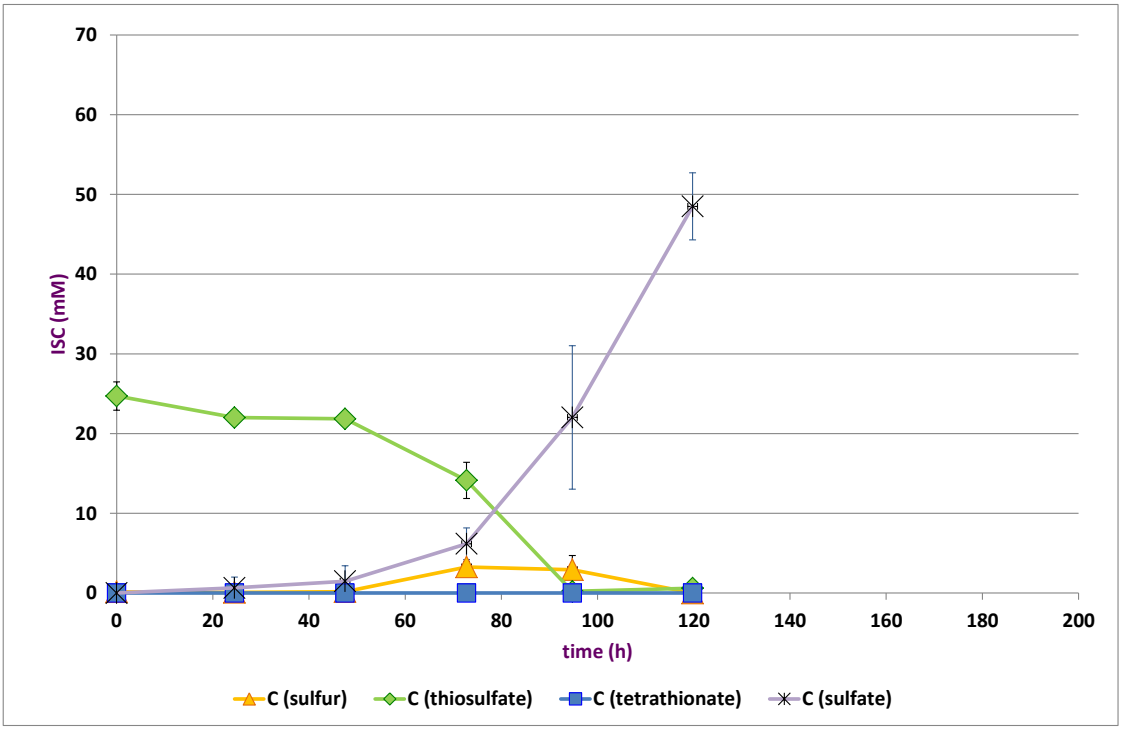

Fig. 11: ISC concentrations during growth of *At. caldus* on thiosulfate at 30 °C.
At. caldus cultures were grown as described. S^0, tetrathionate, thiosulfate and sulfate concentrations were determined daily from the supernatants of cultures as described. ISC concentrations were measured daily. Standard deviations are given from triplicates.

Thiosulfate cultures had an average of 24 mM thiosulfate as start concentration. It was consumed within less than 100 h (~ 4 days). During growth, the apparance of S^0 was observed and a maximum concentration of 3.3 mM after 3 days was measured. After 5 days no S^0 was detected. Concomitantly, 48 mM sulfate was measured after 5 days. Thus, all thiosulfate was converted. Tetrathionate was not detected at any time.

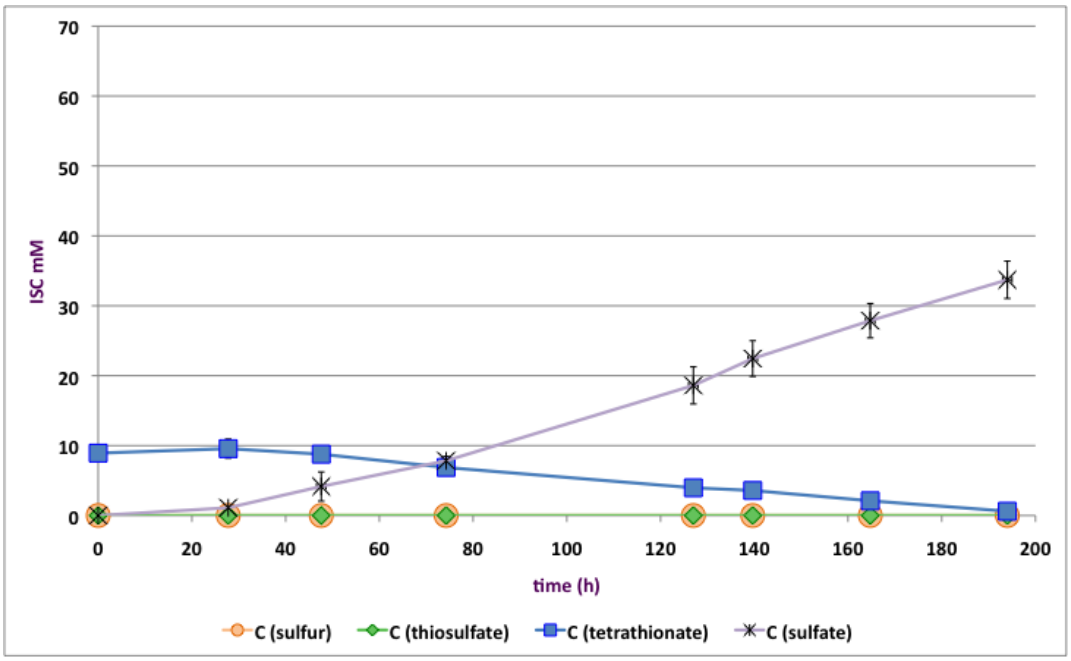

Fig. 12: **ISC concentrations during growth of *At. caldus* on tetrathionate at 30 °C.**
At. caldus cultures were grown as described. S^0, tetrathionate, thiosulfate and sulfate concentrations were determined daily from the supernatants of cultures as described. Standard deviations are given from triplicates.

Measurements showed that during growth of *At. caldus* tetrathionate consumption is slow. 1 mol tetrathionate can be converted to 4 mol sulfate. The cultures started with 9 mM tetrathionate and after 8 days it was fully converted to 34 mM sulfate, which was also almost the case here. During this growth neither S^0 nor thiosulfate could be detected in the culture medium.

4.1.2 *At. caldus* growth at 45 °C

The following figures (Fig. 13-16) show the growth characteristics pH and the concentration of ISCs in *At. caldus* cultures at 45 °C. Cells were grown with S^0, thiosulfate or tetrathionate as described. Additionally, the growth of *At. caldus* in DSM 71 medium with S^0 is shown. This medium was used for *At. caldus* cultivation for the proteomic analyses (Section 4.4). The main differences between the standard S^0 medium and DSM 71 medium is the start pH 4.8 and the increased buffering capacity of the latter at this pH.

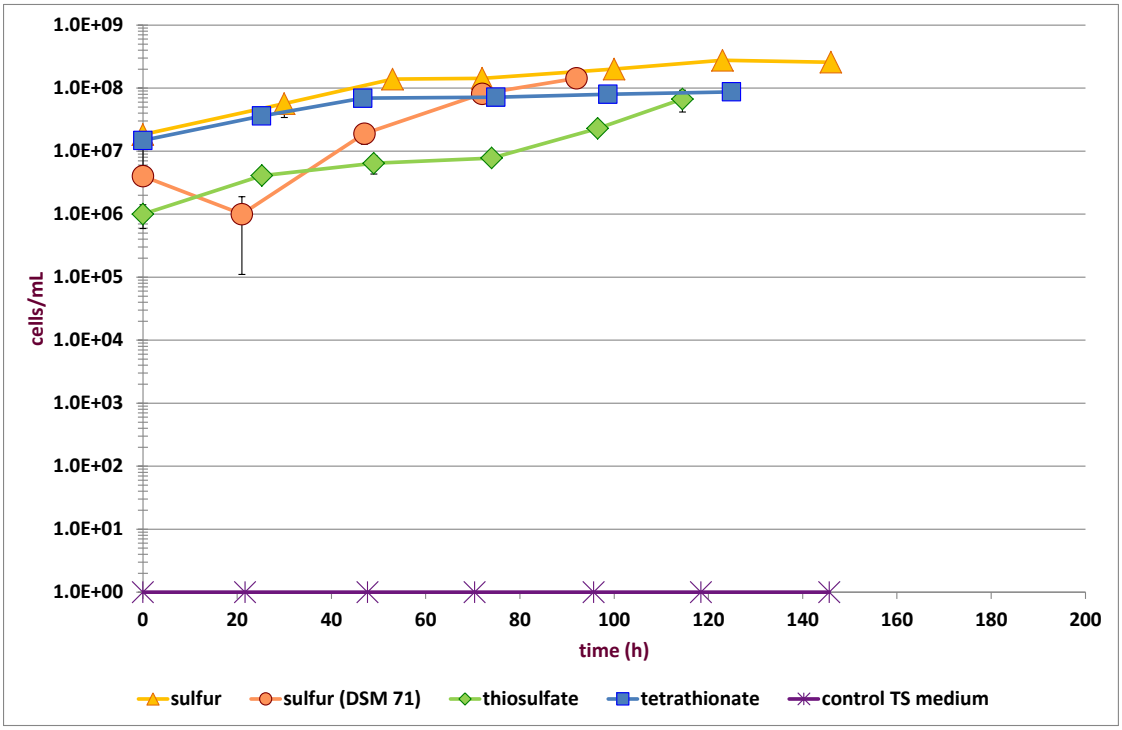

Fig. 13: *At. caldus* growth on different RISC's at 45 °C.
At. caldus cultures were grown at 45°C in standard S^0 medium, DSM 71 medium with S^0 or thiosulfate and in tetrathionate medium as described. Uninoculated control flasks of DSM 71 with thiosulfate were also incubated. TCC were measured daily and the standard deviations are given from triplicates.

At. caldus inocula for standard S^0 medium and tetrathionate medium were $1.2x10^7$ cells/mL. Within 120 h (~ 5 days) cell growth in S^0 medium reached $2.3x10^8$ cells/mL, the cells divided approx. 4 times. With tetrathionate the cells grew less, just reaching $8.7x10^7$ cells/mL during the same time period, they divided approx 3 times. Cells for thiosulfate cultures were inoculated in concentrations of $1x10^6$ cells/mL to minimize a pH drop in the cultures, which could lead to thiosulfate disproportionation and therefore S^0 production. Cells grown in DSM 71 medium with S^0 were grown for proteomic analysis to avoid differences in the proteomes due to different basal medium and starting pH. Afterwards, cell growth constantly increased and reached approx. the same cell density as in S^0 grown cultures. No growth was observed in control flask of DSM 71 with thiosulfate.

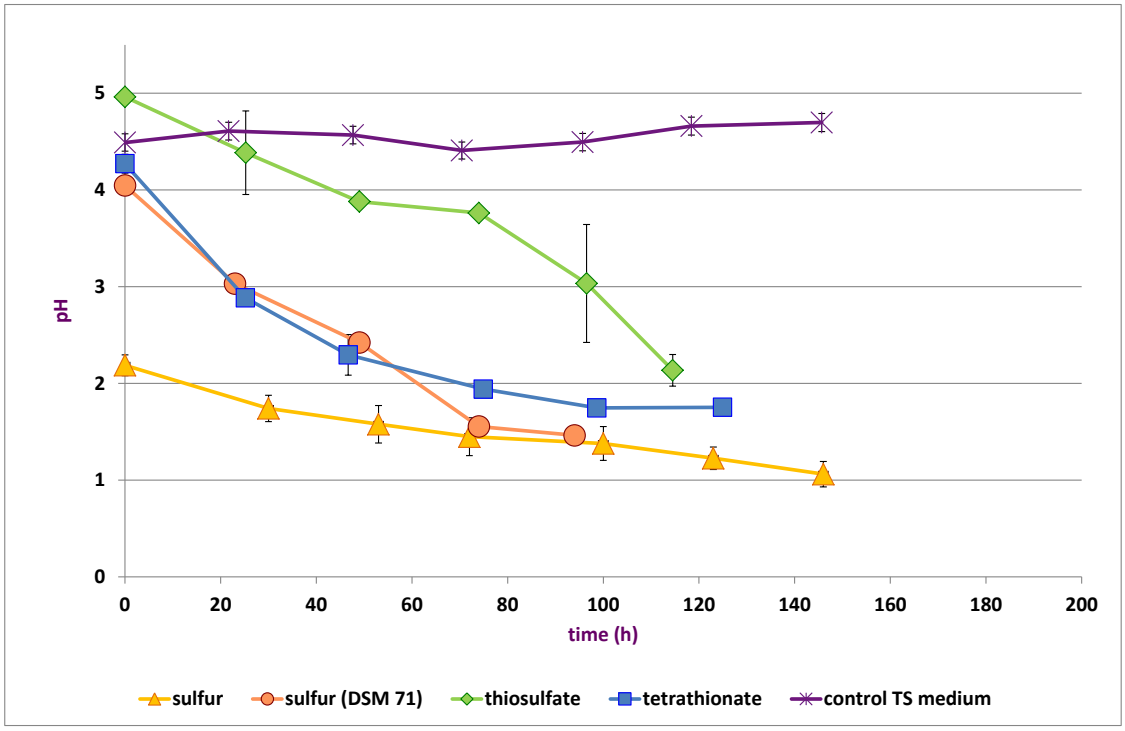

Fig. 14: pH during *At. caldus* growth at 45 °C on different RISC's.
At. caldus cultures were grown at 45 °C in standard S^0 medium, in DSM 71 medium with S^0 or thiosulfate and in tetrathionate medium. Control flasks of DSM71 with thiosulfate were also incubated and pH values were measured daily. The standard deviations are given from triplicates.

The pH values of control assays stayed stable over 145 h (~6 days) at around 4.6. All other pH decreased constantly during growth in the cultures. In cultures of standard S^0 medium pH started at 2.2 and reached after 6 days a value of 1.2. The pH of DSM 71 with S^0 decreased fast, started with pH 4 and reached after 94 h (~ 4 days) pH 1.5. In thiosulfate cultures, the pH started with 5 and decreased in the total time of almost 5 days to pH 2.1. In tetrathionate cultures pH decreased fast over the first 2 days and afterwards slowly to reach after 5 days 1.8.

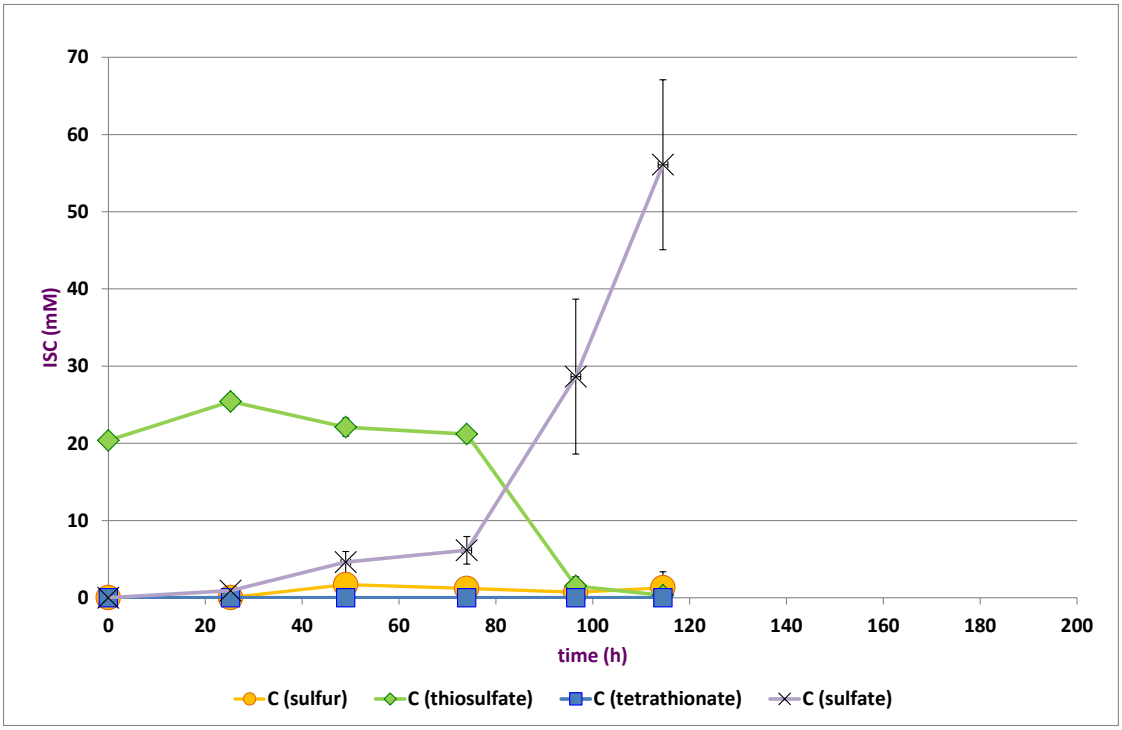

Fig. 15: ISC concentrations during growth of *At. caldus* on thiosulfate at 45 °C.
At. caldus cultures were grown at 45 °C in thiosulfate medium. ISC concentrations were determined daily from supernatants of cultures. Standard deviations are given froms triplicates.

Thiosulfate cultures at 45 °C had an average of 21 mM thiosulfate as starting concentration. It was consumed within less than 100 h. During growth, S^0 was observed and a maximum concentration of 1.7 mM after 2 days could be measured. After almost 5 days still 1.2 mM S^0 was measured. Furthermore, after this time an average of 56 mM sulfate was measured in the supernatant of the cultures. Thiosulfate was fully converted within the incubation time. Start sulfate concentrations were subtracted from all sulfate concentrations. Tetrathionate could not be detected at any time.

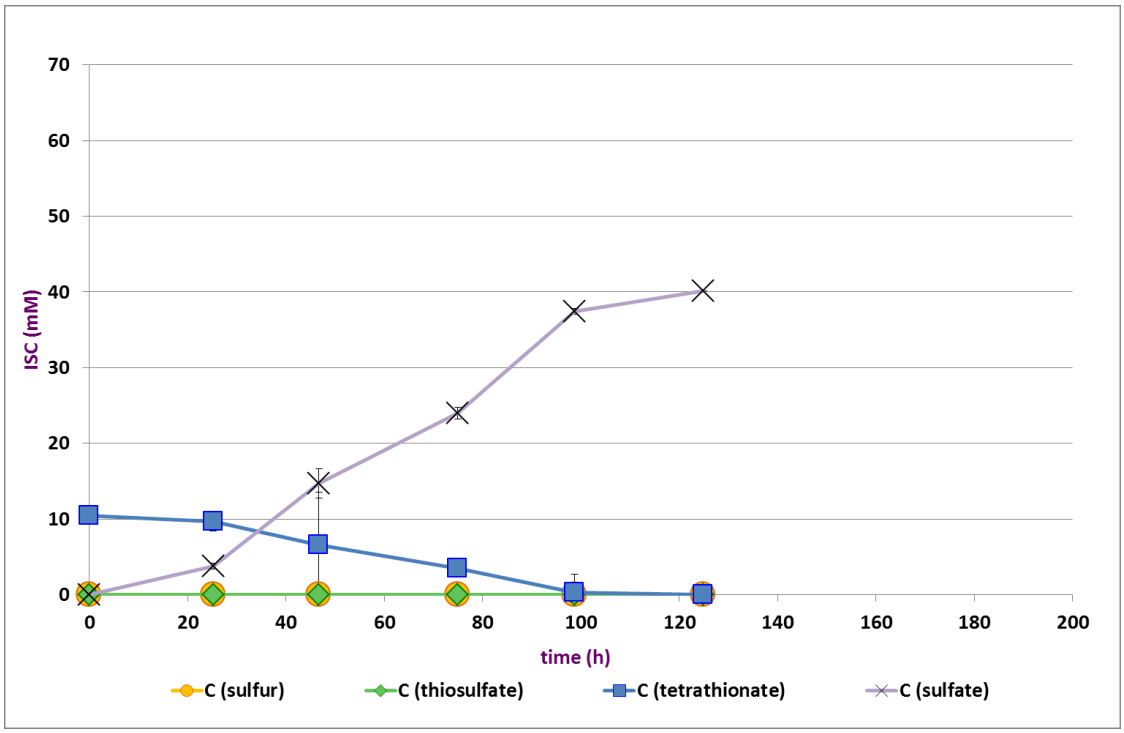

Fig. 16: ISC concentrations during growth of *At. caldus* on tetrathionate at 45 °C.
At. caldus cultures were grown at 45 °C in tetrathionate medium. ISC concentrations were determined daily from supernatants of cultures. Standard deviations are given from triplicates.

Tetrathionate concentration in culture supernatants started with an average of 10.45 mM and within the first day this concentration decreased very slowly. Afterwards, there was an accelerated decrease and in the final 99 h (~ 4 days) tetrathionate was completely converted to an average of 40 mM sulfate in the medium. Tetrathionate and S^0 were not detected in these cultures.

During incubation of three control flasks of thiosulfate medium at 45 °C, the thiosulfate concentration stayed constant at around 24 mM. Standard deviations of thiosulfate and sulfate were very low. Neither S^0 nor tetrathionate could be detected in the medium.

4.2 Expression levels of genes involved in sulfur metabolism of *At. caldus*

The expression levels of six genes, *sor* (ACA_0302), *soxB* (ACA_2394), *soxX* (ACA_2389), *sqr_I* (ACA_0303), *sqr_II* (ACA_2485) and *tth* (ACA_1633), depending on the substrate (S^0, thiosulfate or tetrathionate) and growth T° (30 °C, 45 °C and 50 °C) were measured in order to find out if there is a differential regulation dependent on these factors. Results are shown in Tables 7-12.

All standard curves had a high correlation coefficient, similar amplification efficiency, and a similar slope (Table 5). These values represent a good calibration of the PCRs and the sensitivity of the primers used for amplification of the specific genes at the annealing temperatures given in Table 3C.

Table 5: Efficiency and sensitivity of the designed primers used at the corresponding annealing temperature in the real-time PCR assays

Target gene	Correlation coefficient	Amplification efficiency	Slope
sor	1	99.0 %	-3.342
soxB	0.995	98.0 %	-3.372
soxX	0.998	114.4 %	-3.019
sqr_I	0.967	92.5 %	-3.515
sqr_II	0.995	86.7 %	-3.687
tth	0.977	128 %	-2.794

Table 6 shows the mean amplification threshold (C_T) values (three biological replicates, measured twice) of each gene and the corresponding copy N^o of these genes. The values were normalized to the 16S rDNA values.

Table 6: Amplication threshold (C_T) mean values and copy numbers of target genes in *At. caldus* samples grown in three different RISCs at three growth temperatures.

Gene	Sulfur						Thiosulfate				Tetrathionate			
	30°C		45°C		50°C		30°C		45°C		30°C		45°C	
	C_T (mean)	copy no.	C_T(mean)	copy no.	C_T(mean)	copy no.	C_T (mean)	copy no.	C_T (mean)	copy no.	C_T (mean)	copy no.	C_T (mean)	copy no.
sor	25.81	1.77E+03	28.09	3.68E+02	25.37	2.40E+03	27.74	4.71E+02	26.27	1.29E+03	27.94	4.08E+02	29.14	1.79E+02
soxB	27.12	1.40E+03	29.14	3.52E+02	26.88	1.65E+03	26.44	2.23E+03	29.47	2.82E+02	31.46	7.26E+01	25.60	3.97E+03
soxX	25.99	1.42E+03	28.11	1.50E+03	26.96	3.30E+03	23.40	1.02E+04	26.42	1.02E+03	31.02	3.05E+01	23.42	1.01E+04
sqr_I	21.41	2.36E+04	24.44	3.25E+03	21.89	1.73E+04	22.97	8.54E+03	24.70	2.74E+03	23.40	6.44E+03	24.77	2.63E+03
sqr_II	26.60	2.51E+03	27.05	1.90E+03	25.91	3.89E+03	24.74	8.04E+03	26.34	2.97E+03	28.37	8.36E+02	23.76	1.48E+04
tth	30.22	1.78E+03	29.77	2.57E+03	26.70	3.25E+04	23.66	3.97E+05	25.90	6.24E+04	28.19	9.49E+03	25.56	8.28E+04

It can be observed that cells grown on tetrathionate at 30°C have low copy number of all analyzed genes. The highest copy N^o in all samples was measured for *sqr_I* gene.

All results are mean values given from at least two samples measured three times. The SD values did not exceed 10 %. Only the *tth* SD values of the thiosulfate grown samples at 30 °C, were higher with 18 %.

The comparative quantification of *sor* gene expression levels when *At. caldus* grows on tetrathionate at 45°C is shown in Table 7. Comparing this sample (Sample A) with all other samples (Samples B), all samples B are up-regulated. Consequently, *sor* was down-regulated on tetrathionate at 45°C. In general, values ≥ 3 shows an induction under the compared conditions.

The following Tables 7-12 show the expression levels of *sor, soxB, soxX, sqr_I, sqr_II and tth* at the compared growth temperature and RISCs.

Table 7: Expression levels of ***sor*** in *At. caldus* grown on three different RISCs at three different growth temperatures, harvest in late exponatial growth phase. The values are normalized to the corresponding 16S rDNA expression.

B / A		sulfur			thiosulfate		tetrathionate	
		30 °C	45 °C	50 °C	30 °C	45 °C	30 °C	45 °C
sulfur	30 °C	1.0	0.4	1.1	0.4	1.3	1.2	0.1
	45 °C	6.0	1.0	4.2	1.0	3.3	4.1	0.3
	50 °C	2.0	0.4	1.0	0.3	1.1	1.1	0.1
thiosulfate	30 °C	7.6	3.5	1.4	1.0	4.2	4.1	0.3
	45 °C	1.6	0.2	0.8	0.3	1.0	0.9	0.1
tetrathionate	30 °C	2.1	0.2	0.8	0.4	1.2	1.0	0.1
	45 °C	31.3	5.7	21.6	5.4	17.2	16.8	1.0

The *sor* gene expression was up-regulated in *At. caldus* grown on S^0 at 30 °C compared to all other samples. It was also found to be up-regulated at 50 °C on S^0 compared to cells grown on S^0 at 45 °C. Furthermore, *sor* was down-regulated in cells grown on tetrathionate at 45 °C.

Table 8: Expression levels of ***soxB*** in *At. caldus* grown on three different RISCs at three different growth temperatures, harvest in late exponatial growth phase. The valuesa are normalized to the corresponding 16S rDNA expression.

B / A		sulfur			thiosulfate		tetrathionate	
		30 °C	45 °C	50 °C	30 °C	45 °C	30 °C	45 °C
sulfur	30 °C	1.0	0.6	0.9	2.2	1.2	0.2	2.9
	45 °C	3.0	1.0	11.2	9.3	5.1	1.1	3.3
	50 °C	0.9	0.3	1.0	2.2	1.2	0.2	2.9
thiosulfate	30 °C	0.9	0.3	0.4	1.0	0.6	0.1	0.6
	45 °C	3.2	0.5	1.6	3.7	1.0	0.4	5.0
tetrathionate	30 °C	11.2	1.2	3.9	9.0	4.9	1.0	5.5
	45 °C	0.3	0.1	0.5	1.1	0.6	0.1	1.0

In tetrathionate grown cells at 30 °C and S^0 grown ones at 45°C *soxB* was down-regulated. Levels of *soxB* were up-regulated in cells grown on thiosulfate at 30 °C compared to cells grown on S^0 at 45 °C and 50 °C and also compared to cells grown on thiosulfate at 45 °C and tetrathionate at 30 °C.

Table 9: Expression levels of ***soxX*** in *At. caldus* grown on three different RISCs at three different growth temperatures, harvest in late exponatial growth phase. The values are normalized to the corresponding 16S rDNA expression.

B / A		sulfur			thiosulfate		tetrathionate	
		30 °C	45 °C	50 °C	30 °C	45 °C	30 °C	45 °C
sulfur	30 °C	1.0	0.6	0.4	10.2	5.2	0.3	5.5
	45 °C	23.5	1.0	4.7	23.6	19.5	0.8	18.0
	50 °C	11.7	0.8	1.0	13.1	6.6	0.4	7.1
thiosulfate	30 °C	0.6	0.1	0.2	1.0	0.5	0.0	0.6
	45 °C	0.4	0.3	0.8	4.3	1.0	0.1	2.3
tetrathionate	30 °C	39.0	3.8	2.3	65.0	33.0	1.0	35.2
	45 °C	1.2	0.1	0.4	2.1	1.0	0.1	1.0

The transcript levels of *soxX* were found to be highly up-regulated in thiosulfate grown *At. caldus*, where an even enhanced expression level was measured for cells grown at 30 °C compared to 45 °C. In comparison of all S^0 grown samples an

enhanced expression level was measured for cells grown at 30 °C. Additionally, this gene was down- regulated in cells grown on tetrathionate at 30 °C.

Table 10: Expression levels of ***sqr_I*** in *At. caldus* grown on three different RISCs at three different growth temperatures, harvest in late exponatial growth phase. The values are normalized to the corresponding 16S rDNA expression

B / A		sulfur			thiosulfate		tetrathionate	
		30 °C	45 °C	50 °C	30 °C	45 °C	30 °C	45 °C
sulfur	30 °C	1.0	0.3	0.7	0.6	0.4	2.0	0.1
	45 °C	12.2	1.0	1.9	2.6	1.8	8.1	0.4
	50 °C	4.8	0.4	1.0	1.0	0.6	3.2	0.2
thiosulfate	30 °C	6.3	0.6	1.0	1.0	0.9	4.2	0.2
	45 °C	9.2	0.8	1.4	1.9	1.0	6.1	0.3
tetrathionate	30 °C	2.0	0.2	0.3	0.4	0.3	1.0	0.1
	45 °C	36.5	3.2	8.2	7.7	5.3	24.3	1.0

The expression levels of *sqr_I* were found to be enhanced in cells grown on S^0 and tetrathionate at 30 °C and a decreased expression level on S^0 and tetrathionate at 45 °C was measured. However, in direct comparison this gene was more expressed on S^0 at 45°C than with tetrathionate at this T°.

Table 11: Expression levels of ***sqr_II*** in *At. caldus* grown on three different RISCs at three different growth temperatures, harvest in late exponatial growth phase. The values are normalized to the corresponding 16S rDNA expression.

B / A		sulfur			thiosulfate		tetrathionate	
		30 °C	45 °C	50 °C	30 °C	45 °C	30 °C	45 °C
sulfur	30 °C	1.0	0.7	1.4	4.4	3.5	2.6	5.1
	45 °C	1.8	1.0	4.7	6.0	4.9	3.7	7.2
	50 °C	0.5	0.3	1.0	1.8	1.5	1.1	2.2
thiosulfate	30 °C	0.3	0.2	0.8	1.0	0.8	0.6	1.2
	45 °C	0.4	0.2	1.0	1.3	1.0	0.2	1.6
tetrathionate	30 °C	0.7	0.4	2.0	2.5	2.0	1.0	3.0
	45 °C	0.3	0.2	0.7	1.0	0.8	0.6	1.0

The expression levels *sqr_II* were found decreased in cells grown on S^0 at 45 °C and enhanced for tetrathionate grown cells at the same T°, where the highest induction was detected in comparison to S^0 grown cells.

Table 12: Expression levels of ***tth*** in *At. caldus* grown on three different RISCs at three different growth temperatures, harvest in late exponatial growth phase. The values are normalized to the corresponding 16S rDNA expression.

B / A		sulfur			thiosulfate		tetrathionate	
		30 °C	45 °C	50 °C	30 °C	45 °C	30 °C	45 °C
sulfur	30 °C	1.0	3.8	12.5	206.7	5.2	63.5	59.2
	45 °C	1.3	1.0	5.2	127.2	2.2	26.5	4.8
	50 °C	0.3	0.3	1.0	25.2	0.4	5.2	1.0
thiosulfate	30 °C	0.0	0.0	0.0	1.0	0.0	0.2	0.2
	45 °C	0.1	0.1	0.1	5.0	1.0	1.0	0.2
tetrathionate	30 °C	0.1	0.1	0.2	5.7	0.1	1.0	0.3
	45 °C	0.1	0.2	0.3	12.0	0.2	2.5	1.0

Low expression levels of *tth* were detected in cells grown on S^0, with the lowest value at 30 °C. Interestingly, a high expression level was found in samples of cells grown

on thiosulfate at 30 °C. High induction values were also found for tetrathionate grown cells at 30 °C, as compared to S^0 grown cells.

4.3 Cotranscription of the putative *sox_I* operon of *At. caldus*

The *sox_I* cluster (gi:255019732-25501937; ACA_2389-ACA_2394) of *At. caldus* was analyzed for cotranscription in order to demonstrate the functionality of these genes and their potential operon organization. Cells were grown on S^0 at 45 °C and harvested in exponential phase. After RNA extraction and cDNA synthesis, PCR was performed with primers specific for overlapping sequences of adjacent genes by using cDNA as PCR template. Results are shown in Fig. 18. Expected amplicon sizes were the following: region 1 = 474 bp; region 2 = 389 bp; region 3 = 485bp; region 4 = 546 bp and region 5 = 420 bp (see also Table 3B). Control assays were performed with 20 ng of *At. caldus* genomic DNA (data not shown) for determining optimal annealing temperatures for each primer.

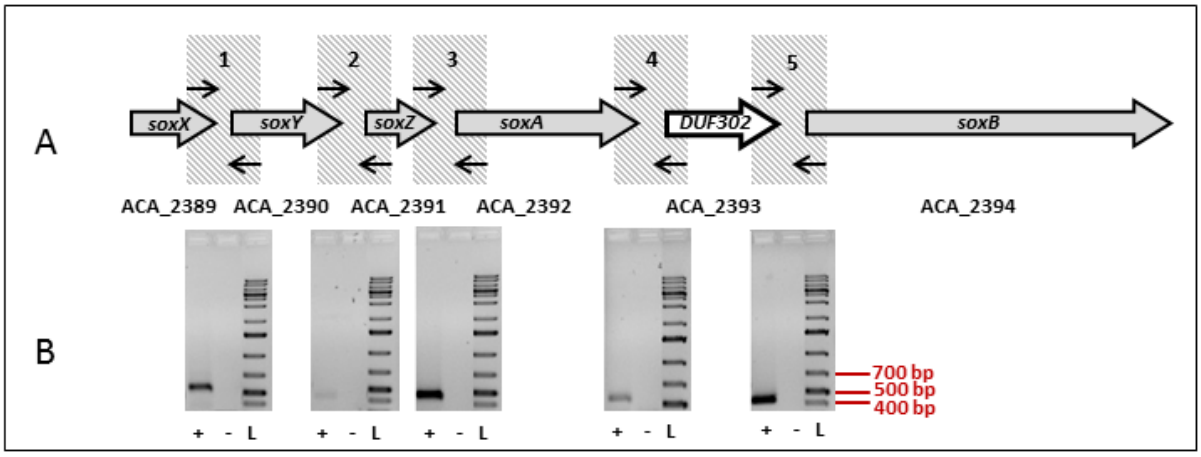

Fig. 17: **Cotranscription of the putative *sox_I* operon of *At. caldus***
A: Experimental design for cotranscription testing of the genes of the putative *sox I* operon: forward and reverse primers (small arrows; Table 3B) were designed to amplify regions (gray shades) within genes (big arrows) of the operon; ACA_xxxx indicates locus tag of genes in the genome. The whole operon has a size of 6.2 kb.
B: Results of the PCR amplification cotranscription: cDNA of *At. caldus* culture grown on S^0 at 45°C; positve (+) and negative (-) controls; L = Ladder; PCRs with 40 cycles. Expected amplicon sizes were the following: region 1 = 474 bp; region 2 = 389 bp; region 3 = 485bp; region 4 = 546 bp and region 5 = 420 bp

The results show that amplicons of the expected sizes were successfully transcribed for all detected adjacent genes, suggesting that the *sox_I* cluster is co-transcribed at least in one transcriptional unit.

4.4 Shot-gun proteomic of *At. caldus* grown on sulfur vs thiosulfate

A major part of this thesis included the analysis of total proteomes from S^0 and thiosulfate grown cells of the *At. caldus* type strain. The good degree of sample purity allowed us to do a high throughput proteomic analysis by tandem mass spectrometry (MS).

4.4.1 General information of the high throughput MS analysis

After semi-quantitative measurement and further statistical analysis of four independent proteome samples from each condition, a total number of 1292 proteins (45.8 %) was identified from 2821 annotated protein coding genes in the genome. 1215 proteins were detected to be present in S^0 grown samples and 1120 proteins were detected in thiosulfate grown samples (Table 13).

In order to do a minimal statistical analysis with 4 independent samples, a Student t-test was performed as described in Material and Methods (chapter 3.3.14). Mean values (n=4) from log2 ratios of the number of peptides found for each protein (normalized against the sum of peptides found in their respective gel lanes) were used to perform a semi-quantitative analysis for proteomes from S^0 or thiosulfate grown cells. Always log2 ratios for S^0 / thiosulfate proteomes were calculated. If the log2 ratio was higher than 1.5 for a protein, this protein was considered to be up-regulated in S^0 growth condition. On the other hand, when the log2 ratio was lower than -1.5, this protein was considered to be up-regulated in the thiosulfate growth condition. Addionally, when the corresponding t-test *p* values were ≤ 0.05, these proteins were considered to be significantly induced or repressed, while proteins with t-test *p* values ≤ 0.1 were considered to be up- or down-regulated.

Table 13: Proteins detected in the proteomes and found to be induced ($p \leq 0.05$)/ up-regulated ($p \leq 0.1$) in samples of *At. caldus* grown in S^0 or thiosulfate medium.
Always log2 ratios for S^0 / thiosulfate proteomes were calculated. If the log2 ratio was higher than 1.5 for a protein, this protein was considered to be up-regulated in S^0 growth condition. On the other hand, when the log2 ratio was lower than -1.5, this protein was considered to be up-regulated in the thiosulfate growth condition.

Total protein amount detected: **1292** Proteins, which could be detected in all proteoms: **334**			
sulfur		thiosulfate	
Total amount of proteins found in any proteome of S^0 grown cells	**1215**	**Total amount** of proteins found in any proteome of thiosulfate grown cells	**1120**
Proteins found **somehow induced** in all proteomes of S^0 grown cells	**271**	Proteins found **somehow induced** in all proteomes of thiosulfate grown cells	**49**
Proteins found significant **induced ($p \leq 0.05$)** in all proteomes of S^0 grown cells	**85**	Proteins found **significant induced ($p \leq 0.05$)** in all proteomes of thiosulfate grown cells	**13**
Proteins found **up-regulated ($p \leq 0.1$)** in all proteomes of S^0 grown cells	**47**	Proteins found **up-regulated ($p \leq 0.1$)** in all proteomes of thiosulfate grown cells	**11**
Proteins found **not significant up-regulated ($p \geq 0.1$)** in all proteomes of S^0 grown cells	**139**	Proteins found not **significant up-regulated ($p \geq 0.1$)** in all proteomes of thiosulfate grown cells	**25**
Proteins **uniquely found** in proteomes of S^0 grown cells	**170**	Proteins **uniquely found** in proteomes of thiouslfate grown cells	**78**

COG analysis of the *At. caldus* genome and proteomes

All genes annotated in the genome, the 1292 proteins found in the proteomes, and the proteins of each type of proteome were classified according to COG categories (Fig. 19, 20).
It is obvious that most of the *At. caldus* proteins annotated in the genome (37.8 %) were of unknown function or poorly characterized ones. In detail, 25.8 % were not in COGs, 6.1 % were in general function only and 5.8 % were with unknown function. Following the categories: replication, recombination and repair (7.3 %), cell wall/ membrane biogenesis (6.1 %) followed by energy production and conversion (5.6 %) were the more represented ones.
In all proteomes 12.6 % of the detected proteins were not in COGs, 7.6 % and 5.5 % were classified in COGs with general function or to have unknown functions,

respectively. In total, 25.6 % of the encoded *At. caldus* proteins were unknown or with poorly characterized functions. Most of the encoded proteins belong to housekeeping functional categories (such as transcription and translation) with 8.6 %, followed by energy production and conversion and amino acid transport and metabolism with 8.0 % and 8.3 %, respectively. A similar frequency of occurrence was observed in the proteomes from S^0 or thiosulfate grown samples, where 26.8 % and 24.8 % of proteins were classified as “poorly characterized function”.

85 proteins were induced and 47 were up-regulated in proteomes of S^0 grown cells. Due to this big amount, only the induced proteins have been discussed, while the up-regulated proteins found in S^0 grown cells are given in the annex (Table S1 and Table S2, respectively). On the other hand, in thiosulfate grown cells 13 and 11 proteins were induced and upregulated, respectively.

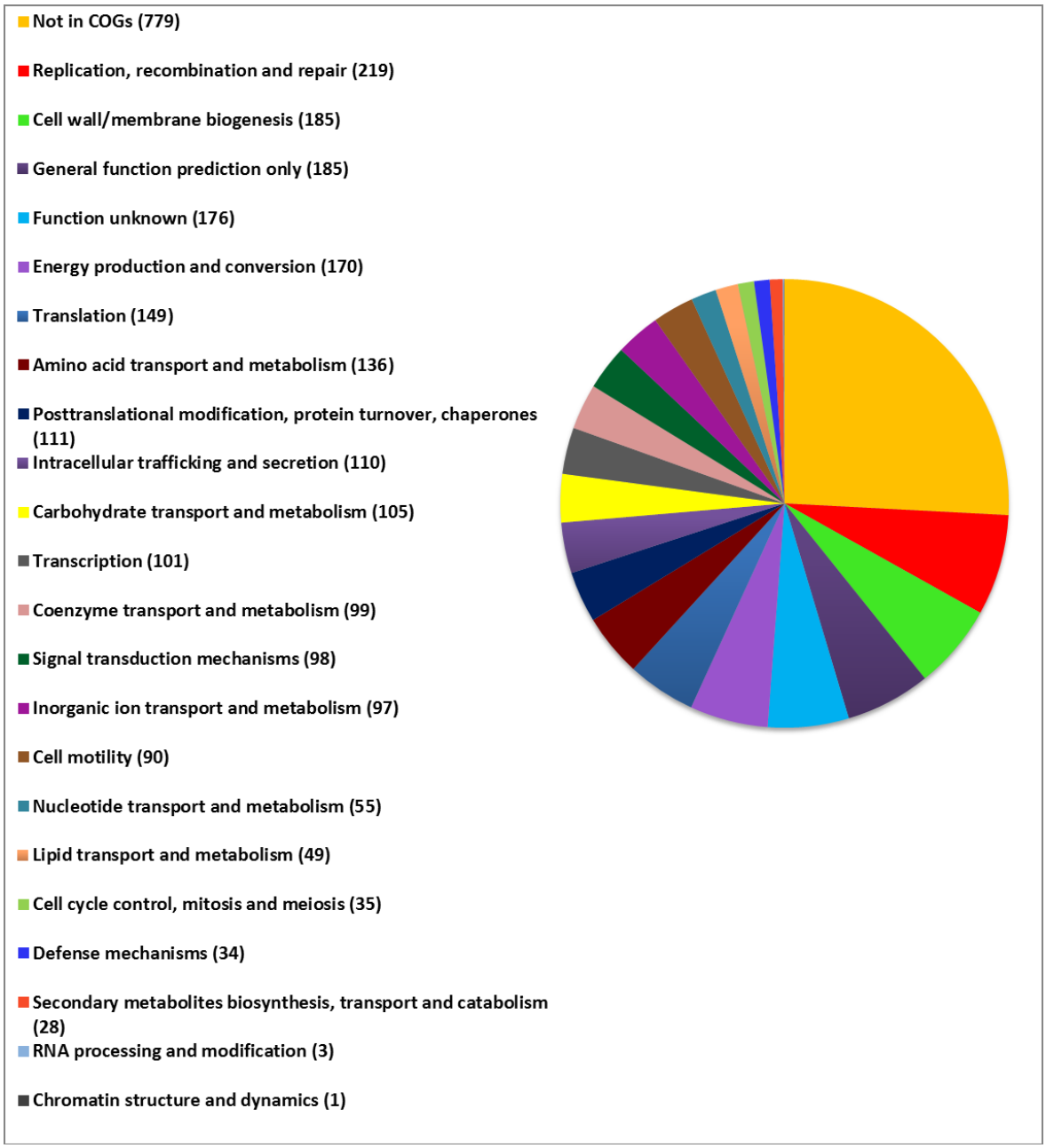

Fig. 18: Pie chart of annotated proteins in the genome of *At. caldus* ordered in COG categories; protein numbers are given in brackets.

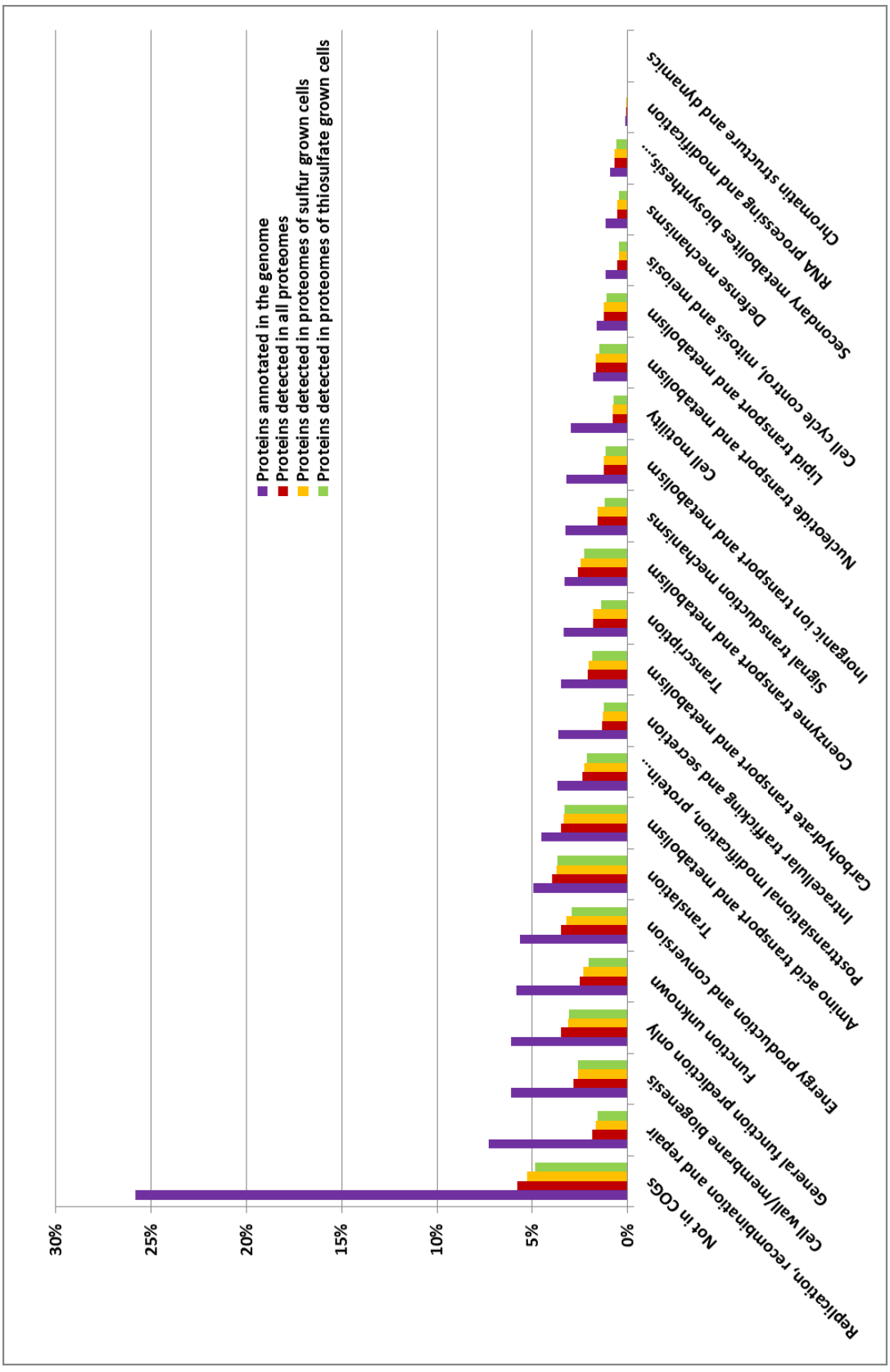

Fig. 19: COG distribution of annotated proteins in the genome of *At. caldus* ATCC 51756 and proteins found in the different proteomes,

Table 14**:** Proteins induced in proteomes of S^0 grown cells. In all subtables, when possible, COGs numbers are shown for each protein

A) Proteins found in the COG categories for: energy production and conversion (C); coenzyme metabolism (H); secondary metabolites biosynthesis, transport and catabolism (Q) and inorganic ion transport and metabolism (P)

Gene description	Locus tag	Reg S/TS	T-test ≤ 0.05	GB	Some remarks	COG category
Uptake hydrogenase large subunit	ACA_2234	7.35	0.000	ZP_05293729	**COG0374** (Ni,Fe-hydrogenase I large subunit) **EC: 1.12.99.6**	C
Uptake hydrogenase small subunit precursor	ACA_2233	6.33	0.000	ZP_05293728	**COG1740** (Ni,Fe-hydrogenase I small subunit) **EC: 1.12.99.6**	C
Ferredoxin, 2Fe-2S	ACA_1179	3.48	0.001	ZP_05293013	**COG0633** (Ferredoxin)	C
Cytochrome d ubiquinol oxidase subunit I	ACA_2617	3.46	0.003	ZP_05291736	**COG1271** (Cytochrome bd-type quinol oxidase, subunit 1) **EC: 1.10.3.-**	C
NADH-ubiquinone oxidoreductase chain I	ACA_2707	3.32	0.004	ZP_05292020	**COG1143** (Formate hydrogenlyase subunit 6/NADH:ubiquinone oxidoreductase 23 kD subunit (chain I)) **EC: 1.6.5.3**	C
NADH-ubiquinone oxidoreductase chain E	ACA_2703	3.12	0.001	ZP_05292016	**COG1905** (NADH:ubiquinone oxidoreductase 24 kD subunit) **EC: 1.6.5.3**	C
Cytochrome c, class I	ACA_1998	2.84	0.084	ZP_05293552	**COG2010** (Cytochrome c, mono- and diheme variants)	C
Pyruvate dehydrogenase (acetyl-transferring)	ACA_0754	2.78	0.064	ZP_05293267	**COG1071** (Thiamine pyrophosphate-dependent dehydrogenases, E1 component alpha subunit) **EC: 1.2.4.1**	C
dihydrolipoamide acetyltransferase	ACA_0752	1.73	0.050	ZP_05293265	**COG0508** (Dihydrolipoamide acyltransferases)	C
ferredoxin, 4Fe-4S	ACA_2756	2.83	0.054	ZP_05293082	**COG1146** (Ferredoxin 3) **COG1145** (Ferredoxin 2) **COG1142** (Fe-S-cluster-containing hydrogenase components 2)	C; C; C
hopanoid biosynthesis associated radical SAM protein HpnJ	ACA_0715	3.09	0.002	ZP_05294193	**COG1032** (Fe-S oxidoreductases family 2) **COG0621** (2-methylthioadenine synthetase)	C; J
uncharacterized flavoprotein	ACA_0313	2.83	0.050	ZP_05293386	**COG0426** (Uncharacterized flavoproteins) **COG0491** (Zn-dependent hydrolases, including glyoxylases)	C; R
Dethiobiotin synthetase	ACA_0385	3.49	0.001	ZP_05294238	**COG0132** (Dethiobiotin synthetase) **EC: 6.3.3.3**	H
HesA/MoeB/ThiF family protein	ACA_2536	2.92	0.022	ZP_05293666	**COG1179** (Dinucleotide-utilizing enzymes involved in molybdopterin and thiamine biosynthesis family 1)	H
Dephospho-CoA kinase	ACA_0924	2.47	0.040	ZP_05292256	**COG0237** (Dephospho-CoA kinase) **EC: 2.7.1.24**	H
efflux transporter, RND family, MFP subunit	ACA_1142	4.53	0.005	ZP_05292976	**COG0845** (Membrane-fusion protein)	Q
rhodanese-like protein	ACA_0025	4.36	0.001	ZP_05292580	**COG0607** (Rhodanese-related sulfurtransferases)	P
Potassium-transporting ATPase B chain	ACA_0010	2.75	0.005	ZP_05292565	**COG2216** (High-affinity K+ transport system, ATPase chain B) **EC: 3.6.3.12**	P

B) Proteins found in the COG categories for: lipid metabolism (I); carbohydrate metabolism (G) and transport and amino acid metabolism and transport (E)

Gene description	Locus tag	Reg S/TS	T-test ≤ 0.05	GB	Some remarks	COG category
4-diphosphocytidyl-2-C-methyl-D-erythritol kinase	ACA_0540	2.74	0.001	ZP_05292733	**COG1947** (4-diphosphocytidyl-2C-methyl-D-erythritol 2-phosphate synthase) **EC: 2.7.1.148**	I
tagatose-6-phosphate kinase	ACA_1396	3.09	0.002	ZP_05293470	**COG1105** (Fructose-1-phosphate kinase and related fructose-6-phosphate kinase (PfkB)) **COG2870** (ADP-heptose synthase, bifunctional sugar kinase/adenylyltransferase) **COG0524** (Sugar kinases, ribokinase family)	G; M; G
putative phosphoglycerate mutase family protein	ACA_2715	2.90	0.039	ZP_05292028	**COG0406** (Fructose-2,6-bisphosphatase) **COG0588** (Phosphoglycerate mutase 1)	G; G
phosphoheptose isomerase	ACA_2240	4.17	0.001	ZP_05293735	**COG0279** (Phosphoheptose isomerase)	G
2,3-diketo-5-methylthiopentyl-1-phosphate enolase	ACA_0171	4.02	0.001	ZP_05291875	**COG1850** (Ribulose 1,5-bisphosphate carboxylase, large subunit)	G
glycoside hydrolase, family 57	ACA_1678	3.46	0.037	ZP_05292774	**COG1449** (Alpha-amylase/alpha-mannosidase)	G
phosphoglucosamine mutase	ACA_1484	2.74	0.001	ZP_05291978	**COG1109** (Phosphomannomutase) **EC: 5.4.2.10**	G
2,3-bisphosphoglycerate-independent phosphoglycerate mutase	ACA_0756	2.71	0.036	ZP_05293269	**COG0696** (Phosphoglyceromutase) **EC: 5.4.2.1**	G
Senescence marker protein-30 (SMP-30)	ACA_2344	2.63	0.032	ZP_05292144	**COG3386** (Gluconolactonase)	G
Lactoylglutathione lyase	ACA_0195	2.77	0.057	ZP_05291899	**COG0346** (Lactoylglutathione lyase and related lyases) **EC: 4.4.1.5**	E
Biosynthetic Aromatic amino acid aminotransferase beta	ACA_1595	2.68	0.038	ZP_05293333	**COG0079** (Histidinol-phosphate aminotransferase/Tyrosine aminotransferase) **COG0436** (PLP-dependent aminotransferases) **EC: 2.6.1.57**	E; E
Imidazole glycerol phosphate synthase amidotransferase subunit	ACA_1730	2.35	0.043	ZP_05292630	**COG0118** (Glutamine amidotransferase) **EC: 2.4.2.-**	E

C) Proteins found in the COG categories for: cell wall structure and biogenesis and outer membrane (M) and secretion, motility and chemotaxis (N)

Gene description	Locus tag	Reg S/TS	T-test ≤ 0.05	GB	Some remarks	COG category
Type IV pilus biogenesis protein PilN	ACA_1360	3.54	0.018	ZP_05293683	**COG3166** (Fimbrial assembly protein)	N
Flagellar assembly protein fliH	ACA_0350	3.00	0.002	ZP_05293423	**COG1317** (Flagellar biosynthesis/type III secretory pathway protein)	N
probable methyl-accepting chemotaxis protein	ACA_0837	2.46	0.042	ZP_05294049	**COG0840** (Methyl-accepting chemotaxis protein)	N
N-acetylglucosamine-1-phosphateuridyl transferase / Glucosamine-1-phosphate N-acetyl transferase	ACA_0980	3.21	0.031	ZP_05292312	**COG1207** (N-acetylglucosamine-1-phosphate uridyltransferase (contains nucleotidyltransferase and I-patch acetyltransferase domains) **COG1208** (Nucleoside-diphosphate-sugar pyrophosphorylases involved in lipopolysaccharide biosynthesis/translation initiation factor eIF2B subunits) **EC: 2.3.1.157**	M; MJ
Glucosamine--fructose-6-phosphate aminotransferase (isomerizing)	ACA_0981	3.21	0.038	ZP_05292313	**COG0449** (Glucosamine 6-phosphate synthetase, contains amidotransferase and phosphosugar isomerase domains) **EC: 2.6.1.16**	M
D-alanyl-D-alanine carboxypeptidase	ACA_2400	2.98	0.026	ZP_05291820	**COG1686** (D-alanyl-D-alanine carboxypeptidase) **EC: 3.4.16.4**	M
Cyclopropane-fatty-acyl-phospholipid synthase	ACA_2714	2.74	0.001	ZP_05292027	**COG2230** (Cyclopropane fatty acid synthase and related methyltransferases) **EC: 2.1.1.79**	M

D) Proteins found in the COG categories for: molecular chaperones and related functions (O); replication, recombination and repair (L); transcription (J); translation (K), including ribosome structure and biogenesis and signal transduction (T)

Gene description	Locus tag	Reg S/TS	T-test ≤ 0.05	GB	Some remarks	COG category
Inactive metal-dependent protease, putative molecular chaperone	ACA_2653	2.74	0.001	ZP_05291772	**COG1214** (Inactive homologs of metal-dependent proteases, putative molecular chaperones) **COG0533** (Metal-dependent proteases with possible chaperone activity)	O; O
NiFe hydrogenase metallocenter assembly protein HypE	ACA_2242	4.89	0.000	ZP_05293737	**COG0309** (Hydrogenase maturation factor)	O
NiFe hydrogenase metallocenter assembly protein HypF	ACA_2238	4.46	0.001	ZP_05293733	**COG0068** (Hydrogenase maturation factor)	O
DNA gyrase subunit B	ACA_0883	2.67	0.043	ZP_05291647	**COG0187** (DNA gyrase (topoisomerase II) B subunit) **EC: 5.99.1.3**	L
RNA polymerase sigma-54 factor RpoN	ACA_1750	4.18	0.002	ZP_05292650	**COG1508** (DNA-directed RNA polymerase specialized sigma subunits, sigma54 homologs)	K
Transcriptional regulator, MerR family	ACA_2018	3.21	0.001	ZP_05293572	**COG1396** (Predicted transcriptional regulators)	K
putative transcriptional regulator	ACA_1258	3.09	0.002	ZP_05292121	**COG0583** (Transcriptional regulator)	K
transcriptional regulator, ArsR family	ACA_2532	3.02	0.047	ZP_05293662	**COG0640** (Predicted transcriptional regulators)	K
Cysteinyl-tRNA synthetase	ACA_0293	3.61	0.012	ZP_05293366	**COG0215** (Cysteinyl-tRNA synthetase) **EC: 6.1.1.16**	J
ribosomal protein L29	ACA_1884	2.85	0.036	ZP_05292831	**COG0255** (Ribosomal protein L29)	J
endoribonuclease L-PSP	ACA_2581	2.75	0.029	ZP_05294104	**COG0251** (Putative translation initiation inhibitor)	J
Translation initiation factor 1	ACA_1898	2.74	0.001	ZP_05292845	**COG0361** (Translation initiation factor IF-1)	J
Peptide chain release factor 3	ACA_2651	2.74	0.001	ZP_05291770	**COG0480** (Translation elongation and release factors (GTPases))	J
two component, sigma54 specific, transcriptionalregulator, Fis family	ACA_2232	3.47	0.001	ZP_05293727	**COG2204** (Response regulator containing CheY-like receiver, AAA-type ATPase, and DNA-binding domains)	T
PAS modulated sigma54 specific transcriptionalregulator, Fis family	ACA_1137	3.00	0.002	ZP_05292971	**COG2204** (Response regulator containing CheY-like receiver, AAA-type ATPase, and DNA-binding domains)	T
sigma54 specific transcriptional regulator, Fis family	ACA_2615	2.87	0.001	ZP_05291734	**COG2204** (Response regulator containing CheY-like receiver, AAA-type ATPase, and DNA-binding domains)	T
hypothetical protein	ACA_1270	3.68	0.001	ZP_05293192	**COG2199** (GGDEF domain) **COG2202** (PAS/PAC domain)	T; T
Chemotaxis regulator - transmits chemoreceptorsignals to flagelllar motor components CheY	ACA_0317	2.96	0.042	ZP_05293390	**COG0784** (CheY-like receiver domain) **COG0745** (Response regulators consisting of a CheY-like receiver domain and a winged-helix DNA-binding domain)	T; TK

E) Proteins found in the "poorly characterized" COG categories (R and S)

Gene description	Locus tag	Reg S/TS	T-test ≤ 0.05	GB	Some remarks	COG category
hypothetical protein	ACA_1144	6.13	0.001	ZP_05292978	**COG0457** (TPR-repeat-containing proteins)	R
FAD-dependent pyridine nucleotide-disulphideoxidoreductase	ACA_0669	4.55	0.001	ZP_05293919	**COG0446** (Uncharacterized NAD(FAD)-dependent dehydrogenases)	R
hypothetical protein	ACA_2411	4.30	0.000	ZP_05291831	**COG2018** (Uncharacterized ACR; distantly related to eukaryotic homeotic protein bithoraxoid)	R
hypothetical protein	ACA_1140	3.60	0.004	ZP_05292974	**COG0457** (TPR-repeat-containing proteins)	R
hypothetical protein	ACA_1244	3.09	0.002	ZP_05292107	**COG2229** (Predicted GTPase)	R
LSU m5C1962 methyltransferase RlmI	ACA_1589	3.06	0.034	ZP_05293327	**COG2802** (Uncharacterized protein, similar to the N-terminal domain of Lon protease)	R
hypothetical protein	ACA_2802	2.68	0.038	ZP_05293128	**COG2802** (Uncharacterized protein, similar to the N-terminal domain of Lon protease)	R
oxidoreductase molybdopterin binding	ACA_1585	2.45	0.048	ZP_05293323	**COG2041** (Uncharacterized enzymes, related to nitrate reductase)	R
Oxidoreductase (flavoprotein)	ACA_0165	3.82	0.000	ZP_05291869	**COG0446** (Uncharacterized NAD(FAD)-dependent dehydrogenases) **COG1252** (NADH dehydrogenase, FAD-containing subunit)	R; C
hypothetical protein	ACA_0091	3.36	0.034	ZP_05291471	**COG1416** (Uncharacterized ACR)	S
hypothetical protein	ACA_0163	3.32	0.000	ZP_05291867	**COG2210** (Uncharacterized ACR)	S
prevent-host-death family protein	ACA_0136	3.21	0.001	ZP_05291714	**COG2161** (Uncharacterized ACR)	S
Propeptide PepSY amd peptidase M4	ACA_0538	3.12	0.001	ZP_05292731	**COG3212** (Uncharacterized membrane protein)	S
hypothetical protein	ACA_0321	3.05	0.026	ZP_05293394	**COG1699** (Uncharacterized BCR)	S
ErfK/YbiS/YcfS/YnhG family protein	ACA_0211	3.00	0.002	ZP_05291915	**COG1376** (Uncharacterized BCR)	S
hypothetical protein	ACA_0092	2.99	0.000	ZP_05291471	**COG1520** (Uncharacterized proteins of WD40-like repeat family)	S
hypothetical protein	ACA_0755	2.88	0.004	ZP_05293268	**COG0599** (Uncharacterized ACR, homolog of gamma-carboxymuconolactone decarboxylase subunit)	S
protein of unknown function DUF74	ACA_0741	2.60	0.045	ZP_05293254	**COG0393** (Uncharacterized ACR)	S
hypothetical protein	ACA_2408	4.70	0.002	ZP_05291828	not in COGs	-
conserved hypothetical protein	ACA_1145	4.37	0.006	ZP_05292979	not in COGs	-
hypothetical protein	ACA_0937	4.20	0.001	ZP_05292269	not in COGs	-
NHL repeat-containing protein	ACA_2237	3.56	0.001	ZP_05293732	not in COGs	-
hypothetical protein	ACA_1767	3.47	0.001	ZP_05292667	not in COGs	-
hypothetical protein	ACA_0508	3.43	0.018	ZP_05292703	not in COGs	-
putative carboxysome peptide A	ACA_2769	3.12	0.001	ZP_05293095	not in COGs	-
hypothetical protein	ACA_0912	3.09	0.002	ZP_05292244	not in COGs	-
hypothetical protein	ACA_0662	2.99	0.000	ZP_05293912	not in COGs	-
Ribulose bisphosphate carboxylase small chain	ACA_2766	2.85	0.101	ZP_05293092	not in COGs; **EC: 4.1.1.39**	-
hypothetical protein	ACA_2787	2.84	0.099	ZP_05293113	not in COGs	-
hypothetical protein	ACA_2699	2.74	0.001	ZP_05292012	not in COGs	-

Energy production and conversion

Thirteen proteins were found to be induced in proteomes of S^0 grown cells belonging to the category energy production and conversion.

ACA_2234 was annotated as uptake hydrogenase, large subunit. [Ni,Fe]-hydrogenase catalyzes: H_2 + A <=> AH_2; Cofactors are iron-sulfur cluster and nickel. The Ni-Fe hydrogenases are found to catalyze both hydrogen evolution and uptake, with low-potential multiheme cytochromes, such as cytochrome C3, acting as either electron donors or acceptors, depending on their oxidation state (Fauque *et al.* 1988; Cammack *et al.* 1994). In *Desulfovibrio*, it uses molecular hydrogen for the reduction of a variety of substances. It recycles the H_2 produced by nitrogenase to increase the production of ATP and to protect nitrogenase against inhibition or damage by O_2 under carbon- or phosphate-limited conditions. The small subunit contains three iron-sulfur clusters (two [4Fe-4S] and one [3Fe-4S]); the large subunit contains a nickel ion (Cammack *et al.* 1994). Several hydrogenase clusters are present in the genome of *At. caldus*. However, only two proteins of the potential gene cluster encoding ACA_2233 till ACA_2245 were found to be induced with the S^0 substrate. But not all of these induced proteins are characterized in this COG category here.

ACA_1179 is annotated as a ferredoxin. Ferredoxins are small, acidic, electron transfer proteins ubiquitous in biological redox systems. They have also either a 4Fe-4S, 3Fe-4S, or a 2Fe-2S cluster. Among them, ferredoxin with one 2Fe-2S cluster per molecule are present in plants, animals, and bacteria, where four conserved cysteine residues coordinate the 2Fe-2S cluster. This conserved region is also found as a domain in various metabolic enzymes (Fukuyama *et al.* 1995).

Cytochrome d ubiquinol oxidase (ACA_2617) is a cytochrome bd type terminal oxidase that catalyses quinol dependent, Na^+ independent oxygen uptake (Sturr *et al.* 1996). Members of this family are integral membrane proteins.

NADH: ubiquinone oxidoreductase (ACA_2707 and ACA_2708; EC: 1.6.5.3) is a respiratory-chain enzyme that catalyzes the transfer of two electrons from NADH to ubiquinone in a reaction that is associated with proton translocation across the membrane (NADH + ubiquinone = NAD^+ + ubiquinol; Walker 1992). This complex is a major source of reactive oxygen species that are predominantly formed by electron transfer from coenzyme flavin mononucleotide (FMN)H_2. In general, the bacterial complex consists of 14 different subunits (A to N). The NADH oxidation domain

harbouring the FMN cofactor is connected via a chain of iron-sulfur clusters to the ubiquinone reduction site.

Cytochromes c (CytC; ACA_2617) are electron-transfer proteins having one or several heme c groups, bound to the protein by one or, more generally, two thioether bonds involving sulphydryl groups of cysteine residues. The fifth heme iron ligand is always provided by a histidine residue. CytC possess a wide range of properties and functions in a large number of different redox processes (Ambier 1991).

Pyruvate dehydrogenase (PDH) is a heterodimer of α and β subunits. The PDH complex catalyzes the overall conversion of pyruvate to acetyl-CoA and CO_2. It contains multiple copies of three enzymatic components: pyruvate dehydrogenase (E1), dihydrolipoamide acetyltransferase (E2) and lipoamide dehydrogenase (E3) (Hawkins *et al.* 1990). E1 and E2 are found closly ordered in the genome ACA_0752 and ACA_0754 (both found to be induced on S^0 grown cells). E3 components (ACA_2840 and ACA_2613) were also found in the proteomes, but not induced on S^0.

The protein ACA_0715, annotated as an hopanoid biosynthesis (ACA_0715) associated radical SAM protein (HpnJ) utilizes an iron-sulfur redox cluster and S-adenosylmethionine (SAM) to carry out diverse radical mediated reactions (Sofia *et al.* 2001).

Coenzyme metabolism

Three proteins belong to the category coenzyme metabolism.

ACA_0385 is annotated as dethiobiotin synthetase. It is involved in biotin biosynthesis using ATP, 7,8-diaminononanoate, and CO_2,and requires Mg^{2+} as a co-factor (Krell and Eisenberg 1970).

Members of the HesA/MoeB/ThiF family of proteins (ACA_2536) include several proteins related of thiamine biosynthetic pathways. The family is also conected with ubiquitin-activating enzymes, which share in their catalytic domains structural similarity with a large family of NAD/FAD-binding proteins (Hershko 1991).

Dephospho-CoA kinases (ACA_0924) catalyze the final step in CoA biosynthesis, the phosphorylation of the 3'-hydroxyl group of ribose using ATP as a phosphate donor. (ATP + 3'-dephospho-CoA <=> ADP + CoA) (Obmolova *et al.* 2001).

Secondary metabolites biosynthesis, transport and catabolism

Only one protein, ACA_1142, encoding an efflux transporter protein belonging to the RND family (MFP subunit), was found in this category. RND refers to resistance, nodulation, cell division. In Gram-negative bacteria, MFPs are proposed to span the periplasm, linking both membranes (Schulein *et al.* 1992).

Inorganic ion transport and metabolism

The protein ACA_0025 is annotated as a rhodanese-like protein. Rhodaneses (i.e. thiosulfate sulfatetransferases) are enzymes catalyzing the transfer of the sulfane atom of thiosulfate to cyanide, to form sulfite and thiocyanate. An increasing number of reports indicate that rhodanese modules are versatile sulfur carriers that have adapted their function to fulfill the need for reactive sulfane sulfur in distinct metabolic and regulatory pathways (Bordo and Bork 2002).
The protein ACA_0010 is annotated as a potassium-transporting ATPase (chain B). Transmembrane ATPases use ATP hydrolysis to drive the transport of protons across a membrane (Rappas *et al.* 2004).

Lipid metabolism

In the category only one protein, the 4-diphosphocytidyl-2C-methyl-D-erythritol kinase (ACA_0540), was found to be induced in proteomes from S^0 grown cells. It is a member of GHMP family, which includes galacto-, homoserine, mevalonate or phospho- kinases. It is an enzyme of the deoxyxylulose phosphate pathway of terpenoid biosynthesis, catalyzing the single ATP-dependent phosphorylation stage affording 4-diphosphocytidyl-2C-methyl-D-erythritol-2-phosphate (Miallau *et al.* 2003).

Carbohydrate metabolism and transport

Eight proteins were induced on S^0. (ACA_1396) is the tagatose-6-phosphate kinase (EC: 2.7.1.144), part of the tagatose-6-phosphate pathway of lactose degradation. The genes encoding for the enzymes of the tagatose 6-phosphate pathway have been found to be part of the lac operon, together with the genes coding for the lactose-phosphotransferase system and the phospho-beta-galactosidase e.g. in

Lactococcus lactis, *Staphlococcus aureus*, and *Streptococcus mutans* (Nobelmann and Lengeler 1995).

Another protein induced is ACA_2715, the phosphoglycerate mutase (PGM) (EC: 5.4.2.1), an enzyme that catalyzes the internal transfer of a phosphate group from C-3 to C-2 resulting in the conversion of 3-phosphoglycerate (3PG) to 2-phosphoglycerate (2PG) through a 2,3-bisphosphoglycerate intermediate, found in glycolysis (Grisolia 1962, Rose 1980). Also the 2,3-bisphosphoglycerate-independent phosphoglycerate mutase (ACA_0756) which catalyzes: 2-phospho-D-glycerate <=> 3-phospho-D-glycerate was found to be induced.

Furthermore, the phosphoheptose isomerase (ACA_2240) was also found to be induced in this category. This protein belongs to the SIS (Sugar ISomerase) superfamily and it is involved in lipopolysaccharide (LPS) biosynthesis. More specifically it is involved in the synthesis of glyceromannoheptose 7-phosphate, which is the first intermediate of the biosynthesis of the inner core LPS precursor, L-glycero-D-mannoheptose in Gram-negative bacteria (Taylor *et al.* 2008).

The protein ACA_0171, encoding a 2,3-diketo-5-methylthiopentyl-1-phosphate enolase, was found to be induced. It is a homologoue of RuBisCO (Tabita *et al.* 2008). Interestingly, also the RuBisCO (small chain), ACA_2766 (listed in the annex 7.1.1), is also found to be up-regulated in proteomes of S^0 grown cells. RuBisCO is a bifunctional enzyme that catalyzes both the carboxylation and oxygenation of ribulose-1,5-bisphosphate, thus fixing carbon dioxide as the first step of the Calvin cycle: D-ribulose 1,5-bisphosphate + CO_2 + H_2O <=> 2 3-phospho-D-glycerate + 2 H^+.

The protein ACA_1678 is an O-Glycosyl hydrolase (family 57; EC: 3.2.1.). Zhese are a widespread group of enzymes that hydrolyse the glycosidic bond between two or more carbohydrates, or between a carbohydrate and a non-carbohydrate moiety. A classification system for glycosyl hydrolases, based on sequence similarity, has led to the definition of 85 different families, while the Glycoside hydrolase family 57 (GH57) comprises enzymes with two known activities: alpha-amylase (EC: 3.2.1.1) and 4-alpha-glucanotransferase (EC: 2.4.1) (Davies and Henrissat 1995).

The protein ACA_1484 is the phosphoglucosamine mutase (PGM), (EC: 5.4.2.3) which belongs to the alpha-D- phosphohexomutase superfamily, involved in the biosynthesis of UDP-N-acetylglucosamine (Mio *et al.* 2000).

The last protein found in this category (ACA_2344) is annotated as “senesence marker protein-30” (SMP30), also known as regucalcin, a class of Ca^{2+} binding proteins (Shimokawa and Yamaguchi 1992, 1993).

Amino acid metabolism and transport

In this category 3 proteins were found to be induced in proteomes of S^0 grown cells.
ACA_1595 is annotated as a “beta biosynthetic aromatic aminoacid aminotransferase”. Aminotransferases are pyridoxal 5′-phosphate (PLP)-dependent enzymes catalyzing the reversible transfer of an amino group, usually the α-amino group of an amino acid, to an α-keto acid such as α-ketoglutarate. These enzymes have been divided into four subfamilies based on structural similarities (Mehta *et al.* 1993). Subfamily I comprises the aspartate, alanine, aromatic and histidinolphosphate aminotransferases.
Another enzyme induced is ACA_0195, a lactoylglutathione lyase (glyoxalase I), which is found mainly in marine members of the gammaproteobacteria. I Glyoxalase I is a ubiquitous enzyme which binds one mole of zinc per subunit. The bacterial and yeast enzymes are monomeric. It catalyzes the first step of the glyoxal pathway in the following reaction: glutathione + methylglyoxal <=> (R)-S-lactoylglutathione.
S-lactoylglutathione can then be converted by glyoxalase II to lactic acid (Kim *et al.* 1993).
The protein ACA_1730 is annotated as an imidazole glycerol phosphate synthetase (IGPS) subunit HisH. This is a key metabolic enzyme, which links amino acid and nucleotide biosynthesis: it catalyzes the closure of the imidazole ring within histidine biosynthesis and provides the substrate for de novo purine biosynthesis. IGPS consists of two different subunits: HisH, a glutamine amidotransferase (glutaminase), and HisF, a synthase (cyclase). HisH functions to provide a source of nitrogen, which is required for the synthesis of histidine and purines (Omi *et al.* 2002).

Secretion, motility and chemotaxis

Three Proteins were found ito be nduced in proteomes from S^0 grown cells.
One protein is the type IV pilus biogenesis protein PilN (ACA_1360). Type IV pili are surface-exposed filaments, which play a major role in pathogenesis, motility, and

DNA uptake in bacteria. PilN is a lipoprotein which is locates at the OM and is part of a thin pilus required only for liquid mating (Karuppiah and Derrick 2011).
FliH (ACA_0350) is the flagellar assembly protein. The bacterial flagellum is a complex structure comprising intracellular, envelope-spanning, and extracellular components. In *Salmonella typhimurium*, FliH is a filament protein and thought to be exported by a unique, flagellum-specific pathway travelling through the hollow core of the nascent structure and assembling at its distal end (Vogler *et al.* 1991).
The protein ACA_0837 is annotated as the probable methyl-accepting chemotaxis protein (MCP). These are a family of bacterial receptors mediating chemotaxis to diverse signals, responding to changes in the concentration of attractants and repellents in the environment by altering bacterial swimming behaviour (Derr *et al.* 2006).

Cell wall structure and biogenesis and outer membrane

Four proteins were induced in this category. The protein ACA_0961 is the glucosamine-fructose-6-phosphate aminotransferase (EC: 2.6.1.16). It catalyzes the formation of glucosamine 6-phosphate and is the first and rate-limiting enzyme of the hexosamine biosynthetic pathway. The final product of the hexosamine pathway, UDP-N-acetyl glucosamine, is an active precursor of numerous macromolecules containing amino sugars (Mouilleron *et al.* 2006).
ACA_0980 encodes a N-acetylglucosamine-1-phosphateuridyltransferase/ Glucosamine-1-phosphate N-acetyltransferase. This enzyme catalyzes two reactions:
Acetyl-CoA + alpha-D-glucosamine-1-phosphate <=> CoA + N-acetyl-alpha-D-glucosamine 1-P ; and uridine 5'-triphosphate (UTP) + N-acetyl-alpha-D-glucosamine 1-P <=> diphosphate + UDP-N-acetyl-D-glucosamine (Olsen *et al*. 2007).
Furthermore, the protein D-alanyl-D-alanine carboxypeptidase (ACA_2400) was also found in this category. It is working in final stages of bacterial peptidoglycan synthesis, where its preferential cleavage site is: $(Ac)_2$-L-Lys-D-Ala-┃-D-Ala. It is inhibited by beta-lactam antibiotics, which acylate at the active site serine in the enzyme (Martin *et al.* 1975).
The protein ACA_2714 is a cyclopropane-fatty-acyl-phospholipid synthase. It transfers a methylene group from S-adenosyl-L-methionine to the cis double bond of an unsaturated fatty acid chain resulting in the replacement of the double bond with a

methylene bridge. Consequently, it catalyzes the reaction: S-adenosyl-L-methionine + phospholipid olefinic fatty acid <=> S-adenosyl-L-homocysteine + phospholipid cyclopropane fatty acid (Wang *et al.* 1992)

Molecular chaperones and related functions

Three proteins belonging to this category were found to be induced.
The protein ACA_2653 is annotated as “inactive metal-dependent protease (putative molecular chaperone)”. Metalloproteases are the most diverse of the four main types of proteases, with more than 50 families identified to date. In these enzymes, a divalent cation, usually zinc, activates the water molecule. Of the known metalloproteases around half contain an HEXXH motif, which has been shown in crystallographic studies to form part of the metal-binding site (Rawlings and Barrett 1995).
The other two proteins are assembly proteins of [NiFe]-hydrogenase (ACA_2238; ACA_2242), named HypE and HypF respectively. These as well as other nickel metalloenzymes, are synthesized as a precursor devoid of the metalloenzyme active site. This precursor then undergoes a complex post-translational maturation process that requires a number of accessory proteins. Members of the HypF family are accessory proteins involved in hydrogenase maturation (Paschos *et al.* 2002). Strongly related is also the enzyme containing HypE (or HupE), a protein required for expression of catalytically active Ni-Fe hydrogenase in systems, where it appears to be an accessory protein involved in maturation rather than a regulatory protein involved in expression (Watanabe *et al.* 2007).

Replication, recombination and repair

The protein ACA_0883, the DNA gyrase subunit B, was found to be induced. This enzyme is responsible for ATP-dependent breakage, passage and rejoining of double-stranded DNA (Roca 1995).

Transcription

Four proteins were found to be induced in this category.
The protein ACA_1750 encodes the RNA polymerase sigma-54 factor RpoN. Sigma factors are bacterial transcription initiation factors that promote the attachment of the

core RNA polymerase to specific initiation sites and are then released. They alter the specificity of promoter recognition. The sigma-54 (gene *rpoN* or *ntrA*) directs the transcription of a wide variety of genes (Helmann and Chamberlin 1988; Merrick 1993). It interacts with ATP-dependent positive regulatory proteins that bind to upstream activating sequences (Chaney *et al.* 2001).

Three other proteins (ACA_1258, ACA_2018 and ACA_2532) are annotated as transcriptional regulators. In prokaryotes, regulation of transcription is needed for a cell to quickly adapt to the ever-changing outer environment. ACA_2018 belongs to the MerR family, which responds to stress-inducing concentrations of di- and multivalent heavy metal ions. MerR regulators are found in many bacterial species mediating the mercuric-dependent induction of the mercury resistance operon (Helmann *et al.* 1989). The protein ACA_2532 is annotated as the metalloregulatory transcriptional repressor ArsR, which represses the expression of operons linked to stress-inducing concentrations of di- and multivalent heavy metal ions (Busenlehner *et al.* 2003; Eicken *et al.* 2003). The gene ACA_1258 contains a region encoding a binding domain of the LysR-type transcriptional regulators (LTTR). Genes controlled by the LTTRs have diverse functional roles including amino acid biosynthesis, CO_2 fixation, antibiotic resistance, degradation of aromatic compounds, oxidative stress responses, nodule formation of nitrogen-fixing bacteria, synthesis of virulence factors, toxin production, attachment and secretion (Maddocks and Oyston 2008).

Translation, including ribosome structure and biogenesis

Five proteins were detected induced in this category.
The cysteinyl-tRNA synthetase (ACA_0293) (EC: 6.1.1.16) catalyzes the attachment of cystein to its cognate transfer RNA molecule (Delarue and Moras 1993).
The protein ACA_1884 is the ribosomal protein L29. It participates in forming a protein ring that surrounds the polypeptide exit channel, providing structural support for the ribosome (Hashimoto *et al.* 1993).
The protein ACA_2581 is annotated as an endoribonuclease L-PSP (liver perchloric acid-soluble protein). In rats it causes inhibition of protein synthesis by cleaving mRNA and affecting mRNA template activity. In addition, this gene functions in purine biosynthesis and in negative regulation of translation (Morishita *et al.* 1999).

The protein ACA_1898 is the translation Initiation Factor IF1. It contains a RNA-binding domain, which is found in a wide variety of RNA-associated proteins (Croitoru *et al.* 2006)

Signal transduction

5 proteins belonging to in the category were found.
Among them, 3 proteins belong to the sigma 54 Fis family transcriptional regulators (ACA_2232; ACA_1137; ACA_2615). These activators of the sigma 54-holoenzyme are members of the large AAA+ protein family, which use ATP binding and hydrolysis to remodel their substrates. The greater part of the central domain of sigma 54 activators corresponds to the AAA core structure, and includes ATP-binding and hydrolyzing determinants. The sigma 54 protein is known to be the primary target for the NTPase of activators (Chaney *et al.* 2001).
The hypothetical protein (ACA_1270) contains a PAS/PAC domain. Proteins containing a PAS domain are direct oxygen sensors and PAS-domain containing proteins are known to detect their signal by way of an associated cofactor as heme, flavin, or 4-hydroxycinnamyl chromophore (Delgado-Nixon *et al.* 2000).
The protein ACA_0317 is annotated as the chemotaxis regulator CheY. In bacteria with active chemotaxis systems, these proteins localize to the cell poles and information is transferred to the flagellar motors through the phosphorylation of a soluble CheY form. This phosphorylated CheY (CheY-P) interacts with the flagellar switch consisting of FliM, FliN, and FliG in *E. coli*. FliM has been shown to directly interact with CheY-P and induce change of direction of flagellar rotation (Rao *et al.* 2005; Szurmant *et al.* 2003).

General functional prediction only

Ten proteins found to be induced in S^0 grown cells fell into the poorly characterized categories. Two proteins (ACA_0165; ACA_0669) are annotated as flavoproteins.
BlastP results of ACA_1144 and ACA_1140 led only to other hypothetical proteins. ACA_1144 possesses a tetratricopeptide repeat region (TPR repeat; pfam13414). This is a structural motif present in a wide range of proteins, involved in cell cycle regulation, transcriptional control, mitochondrial and peroxisomal protein transport, neurogenesis and protein folding (Lamb *et al.* 1995).

The hypotethical protein ACA_2411 contains a Roadblock/LC7 domain. Members of this family of proteins are associated e.g. with flagellar outer arm motor protein (Bowman *et al.* 1999). This family also includes Golgi-associated MP1 adapter protein and MglB from *Myxococcus xanthus*, a protein involved in gliding motility. However, the family also includes members from non-motile bacteria such as *Streptomyces coelicolor*, suggesting that the protein may play a structural or regulatory role (Stephens *et al.* 1989).

BlastP results with the hypothetical protein ACA_1244 showed 41% identity to phosphoglycerate mutase (PGM) of *Neisseria shayeganii* 871, see also page 61.

Two proteins (ACA_1589 and ACA_2802) were predicted to contain an ATP-dependent protease La (LON) domain; pfam02190.

The hypothetical protein encoded by ACA_1585 contains a region belonging to SO_family_MoCo Superfamily: Sulfite oxidase (SO) family, molybdopterin binding domain. This molybdopterin cofactor (MoCo) binding domain is found in a variety of oxidoreductases. The main members of this family are nitrate reductase (NR) and SO, which catalyzes the terminal reaction in the oxidative degradation of the sulfur-containing amino acids cysteine and methionine. Assimilatory NRs catalyze the reduction of nitrate to nitrite, which is subsequently converted to NH_4^+ by nitrite reductase. NR and SO are found in several bacteria, as *E. coli* or *Desulfovibrio desulfuricans* (Kappler and Bailey 2004; Loschi *et al.* 2004; Moura *et al.* 2004).

No functional prediction

Nine proteins were found to belong to this category.

The hypothetical proteins encoded by ACA_0091 and ACA_0163 may belong to DsrE/DsrF-like family: DsrE is a small soluble protein involved in intracellular sulfur reduction encoded e.g. in the *dsr* gene region of the phototrophic sulphur bacterium *Chromatium vinosum*. (Pott and Dahl 1998; see also chapter 4.4.2)

Several proteins in this category were found in COGs with „uncharacterized Acient Conserved Region (ACR)“ protein function, meaning that portions of the gene sequences are highly conserved, reflecting evolutionary constraints placed upon these regions.

ACA_0136 encodes a prevent-host-death family protein related to the Phd_YefM, type II toxin-antitoxin system. When bound to their toxin partners, they can bind DNA

via the N terminus and repress the expression of operons containing genes encoding the toxin and the antitoxin (Garcia-Pino *et al.* 2010).

ACA_0538 encodes a propeptide PepSY. This signature, PepSY, is found in the propeptide of members of the MEROPS peptidase family M4, which contains the thermostable thermolysins (EC: 3.4.24.27), and related thermolabile neutral proteases (bacillolysins; EC: 3.4.24.28) from various species of Bacillus (Yeats *et al.* 2004). The hypothetical protein ACA_0321 contains a domain similar to the FliW protein from *Bacillus subtilis*, which has been characterized as a flagellar assembly factor (Titz *et al.* 2006).

The protein ACA_0211 contains a L,D-transpeptidase catalytic domain (former called ErfK/YbiS/YcfS/YnhG family), which has been suggested to be involved in peptidoglycan metabolism (Biarrotte-Sorin *et al.* 2006).

The hypothetical protein ACA_0092 contains a PQQ-dependent dehydrogenasedomain. This domain is also found in tetrathionate hydrolases. In addition, BlastP results matched with a putative tetrathionate hydrolase (53 % max. identity) from an acid mine drainage metagenome sequence (CBH95240.1).

The protein ACA_0755 contains a domain belonging to the carboxymuconolactone decarboxylase family, which catalyzes 2-carboxy-2,5-dihydro-5-oxofuran-2-acetate <=> 4,5-dihydro-5-oxofuran-2-acetate + CO_2. It belongs to the family of lyases, specifically the carboxy-lyases, which cleave carbon-carbon bonds (Ito *et al.* 2006).

ACA_0744 encodes a protein partially belonging to the YbjQ_1 Superfamily, which is a putative heavy-metal-binding protein.

Not in COGs

Twelve proteins could not be classified to belong to any COG category. However, very often these hypothetical proteins were identical with hypothetical proteins encoded in *At. caldus* SM-1 genome sequence.

The hypothetical protein ACA_2408 gave 45% max. identity in BlastP results with Lferr_2205 (*At. ferrooxidans*). It is annotated as a response regulator receiver protein. It acts as phosphorylation-activated switch to affect a cellular response, usually by transcriptional regulation. This domain receives the signal from the sensor partner in a two-component system (Pao and Saier 1995).

The NHL repeat, found in the protein ACA_2237, named after NCL-1, HT2A or Lin-41, is found largely in a large number of eukaryotic and prokaryotic proteins. For example, the repeat is found in a variety of enzymes of the copper type II, ascorbate-dependent monooxygenase family, which catalyses the C terminus alpha-amidation of biological peptides (Husten and Eipper 1991).
ACA_2769 encodes a putative carboxysome peptide A. The carboxysome is a bacterial microcompartment that functions as a simple organelle by sequestering enzymes involved in carbon fixation (Tanaka *et al.* 2008).
The hypothetical protein ACA_0662 contains a domain similar to Hemerythrin (Hr), which is a non-heme di-iron oxygen transport protein found in marine invertebrate phyla, in protozoa and a broader collection of bacterial and archaeal homologues. In prokaryotes many hemerythrin proteins are multi-domain proteins containing signal-transducing domains. It might also be involved in cadmium fixation and host anti-bacterial defense (Takagi and Cox 1991).
The RuBisCO small subunit (ACA_2766) is also found here. The function of RuBisCO is already discussed in “carbohydrate metabolism and transport”.

Table 15 shows the 13 proteins found to be induced in proteomes from thiosulfate grown samples.

Table 15: Proteins induced in thiosulfate samples. COGs numbers are shown for each protein in order to get information about their putative functions:

Proteins found in the COG categories for: energy production and conversion (C); coenzyme metabolism (H); inorganic ion transport and metabolism (P) replication, recombination and repair (L); translation (K), including ribosome structure and biogenesis and signal transduction (T); transport and amino acid metabolism and transport (E); secretion, motility and chemotaxis (N) and "poorly characterized" (R and S)

Gene description	Locus tag	Reg S/TS	T-test ≤ 0.05	GB	Some remarks	COG category
Phosphoenolpyruvate carboxylase	ACA_1379	-1.74	0.045	ZP_05293702	**COG2352** (Phosphoenolpyruvate carboxylase) **EC: 4.1.1.31**	C
ATP synthase gamma chain	ACA_0977	-1.53	0.033	ZP_05292309	**COG0224** (F0F1-type ATP synthase gamma subuni) **EC: 3.6.3.14**	C
NADH dehydrogenase, subunit 5	ACA_1268	-4.26	0.030	ZP_05293190	**COG1009** (NADH:ubiquinone oxidoreductase subunit 5 (chain L)/Multisubunit Na+/H+ antiporter, MnhA subunit) **COG0651** (Formate hydrogenlyase subunit 3/Multisubunit Na+/H+ antiporter, MnhD subunit)	CP; CP
N-succinyl-L,L-diaminopimelate aminotransferase alternative	ACA_0762	-3.59	0.001	ZP_05293275	**COG0436** (PLP-dependent aminotransferases) **EC: 2.6.1.17**	E
Thiamin biosynthesis protein ThiC	ACA_2622	-3.21	0.047	ZP_05291741	**COG0422** (Thiamine biosynthesis protein ThiC)	H
3-methyl-2-oxobutanoatehydroxy methyltransferase	ACA_0373	-1.54	0.011	ZP_05293446	**COG0413** (Ketopantoate hydroxymethyltransferase) **EC: 2.1.2.11**	H
2-octaprenyl-3-methyl-6-methoxy-1,4-benzoquinol hydroxylase	ACA_2539	-4.03	0.001	ZP_05293669	**COG0654** (2-polyprenyl-6-methoxyphenol hydroxylase and related FAD-dependent oxidoreductases) **EC: 1.14.13.-**	H; C
Phage antirepressor protein	ACA_1546	-4.08	0.050	ZP_05293973	**COG3561** (Phage anti-repressor protein)	K
Ribonuclease III	ACA_2635	-2.96	0.017	ZP_05291754	**COG0571** (dsRNA-specific ribonuclease) **EC: 3.1.26.3**	K
regulatory protein, ArsR	ACA_0465	-2.54	0.049	ZP_05294001	**COG0187** (DNA gyrase (topoisomerase II) B subunit) **COG0642** (Signal transduction histidine kinase)	L; T
hypothetical protein	ACA_2563	-1.62	0.013	ZP_05293941	**COG0840** (Methyl-accepting chemotaxis protein)	N
hypothetical protein	ACA_0896	-2.49	0.041	ZP_05292228	**COG0767** (ABC-type toluene export system, permease component)	R
hypothetical protein	ACA_2798	-1.55	0.013	ZP_05293124	**COG0393** (Uncharacterized ACR)	S

In case of proteomes from thiosulfate grown cells 4 proteins were classified to belong to in the energy production and conversion COG category (C). ACA_1379 encodes a phosphoenolpyruvate carboxylase (PEPCase), which supplies oxaloacetate to the TCA cycle requiring continuous input of C_4 molecules in order to replenish the intermediates removed for amino acid biosynthesis (Eikmanns *et al.* 1989).

The protein ACA_0977 protein is annotated as an ATP synthase (γ chain).
The protein ACA_1268 is the NADH-ubiquinone oxidoreductase chain 5. This complex (complex I) catalyzes the transfer of two electrons from NADH to ubiquinone in a reaction that is associated with proton translocation across the membrane (Walker 1992).
The last protein classified in this category is ACA_2539, the 2-octaprenyl-3-methyl-6-methoxy-1,4-benzoquinol hydroxylase. This protein probably belongs to the FAD-dependent hydroxylases (monooxygenases), which are all believed to act in the aerobic ubiquinone biosynthesis pathway (Meganathan 2001).
The protein ACA_0762 was classified in the amino acid metabolism and transport COG category (E). It is annotated as a N-Succinyl-LL-diaminopimelate aminotransferase (DAP-AT). This is a key enzyme in the bacterial L-lysine biosynthetic pathway (Cox *et al.* 1996).
Three proteins were classified in the COG category “coenzyme metabolism” (H). One is the thiamine biosynthesis protein ThiC (ACA_2622; Begley *et al.* 1999).
The protein ACA_0373 is annotated as 3-methyl-2-oxobutanoate hydroxymethyltransferase, also called ketopantoate hydroxymethyltransferase (KPHMT). It catalyzes the first step in the biosynthesis of pantothenate (vitamin B5), the precursor of coenzyme A and the acyl carrier protein cofactor (von Delft 2003).
Two proteins were classified in the COG category “transcription” (K). One is the phage antirepressor protein ACA_1546. The protein ACA_2635 is the ribonuclease III. This ubiquitous enzyme specifically cleaves double-stranded rRNA and is found in all bacteria and eukaryotes (Conrad and Rauhut 2002). In bacteria its main role is the processing of pre-rRNAs, where the large precursor ribosomal RNA molecules are cleaved at specific sites to produce the immediate precursors of the functional molecules.
Some proteins, which were found to be induced, are classified in other COG categories. The protein ACA_0465 is annotated as an ArsR regulatory protein. This finding supports the differential ultilization of ArsR type regulators in *At. caldus,* since the protein ACA_2532, also annotated as ArsR type regulator, was found to be induced in proteomes of S^0 grown cells.
The hypothetical protein encoded by ACA_2563 induced was classified also in COG0840 (Methyl-accepting chemotaxis protein), as well as ACA_0837, which was

found to be induced on S^0, suggesting also differential chemotactic behaviours among S^0 and thiosulfate grown cells.
Another hypothetical protein is encoded by ACA_0893. BlastP results showed 57 % max. identity with an ABC-type transporter, a permease component involved in toluene tolerance [beta proteobacterium KB13]. This protein is probably part of the ABC transporter complex ykoCDEF that could transport hydroxymethylpyrimidine (HMP) and/or thiamine (Poretsky *et al.* 2010).
Finally, BlastP results of the last hypothetical protein (ACA_2798) found to be induced on thiosulfate indicated only to other hypothetical proteins. No gene encoding a homologues protein was found in the *At. caldus* SM-1 genome. A part of this protein is predicted to belong to the YbjQ_1 superfamily. From comparative structural analysis this family is likely to be a heavy-metal binding domain. One protein (ACA_0744) belonging to this family was also found to be significantly induced in S^0 grown cells.

The 11 proteins found to be up-regulated on thiosulfate grown cells are shown in the annex (Table S2).

4.4.2 **Proteins related to sulfur metabolism**

Since this is the first high troughput proteomic study performed in *At. caldus,* a search of proteins related to sulfur metabolism was done. Two putative Sox systems are encoded in the genome. However, $Sox(CD)_2$ is missing in this bacterium. Sox systems in *At. caldus* might catalyze sulfite or thiosulfate oxidation with low activity or when forming S^0 globules. The latter has not been reported in *At. caldus* until now. No gene encoding direct sulfite oxidation like SAR has been found in either the type strain (Valdes *et al.* 2009) or *At. caldus* SM-1 (You *et al.* 2011). Also, no candidate gene encoding the enzyme APS- reductase has been found (Mangold *et al.* 2011). However, the presence of some genes like *sat* and *dsrABC* could indicate indirect sulfite oxidation.
The *At. caldus* genome also possesses a *sor* gene, two putative orthologs of *hdr* and two orthologs of *sqr*. Also the Tth has been purified and products of its reaction are thiosulfate and pentathionate (Bugaytsova and Lindström 2004). The gene *tth* is located in a putative operon with genes in the following order: *IsaC1* (transposase), *rsrR*, *rsrS* (two component transcriptional regulator system), *tth*, *doxD* (quinol oxidase

subunit) and *IsaC2* (transposase). Dsr proteins found in the genome of *At. caldus* (DsrEFH and DsrC) are proposed to be involved in S^0 substrate binding and transport of S^0 from the periplasmic S^0 globules to the cytoplasm (Cort *et al.* 2008). Fig. 19 shows these enzymes and the respective organization of their encoding genes in putative operons. Also the proteins found in this study are highlighted.

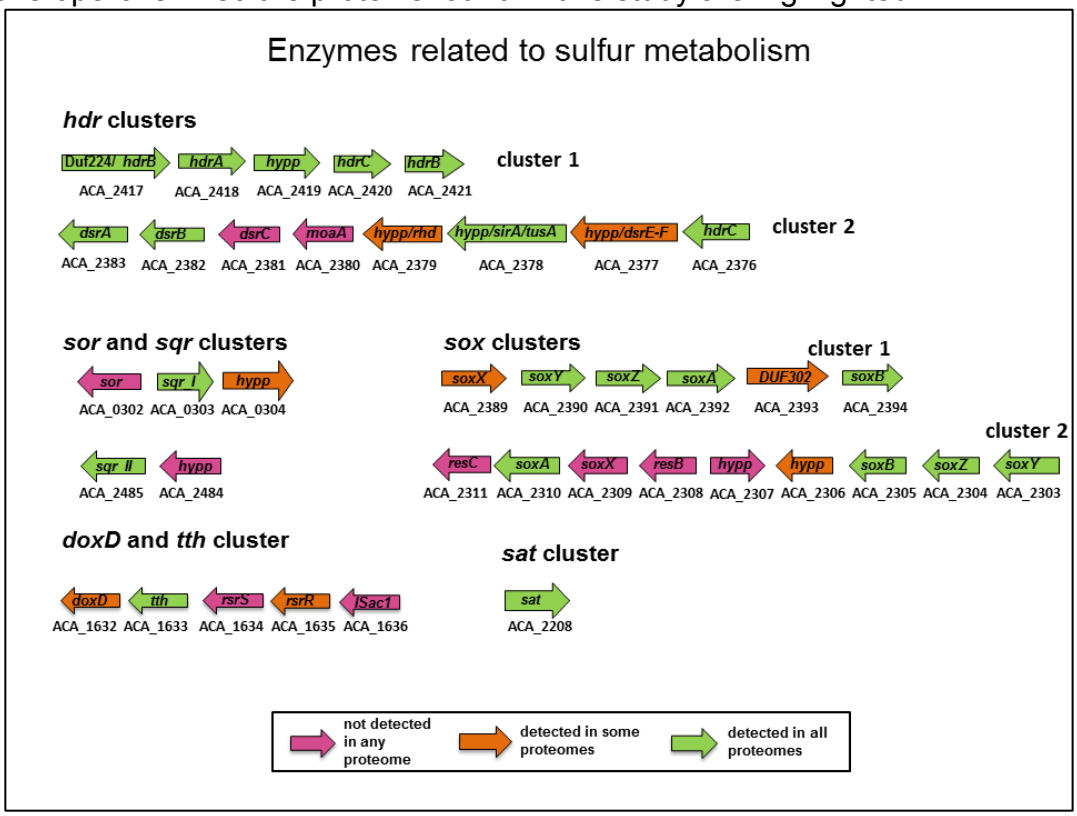

Fig. 20: Gene clusters of enzymes potentially involved in ISC metabolism, as derived from proteomic results.

Gene clusters and gene orientation are taken from the gene data base of the NCBI (www.ncbi.nlm.nih.gov).

Relevant genes/ proteins are abbreviated as follows: *sox*, sulfur oxidation system; *doxD*, thiosulfate:quinol oxidoreductase; *tth*, tetrathionate hydrolase; *hdr*, heterodisulfide reductase; *sqr*, sulfide quinone reductase; *sor*, sulfur oxygenase reductase; *dsr*, dimethyl sulfoxide reductase; *muoA*, molybdenum cofactor biosynthesis protein A; *sirA*, sulfurtransferase; *rsr*, two component regulator; *Isac1*, transposase; *rhd,* rhodanase-like protein; *sat*, sulfate adenylyltransferase; *res*, cytochrome c-type biogenesis protein; *DUFxxx*, protein of unknown function; *hypp*, hypothetical protein.

The following tables (Table 16- 20) summarize the results for proteins related to the sulfur metabolism of *At. caldus*.

The following Legend should describe all abbreviations used in the following Tables 16-25.

Legend:

Product name = protein name of the gene annotated in the genome according to the data base of the NCBI

Short cut = abbreviation, which is often used for the gene/ protein name

GB = GeneBank accession number of proteins used in NCBI

Locus_tag = locus tag of the *At. caldus* type strain gene used in genome databases

COG(s) = number of the cluster of the ortholog group

reg S/TS = gives the log2 (normalized spectral count) ratio between the protein counts found between sulfur and thiosulfate grown cells. If the log2 was greater than 1,5 for a protein, this protein was considered to be induced in sulfur grown cells. When log2 ratio was less than −1.5, the protein was considered to be induced in thiosulfate grown cells. Calculation were done for n=8 proteomes.

t-test = Statistical Student's t-test *p* values of n=8 proteomes

Table 16: Proteomic data of heterodisulfide reductase (Hdr) complexes in *At. caldus*

A) Hdr cluster 1

Product name	Short cut	GB	Locus_tag	COG(s)	reg S/TS	t-test
Heterodisulfide reductase chain B	Duf224 (HdrB)	ZP_05291837	ACA_2417	COG2048	0.78	0.243
Heterodisulfide reductase chain A	HdrA	ZP_05291838	ACA_2418	COG1148	-0.11	0.993
Hypotetical protein	Hypp	ZP_05291839	ACA_2419	not in COGs	-1.02	0.376
Heterodisulfide reductase chain C	HdrC	ZP_05291840	ACA_2420	COG1150	0.15	0.792
Heterodisulfide reductase chain B	HdrB	ZP_05291841	ACA_2421	COG2048	-0.05	0.933

B) Hdr cluster 2

Product name	Short cut	GB	Locus_tag	COG(s)	reg S/TS	t-test
Heterodisulfide reductase chain C	HdrC	ZP_05291796	ACA_2376	COG1150	-0.18	0.641
Hypotetical protein (dimethyl sulfoxide reductase chain E/F-like)	Hypp (DsrE/DsrF)	ZP_05291797	ACA_2377	COG2210	2.21	0.196
Hypotetical protein (Sulfurtransferase)	Hypp (SirA)	ZP_05291798	ACA_2378	COG0425	0.32	0.580
Hypotetical protein (Rhodanase)	Hypp (Rhd)	ZP_05291799	ACA_2379	COG0607	2.67	0.059
Molybdenum cofactor biosynthesis protein A	MoaA	ZP_05291800	ACA_2380	COG2896	/	/
Dimethyl sulfoxide reductase chain C	DsrC	ZP_05291801	ACA_2381	COG3302	/	/
Dimethyl sulfoxide reductase chain B	DsrB	ZP_05291802	ACA_2382	COG0437	-0.15	0.583
Dimethyl sulfoxide reductase chain A	DsrA	ZP_05291803	ACA_2383	COG0243	0.25	0.642

In cells of *At. caldus* two orthologs of heterodisulfide reductase (Hdr; EC 1.8.98.1) have been found in the genome (Table 16A and 16B). It catalyses the reversible

reduction of the heterodisulfide (CoM-S-S-CoB) to the thiol-coenzymes: coenzyme M (H-S-CoM) and coenzyme B (H-S-CoB). Hdr is composed of three subunits: hdrA (subunit A), hdrB (subunit B) and hdrC (subunit C; Madadi-Kahkesh *et al.* 2001). Cluster I was found in all proteomes (Table 16A). BlastP results of the hypothetical protein (ACA_2419) lead only to other hypothetical proteins. However, it has 69 % max. identity with a protein found in *At. ferrooxidans* (AFE_2552), which is found in the same context of a Hdr complex of *At. ferrooxidans* (Quatrini *et al.* 2009). Furthermore, in *At. caldus* SM-1 this hypothetical protein is also found in a Hdr complex with 92 % max. identity (Atc_2349).
The predicted rhodanese (ACA_2379) was found to be induced in S^0 grown cells.

The Hdr has been discussed in the connection with sulfate adenylyltransferase (Sat), ACA_2309 (EC: 2.7.7.4; Quatrini *et al.* 2009). It forms adenosine 5'-phosphosulfate (APS) from ATP and free sulfate, the first step in the formation of the activated sulfate donor 3'-phosphoadenylylsulfate (PAPS; Rosenthal and Leustek 1995). It uses the formed APS by SirA/ Rhd to form sulfate and ATP (Fig. 32). It was found in all proteomes of S^0 grown cells and in two thiosulfate proteomes (reg S/TS: 2.41; t-test: 0.116).

Table 17: Proteomic data of sulfur oxidizing (Sox) complexes in *At. caldus*
A) Sox cluster 1

Product name	Short cut	GB	Locus_tag	COG(s)	reg S/TS	t-test
Sulfur oxidizing protein X	SoxX	ZP_05291809	ACA_2389	not in COGs	2.30	0.191
Sulfur oxidizing protein Y	SoxY	ZP_05291810	ACA_2390	not in COGs	-0.40	0.603
Sulfur oxidizing protein Z	SoxZ	ZP_05291811	ACA_2391	not in COGs	0.59	0.113
Sulfur oxidizing protein A	SoxA	ZP_05291812	ACA_2392	not in COGs	0.00	0.998
Protein of unknown function	Duf302	ZP_05291813	ACA_2393	COG3439	1.65	0.300
Sulfur oxidizing protein B	SoxB	ZP_05291814	ACA_2394	COG0737	0.18	0.712

B) Sox cluster 2

Product name	Short cut	GB	Locus_tag	COG(s)	reg S/TS	t-test
Cytochrome c-type biogenesis protein, chain C	ResC	ZP_05291685	ACA_2311	COG0755	/	/
Sulfur oxidizing protein A	SoxA	ZP_05291686	ACA_2312	not in COGs	-0.87	0.305
Hypothetical protein/ sulfur oxidizing protein X	Hypp/ SoxX	ZP_05291687	ACA_2313	not in COGs	/	/
Cytochrome c-type biogenesis protein, chain B	ResB	ZP_05291688	ACA_2314	COG1333	/	/
Protein of unknown function	Hypp/ ResC	ZP_05291689	ACA_2315	not in COGs	/	/
Hypopthetical protein	Hypp	ZP_05291690	ACA_2316	not in COGs	0.08	0.960
Sulfur oxidizing protein B	SoxB	ZP_05291691	ACA_2317	COG0737	-1.84	0.104
Sulfur oxidizing protein Z	SoxZ	ZP_05291692	ACA_2318	not in COGs	-1.41	0.030
Sulfur oxidizing protein Y	SoxY	ZP_05291693	ACA_2319	not in COGs	-0.66	0.358

In the Sox cluster 1(Table 17A) only SoxX is up-regulated in S^0 grown cells. In the Sox cluster 2 (Table 17B), the proteins ResB and ResC were not found in any proteome. These proteins might be essential proteins in system II c-type cytochrome biogenesis (Feissner *et al.* 2005). The hypothetical protein ACA_2313 was also not found in any proteome. The BlastP results suggested this protein to be a paralog of SoxX, since they share 92 % identity with SoxX (ACA_2389) and 100 % identity with SoxX of *At. caldus* SM-1 (Atc_2212).

Table 18: Proteomic data of the DoxD and TTH complex in *At. caldus*

Product name	Short cut	GB	Locus_tag	COG(s)	reg S/TS	t-test
Putative terminal quinol oxidase, subunit DoxD	DoxD	ZP_05294206	ACA_1632	COG2259	-1.90	0.336
Tetrathionate hydrolase	Tth	ZP_05294207	ACA_1633	COG1520	-2.13	0.091
Integral membrane sensor signal transduction histidine kinase	RsrS	ZP_05294208	ACA_1634	COG0642	/	/
Two-component system response regulator OmpR	OmpR/ RsrR	ZP_05294209	ACA_1635	COG0745	-0.21	0.843
Transposase, mutator type	ISac1	ZP_05294210	ACA_1636	COG3328	/	/

In the DoxD and TTH cluster the proteins RsrS and ISac1 were not found in any proteome. RsrS belongs with RsrR to a two component response regulator system enabling the cells to sense, respond, and adapt to a wide range of environments, stressors, and growth conditions. ISac1 encodes a transposase. TTH and DoxD were up-regulated in thiosulfate grown cells. The proteins are responsible for the oxidation of thiosulfate to tetrathionate (DoxD/ TQO) by reducing a quinone or for regenerating thiosulfate by a reduction of tetrathionate,

Table 19: Proteomic data of the Sor and Sqr complexes in *At.caldus*

A) Sor and Sqr cluster 1

Product name	Short cut	GB	Locus_tag	COG(s)	reg S/TS	t-test
Sulfur oxygenase reductase	Sor	ZP_05293375	ACA_0302	not in COGs	/	/
Sulfide-quinone reductase	Sqr_I	ZP_05293376	ACA_0303	COG0446 COG1252	0.42	0.52
Hypothetical protein	Hypp	ZP_05293377	ACA_0304	not in COGs	-0.26	0.26

B) Sqr cluster 2

Product name	Short cut	GB	Locus_tag	COG(s)	reg S/TS	t-test
Hypothetical protein	Hypp	ZP_05293614	ACA_2484	COG1187	/	/
Sulfide-quinone reductase	Sqr_II	ZP_05293615	ACA_2485	COG0446 COG1252	-0.74	0.22

The Sor enzyme was not detected in any proteome. Furthermore, the *sor* gene is divergent to the *sqr_I* (ACA_0303) gene, which is located in a potential transcription unit together with a hypothetical protein (ACA_0304). Sqr_I was found in all proteomes (Table 19A). It is responsible for the oxidation of sulfide to S^0. BlastP and COG analysis of this hypothetical protein (ACA_0304) resulted only in "unknown function" predictions. In the second Sqr cluster (Table 19B), Sqr_II was also found in all proteomes. The hypothetical protein (ACA_2484) which encoding gene is adjacent to *sqr_II*, was not found in any proteome. This hypothetical protein includes a region with similarities to a S4/Hsp/ tRNA synthetase RNA-binding domain, which has also been found in proteins related to stress respons, ribosomal proteins and tRNA synthetases (Aravind and Koonin 1999).

4.4.3 **Proteins related to respiratory complexes**

At. caldus is able to fix CO_2. The energy for this fixation is obtained from the electron transfer pathway. NADH ubiquinone oxidoreductase (EC: 1.6.5.3) is a respiratory-chain enzyme that catalyzes the transfer of two electrons from NADH to ubiquinone in a reaction that is associated with proton translocation across the membrane (NADH + ubiquinone = NAD^+ + ubiquinol; Walker 1992). In general, the bacterial complex consists of 14 different subunits (*nuoA* to *nuoN*).

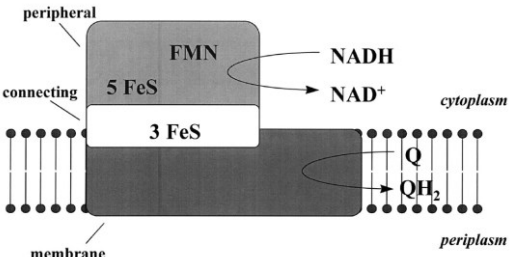

Fig. 21: Schema of NADH complex 1 in *E. coli*.
The complex consits of tree distinct fragments: the peripheral (light gray), connecting (white) and membrane fragments (Falk-Krzesinski and Wolfe 1997). FMN, flavin mononucleotide; Q, ubiquinone; FeS, iron-sulfur cluster.

In *E. coli* it consists of three subcomplexes referred to as the peripheral (NuoE, NuoF, and NuoG), connecting (NuoB, NuoC, NuoD, and NuoI), and membrane fragments (NuoA, NuoH, NuoJ, NuoK, NuoL, NuoM, and NuoN). NuoG is essential for this complex. It plays a role in the regulation of *nuo* expression and/ or its assembly (Falk-Krzesinski and Wolfe 1997). In the reaction mechanism, two electrons are carried to the flavin mononucleotide (FMN) prosthetic group. The electrons are then transferred through the second prosthetic group of NADH dehydrogenase via a series of iron-sulfur (Fe-S) clusters, and finally to coenzyme Q (ubiquinone), which accepts two electrons to be reduced to ubiquinol (CoQH2).

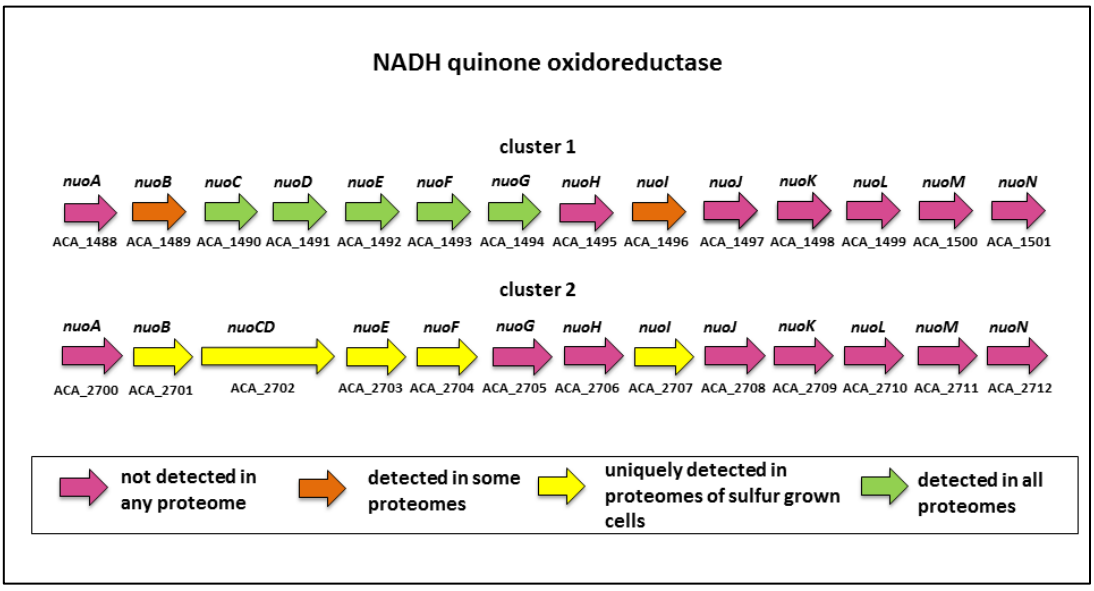

Fig. 22: Gene clusters for proteins in the NADH quinone oxidoreductase of *At. caldus* in correlation with proteomic data.
Gene clusters and gene orientation are taken from the gene database of the NCBI (www.ncbi.nlm.nih.gov).

Detailed information on the proteomic results of NADH quinone oxidoreductase components proteins is shown in the Annex (Table S3).

Within the cluster 1 only NuoB-NuoF and NuoI were found in the proteomes (Fig. 21). NuoB-NuoF showed no differential regulation between S^0 and thiosulfate grown cells, but NuoI was found to be up-regulated in S^0 grown cells. The proteins encoded in the second gene cluster were found in S^0 grown cells, with Nuo E and NuoI were induced. All proteins of the connecting part of the NADH ubiquinone oxidoreductase were detected in all proteomes, as well as most of the proteins belonging to the peripheral fraction. No membrane, (NuoA, NuoH, NuoJ-NuoN) components were identified in this analysis (Fig.21; Table S3)

Terminal oxidases

When bacteria grow in aerobic environments, the terminal electron acceptor O_2 is reduced to water by oxidases. Cytochrome bo_3 is a membrane bound terminal oxidase catalyzing the oxidation of ubiquinol and the reduction of oxygen to water in a process coupled to a translocation of protons across the cell membrane. It belongs to the family of heme-copper oxidases, which also includes aa_3-type cytochrome C oxidases (Garcia-Horsman *et al.* 1995). In the genome of the *At. caldus* type strain two complexes of this bo_3 type and one of the aa_3 type are present (Mangold *et al.* 2011). Complex 1 is composed of the proteins ACA_0257 till ACA_0262, complex 2 of ACA_1043 till ACA_1046 and complex aa_3 at ACA_2321 till ACA_2324. Furthermore, 6 complexes of the cytochrome bd type are encoded in the genome (complex 1: ACA_0473 till ACA_0476; complex 2: ACA_0525 till ACA_0529; complex 3: ACA_1110 till ACA_1114; complex 4: ACA_1968 till ACA_1971; complex 5: ACA_2069 till ACA_2072; complex 6: ACA_2616 till ACA_2619).

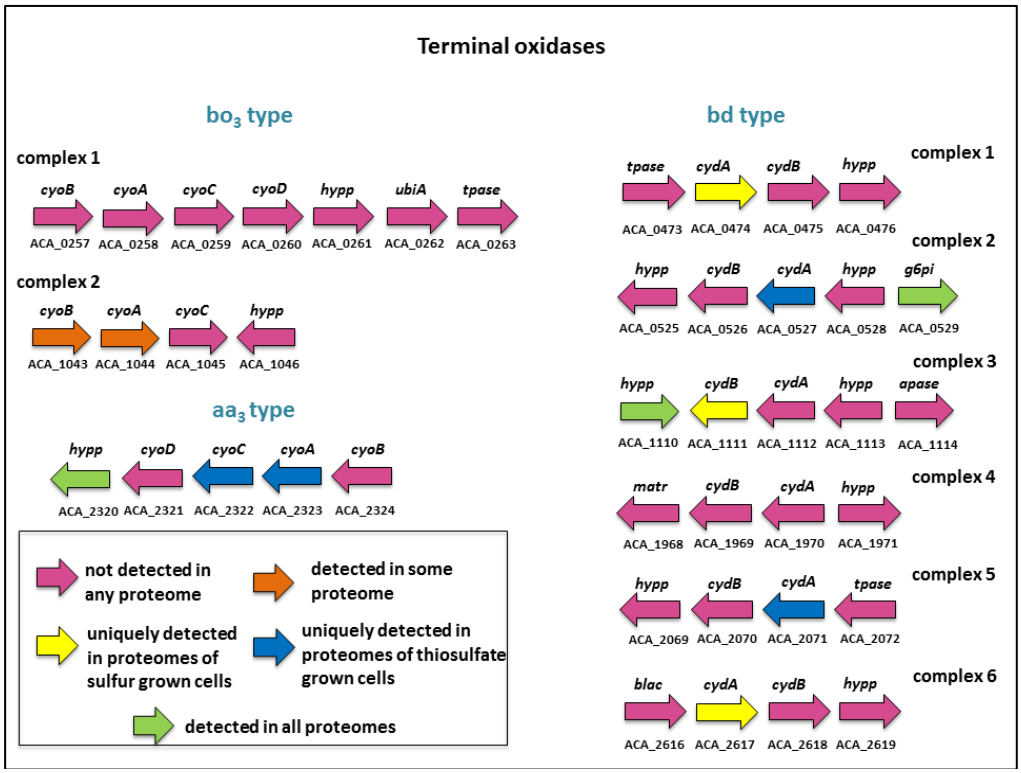

Fig. 23: Gene clusters of the terminal oxidases probably involved in electron transfer for respiration in *At. caldus*, in correlation with the proteomic data.

Gene clusters and gene orientation are taken from the gene database of the NCBI (www.ncbi.nlm.nih.gov).

Arrows indicate gene direction in the genome. Abbreviations: *cyoA*: cytochrome O ubiquinol oxidase I; *cyoB*: cytochrome O ubiquinol oxidase II; *cyoC*: cytochrome O ubiquinol oxidase III; *cyoD*: cytochrome O ubiquinol oxidase IV; *ubiA*: Heme O synthase, protoheme IX farnesyltransferase; *hypp*: hypothetical proteins; *tpase*: transposase; *cydA*: cytochrome d ubiquinol oxidase, subunit I; *cydB*: cytochrome d ubiquinol oxidase, subunit II. *g6pi*: glucose-6-phosphate isomerase; *apase*: amino acid permease; *matr*: C4-dicarboxylate transporter/ malic acid transport protein; *blac*: beta-lactamase domain protein. For details see text.

Detailed information on the proteomic results of the terminal oxydase proteins is shown in the Annex (Table S4).

None protein encoded in the gene cluster bo_3 (complex 1, Fig. 22) was detected in this study.

The hypothetical protein ACA_2320 in the aa_3 type cluster (Fig. 22) was found in all proteomes and BlastP results pointed only to other hypothetical proteins. Many proteins (ACA_2071; ACA_2617; ACA_2322; ACA_2323 and ACA_1111) of the terminal oxidases were only found in one out of eight proteome Thus, they have no statistical relevance. The glucose-6-phosphate isomerase (ACA_0529) was found in all proteomes. This is a multifunctional enzyme which as an intracellular dimer catalyzing the reversible isomerization of glucose-6-phosphate to fructose-6-phosphate.

The hypothetical protein (ACA_1110) was found in all proteomes. It has a region predicted to be a putative transmembrane protein.
The protein CydA (ACA_2617) of bd complex 6 was found to be induced in S^0 grown cells.

4.4.4 **Proteins related to carbon metabolism**

In comparison with the knowledge accumulated on RISC oxidation and energy metabolism, much little has been done to study CO_2-fixation and central metabolism of carbon compounds in cells of *At. caldus*. Uptake and fixation of the CO_2 under extremely acidic condition has been less studied. However, recently a form II ribulose-1,5-bisphosphate carboxylase/ oxygenase (RubisCO) was shown to be expressed in *At. ferrooxidans* suggesting that this could promote the ability to fix CO_2 at different concentrations of CO_2 (Esparza *et al.* 2010). The *At. caldus* SM-1 genome has been analyzed with focus on the central carbon metabolism (You *et al.* 2011). Five clusters involved in the classical Calvin-Bassham-Benson (CBB) cycle were found encoded in the genomes of both the *At. caldus* SM-1 and the *At. caldus* type strain. The product of the CBB is glucose. This is the educt metabolized in the Embden-Meyerhof-Parnas pathway (EMP; also called glycolysis) to build pyruvate wich is further metabolized in the citrate cycle (TCA). The central role of the TCC is to regerenate the used ATP and $NADPH^+ + H^+$ which are required in other metabolism pathways e.g. CBB. Additionally, phospholiated glucose is used in the pentose phosphate pathway (PPP). It is a process of glucose turnover that produces $NADPH + H^+$ as reducing equivalents and pentoses as essential parts of nucleotides. In this thesis, the presence of the proteins involved in the EMP, TCA and the PPP were analyzed in the context of our proteomic results. However, due to the big amount of data, proteomic tables and detailed proteomic analyses are only directly presented here in case of the CBB cycle. All other detailed information of the other carbon pathways is given in the Annex.

Calvin Bassham- Benson cycle

The CBB cycle is one of 6 possible carbon fixation pathways present in autotrophic bacteria and archaea. They differ in reducing copounds, energy source and oxygen sensitivity of enzymes (Berg 2011). The key enzymes of the CBB cycle are RubisCO and phosphoribulokinase. The cycle is divided in 3 phases: 1. CO_2 fixation,

2. Reduction of 3-PG and 3. Regeneration of ribulose-1,5-bisphosphate. Genes involved in the CBB cycle of *At. caldus* are given in Fig. 23.

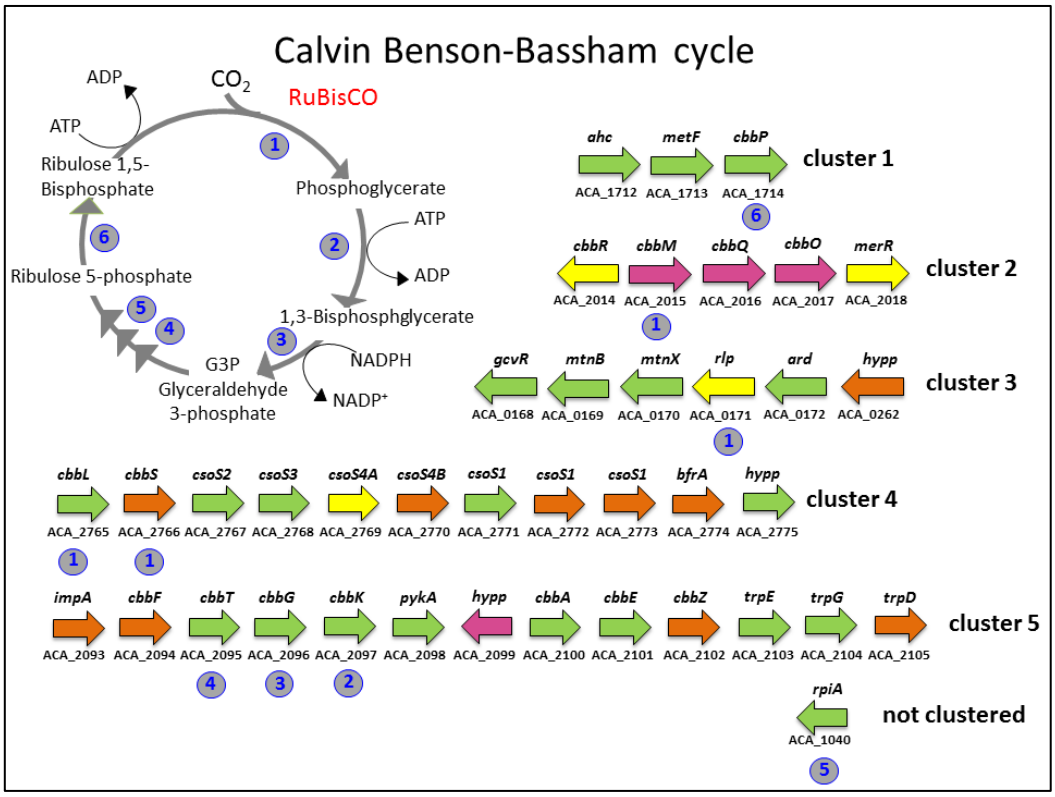

Fig. 24: **The CBB cycle of *At. caldus* in relation to the proteomic data.**
Gene clusters and gene orientation are taken from the gene database of the NCBI (www.ncbi.nlm.nih.gov).
Numbers in the CBB cycle indicate the enzymes involved in this cycle: 1. RuBisCO; 2. Transketolase; 3. NAD-dependent glyceraldehyde-3-phosphate dehydrogenase; 4. Phosphoglycerate kinase; 5. Ribose 5-phosphate isomerase A and 6. Phosphoribulokinase. Arrows in the clusters indicates gene oriantation in the genome: green = protein found in all proteomes; orange = protein found in some proteomes; yellow = proteins found only proteomes of S^0 grown cells. For more details see text.
Abbreviations: *ahc*: Adenosylhomocysteinase; *metF*: 5,10-methylenetetrahydrofolate reductase; *cbbP*: Phosphoribulokinase; *cbbR*: transcriptional regulator, PadR-like family; *cbbM*: Ribulose bisphosphate carboxylase; *cbbQ* and *cbbO*: Rubisco activation protein; *merR*: Transcriptional regulator, MerR family; *gcvR*: Glycine cleavage system transcriptional antiactivator; *mtnB*: Methylthioribulose-1-phosphate dehydratase; *mtnX*: 2-hydroxy-3-keto-5-methylthiopentenyl-1- phosphate phosphatase; *rlp*: 2,3-diketo-5-methylthiopentyl-1-phosphate enolase; *ard*: 1,2-dihydroxy-3-keto-5-methylthiopentene dioxygenase; *hypp*: hypothetical protein; *cbbL*: Ribulose bisphosphate carboxylase large chain; *cbbS*: Ribulose bisphosphate carboxylase small chain; *csoS1-csoS4*: carboxysome shell protein; *bfrA*: bacterioferritin possible associated with carboxysome; *impA*: Myo-inositol-1(or 4)-monophosphatase; *cbbF*: Fructose-1,6-bisphosphatase, GlpX type; *cbbT*: Transketolase; *cbbG*: NAD-dependent glyceraldehyde-3-phosphate dehydrogenase; *cbbK*: Phosphoglycerate kinase; *pykA*: Pyruvate kinase; *cbbA*: Fructose-bisphosphate aldolase class II; *cbbE*: Ribulose-phosphate 3-epimerase; *cbbZ*: Phosphoglycolate phosphatase; *trpE*: Anthranilate synthase, aminase component; *trpG*: Anthranilate synthase, amidotransferase component; *trpD*: Anthranilate phosphoribosyltransferase; *cbbFA*: Fructose-bisphosphate aldolase, archaeal class I; *rpiA:* Ribose 5-phosphate isomerase A; *tim*: Triosephosphate isomerase.

Phase 1. CO_2 fixation:

RubisCO catalyzes the electrophilic addition of CO_2 to the C_5 sugar ribulose-1,5-bisphosphate (RuBP) in its enediolate form, giving rise to an unstable C_6 intermediate. This splits immediately in half, forming two molecules of 3-phosphoglycerate (3-PG).

Phase 2. Reduction of 3-PG:

The 3-PG is further reduced with NADPH to glyceraldehyde-3-phosphate (G3P; GAP) by dehydrogenase. In each cycle one CO_2 molecule is fixed. Conseqeuntly, it needs 3 cycles to give one G3P molecule free for biosynthesis.

Phase 3. Regeneration of ribulose-1,5-bisphosphate:

The regeneration part of ribulose-1,5-bisphosphate in the cycle comprises the interconversion of triose phosphates via various sugar phosphates to ribulose-5-phosphate, which is phosphorylated by phosphoribulokinase to RuBP, closing the cycle (Fig. 23).

The total reaction bilanz is given as follows:

$6CO_2 + 12\ NADPH + H^+ + 18\ ATP \rightarrow C_6H_{12}O_6 + 12\ NADP^+ + 18\ ADP + 18\ P_i + 6\ H_2O$

Tables 20 and 21 show the proteomic data regarding the CBB clusters (Fig. 23). Abbreviations used in these tables are explained in the Legend page 78.

Table 20: Proteomic data of the CBB clusters in *At. caldus*

A) Cluster 1

Product name	Short cut	GB	Locus_tag	COG(s)	reg S/TS	t-test
Adenosylhomocysteinase	Ahc	ZP_05292612	ACA_1712	COG0499	-0.61	0.065
5,10-methylenetetrahydrofolate reductase	MetF	ZP_05292613	ACA_1713	COG0685	-0.90	0.106
Phosphoribulokinase	CbbP	ZP_05292614	ACA_1714	not in COGs	0.30	0.435

All three proteins were found in all proteomes. No significant differential regulation could be detected between S^0 and thiosulfate grown cells.

B) Cluster 2

Product name	short cut	GB	Locus_tag	COG(s)	reg S/TS	t-test
transcriptional regulator, PadR-like family	CbbR	ZP_05293568	ACA_2014	COG1695	0.58	0.391
Ribulose bisphosphate carboxylase	CbbM	ZP_05293569	ACA_2015	COG1850	/	/
Rubisco activation protein CbbQ	CbbQ	ZP_05293570	ACA_2016	COG0714	/	/
Rubisco activation protein CbbO	CbbO	ZP_05293571	ACA_2017	not in COGs	/	/
Transcriptional regulator, MerR family	MerR	ZP_05293572	ACA_2018	COG1396	3.21	0.001

Rubisco activation protein CbbQ (ACA_2016) and CbbO (ACA_2017) belong to a family of proteins, which play a role in the post-translational activation of RubisCO

(Hayashi *et al.* 1999). Both together the protein CbbM (ACA_2015) were not detected in any proteome. Form II RubisCO proteins were shown to catalyze the same reaction as is done by form I RubisCO (comprised of a large and a small subunit). Both enzymes catalyze as a sidereaction an oxygen fixation reaction, whereby the enediol (unsaturated diols of the form R-C(OH)=C(OH)-R) of RuBP is attacked by molecular oxygen. In general, the form II enzyme, comprised only of multimers of the large-subunits, shows only about 30% amino acid sequence identity to form I large subunits of the photosynthetic bacterium *Rhodospirillum rubrum* (Tabita *et al.* 2008). The same is valid for *At. caldus*, where 32 % max protein sequence identity of CbbM (ACA_2015) is shared with the large sununit of RuBisCO, CbbL (ACA_2765).

C) Cluster 3

Product name	Short cut	GB	Locus_tag	COG(s)	reg S/TS	t-test
Glycine cleavage system transcriptional antiactivator	GcvR	ZP_05291872	ACA_0168	COG2716	0.13	0.756
Methylthioribulose-1-phosphate dehydratase	MtnB	ZP_05291873	ACA_0169	COG0235	-0.65	0.099
2-hydroxy-3-keto-5-methylthiopentenyl-1-phosphate phosphatase	MtnX	ZP_05291874	ACA_0170	COG0560	-0.10	0.751
2,3-diketo-5-methylthiopentyl-1-phosphate enolase	RLP	ZP_05291875	ACA_0171	COG1850	4.02	0.001
1,2-dihydroxy-3-keto-5-methylthiopentene dioxygenase	Ard	ZP_05291876	ACA_0172	COG1791	-0.88	0.195
Uncharacterized conserved protein	Hypp	ZP_05291877	ACA_0173	COG1496	0.08	0.955

GcvR (ACA_0168) is a protein required for the glycine cleavage enzyme system (Ghrist and Stauffer 1995) and ACA_0169 and ACA_0170 encode proteins involved in a methionine salvage pathway. This pathway allows methylthioadenosine, left over from polyamine biosynthesis, to be recycled to methionine (Sekowska *et al.* 2004).

The protein ACA_0171, found to be induced in S^0 grown cells, is an homologue of the large subunit of RuBisCO. This RuBisCO-like protein (RLP), nowadays classified as RubisCO form IV (EC: 5.3.2-), catalyzes in *B. subtilis* cells the 2,3-diketo-5-methylthiopentyl-1-phosphate enolase reaction in the methionine salvage pathway.

The uncharacterized conserved protein (ACA_0172) contains a protein region belonging to a multicopper polyphenol oxidase (laccase), COG1496.

D) Cluster 4

Product name	Short cut	GB	Locus_tag	COG(s)	reg S/TS	t-test
Ribulose bisphosphate carboxylase large chain	CbbL	ZP_05293091	ACA_2765	COG1850	-0.13	0.730
Ribulose bisphosphate carboxylase small chain	CbbS	ZP_05293092	ACA_2766	not in COGs	2.85	0.101
carboxysome shell protein CsoS2	CsoS2	ZP_05293093	ACA_2767	not in COGs	-1.08	0.063
carboxysome shell protein CsoS3	CsoS3	ZP_05293094	ACA_2768	not in COGs	-1.09	0.241
putative carboxysome peptide A	CsoS4A	ZP_05293095	ACA_2769	not in COGs	3.12	0.001
putative carboxysome peptide B	CsoS4B	ZP_05293096	ACA_2770	not in COGs	1.82	0.144
carboxysome shell protein CsoS1	CsoS1	ZP_05293097	ACA_2771	not in COGs	-0.43	0.615
carboxysome shell protein CsoS1	CsoS1	ZP_05293098	ACA_2772	not in COGs	2.33	0.164
carboxysome shell protein CsoS1	CsoS1	ZP_05293099	ACA_2773	not in COGs	-0.33	0.856
bacterioferritin possible associated with carboxysome	BfrA	ZP_05293100	ACA_2774	COG2193	2.33	0.083
hypothetical protein	Hypp	ZP_05293101	ACA_2775	not in COGs	0.97	0.422

RuBisCO is often found packaged in organelles called carboxysomes, which are polyhedral cytoplasmatic inclusion bodies. These are considered to enhance CO_2 fixation by increasing the concentration of HCO_3^- in the organelle, where is it converted to CO_2 by carbonic anhydrases in the immediate vicinity of RuBisCO (So *et al.* 2004; Kinney *et al.* 2011). Consequently, carboxysomes are metabolic modules for CO_2 fixation that are found in all cyanobacteria and some chemoautotrophic bacteria. Cluster 4 is also known as carboxysome operon, which has been investigated in *Halothiobacillus neapolitanus* and *At. ferrooxidans* (Baker *et al.* 1999; Esparza *et al.* 2010). The amount of peptides belonging to this operon varies between 7 and 15 (Shively and English 1991). CbbL (ACA_2765) and CbbS (ACA_2765) are the large and small subunits of the RuBisCO form I. The big subunit was found in all proteomes, wheras the small subunit was found to be up-regulated in proteomes from S^0 grown cells. The following 7 proteins in this putative operon are the carboxysome shell proteins and associated ones, including a bacterioferritin (BfrA; also known as cytochrome b1 or cytochrome b557; ACA_2774), which is predicted in *E. coli* as an iron-storage protein consisting of 24 identical subunits. It was also found to be up-regulated in S^0 grown cells.

The hypothetical protein (ACA_2775) contains a region predicted to belong to the PCD_DCoH superfamily, working as both a transcription activator and a metabolic enzyme (Rose *et al.* 2004).

E) Cluster 5

Product name	Short cut	GB	Locus_tag	COG(s)	reg S/TS	t-test
Myo-inositol-1(or 4)-monophosphatase	ImpA	ZP_05292343	ACA_2093	COG0483 COG1218	1.54	0.183
Fructose-1,6-bisphosphatase, GlpX type	CbbF	ZP_05292344	ACA_2094	COG1494	-0.35	0.621
Transketolase	CbbT	ZP_05292345	ACA_2095	COG0021	0.41	0.314
NAD-dependent glyceraldehyde-3-phosphate dehydrogenase	CbbG	ZP_05292346	ACA_2096	COG0057	0.38	0.667
Phosphoglycerate kinase	CbbK	ZP_05292347	ACA_2097	COG0126	0.15	0.726
Pyruvate kinase	pykA	ZP_05292348	ACA_2098	COG0469	0.56	0.218
hypothetical protein	Hypp	ZP_05292349	ACA_2099	not in COGs	/	/
Fructose-bisphosphate aldolase class II	CbbA	ZP_05292350	ACA_2100	COG0191	0.42	0.661
Ribulose-phosphate 3-epimerase	CbbE	ZP_05292351	ACA_2101	COG0036	-0.18	0.567
Phosphoglycolate phosphatase	CbbZ	ZP_05292352	ACA_2102	COG0546 COG1011	-0.58	0.707
Anthranilate synthase, aminase component	TrpE	ZP_05292353	ACA_2103	COG0147	0.48	0.299
Anthranilate synthase, amidotransferase component	TrpG	ZP_05292354	ACA_2104	COG0512	-0.35	0.373
Anthranilate phosphoribosyltransferase	TrpD	ZP_05292355	ACA_2105	COG0547	1.92	0.145

Apart from the hypothetical protein ACA_2099, all proteins in this cluster were found (Cluster E). However, none of these shows a differential regulation between S^0 or thiosulfate grown cells. Several of these proteins here have more than one function and are also found in other context of carbon metabolism, like the glycolysis (ACA_2095; ACA_2096; ACA_2098; ACA_2100) or PPP (ACA_2095; ACA_2101).

The transketolase (CbbT; EC: 2.2.1.1; ACA_2095) catalyzes the reversible transfer of a two-carbon ketol unit from xylulose 5-phosphate to an aldose receptor. Together with transaldolase, provides a link between the glycolytic and pentose-phosphate pathways (Fletcher *et al.* 1992).

The NAD-dependent glyceraldehyde-3-phosphate dehydrogenase (CbbG; ACA_2096; EC: 1.2.1.12) is responsible for the interconversion of 1,3-diphosphoglycerate and glyceraldehyde-3-phosphate, a central step in glycolysis and gluconeogenesis. (Fillinger *et al.* 2000).

The phosphoglycerate kinase (CbbK; EC: 2.7.2.3; ACA_2097) is an enzyme that catalyzes the formation of ATP to ADP and vice versa. It is found in all living organisms and its sequence has been highly conserved throughout evolution (Yon *et al.* 1990).

Table 21: Proteomic data of other proteins involved in the calvin cycle in *At. caldus*

Product name	Short cut	GB	Locus_tag	COG(s)	reg S/TS	t-test
Fructose-bisphosphate aldolase, archaeal class I	CbbFA	ZP_05293468	ACA_1394	COG1830	0.19	0.731
Fructose-1,6-bisphosphatase, type I	CbbF	ZP_05292258	ACA_0926	COG0158	-0.07	0.775
Ribose 5-phosphate isomerase A	RpiA	ZP_05292874	ACA_1040	COG0120	-0.64	0.100
Triosephosphate isomerase	TIM	ZP_05291980	ACA_1486	COG0149	-1.05	0.099

Fructose-bisphosphate aldolase (EC: 4.1.2.13; ACA_1394) is a glycolytic enzyme that catalyzes the reversible aldol cleavage or condensation of fructose-1,6-bisphosphate into dihydroxyacetone-phosphate and glyceraldehyde 3-phosphate (Perham 1990) .
Ribose 5-phosphate isomerase (EC: 5.3.1.6; ACA_1040), also known as phosphoriboisomerase, catalyzes the reversible conversion of D-ribose 5-phosphate to D-ribulose 5-phosphate, the first step in the non-oxidative branch of the pentose phosphate pathway (Zhang *et al.* 2003).
Triosephosphate isomerase (TIM; ACA_1486; EC: 5.3.1.1) is the glycolytic enzyme that catalyzes the reversible interconversion of glyceraldehyde 3-phosphate and dihydroxyacetone phosphate (Alahuhta *et al.* 2008; Lolis *et al.* 1990).

Embden-Meyerhof-Parnas pathway (EMP), citrate cycle (TCA) and the pentose phosphate pathway (PPP)

For glucose metabolism *At. caldus* uses the Embden-Meyerhof-Parnas pathway, which is the most common sequence of reactions for the conversion of glucose-6-phosphate (glucose-6-P) into pyruvate in all domains of life (Romano and Conway 1996; Ronimus and Morgan 2003). Interestingly, the tagatose-6-phosphate kinase (ACA_1396) was found to be induced in proteomes from S^0 samples as well as all phosphoglycerate mutases (ACA_0756; ACA_2715; ACA_1231). The latter enzyme relocates the phosphate from 3-phosphoglycerate (3PG) to form 2-phosphoglycerate (2PG).
Considering the TCA, the cycle almost certainly evolved first as a reductive biosynthetic pathway in anaerobic organisms. It has a central role in the oxidative energy metabolism of aerobic organisms (Romano and Conway 1996). *At. caldus*, possess an incomplete TCA cycle since it lacks the genes encoding for the succinate dehydrogenase and 2-oxoglutarate dehydrogenase (You *et al.* 2011). The latter is a key enzyme, converting 2-oxoglutarate, coenzyme A and NAD^+ to succinyl-CoA, NADH and carbon dioxide. The succinate dehydrogenase (EC: 1.3.99.1) is responsible for the interconversion of fumarate and succinate and is used in aerobic growth (Horesfield *et al.* 2006). Appart from pyruvate dehydrogenase (acetyl-transferring; ACA_0754), which was found to be up-regulated in S^0 grown cells and the fumarase (ACA_1787), all proteins were detected in all proteomes.

The PPP is a process of glucose turnover producing NADPH as reducing equivalents and pentoses as essential parts of nucleotides. There are two different phases in the pathway. The first is an irreversible oxidative phase in which glucose-6P is converted to ribulose-5P by oxidative decarboxylation, and NADPH is generated. The other is a reversible non-oxidative phase, in which phosphorylated sugars are interconverted to generate xylulose-5P, ribulose-5P, and ribose-5P (Papagianni 2012). Apart from glucose-6P-1-dehydrogenase (G6PD; ACA_2792), which was found to be up-regulated in S^0 grown cells, all the other enzymes involved in PPP were found and did not show significantly differential regulation between S^0 and thiosulfate grown cells.
Detailed information of these proteomic results of these pathways are given in the Annex (7.1.5).

4.4.5 **Proteins related to EPS production and cell motility**

As it was already mentioned, leaching bacteria have a strong affinity towards metal sulfides (Rawlings 2002) and form biofilms on their surfaces, which are embedded in EPS (Fig. 1; Kinzler *et al.* 2003). EPS consist of different kinds of (poly-)saccharides, proteins, uronic acids, lipids and nucleic acids. Many authors distinguish polysaccharides with strong or with limited association with the cell surface. The latter is described as a component of the EPS, while the first is denoted as capsular polysaccharide (CPS). EPS and CPS are important parts mediating attachment, biofilm formation and leaching, as highlighted in the introduction. A bioinformatic search for putative CPS biosynthesis pathways in *At. caldus* was included in this work.
Earlier studies from our laboratory have shown that cells of *At. ferrooxidans* possess two systems for capsular polysaccharide biosynthesis and export (Fig. 25).

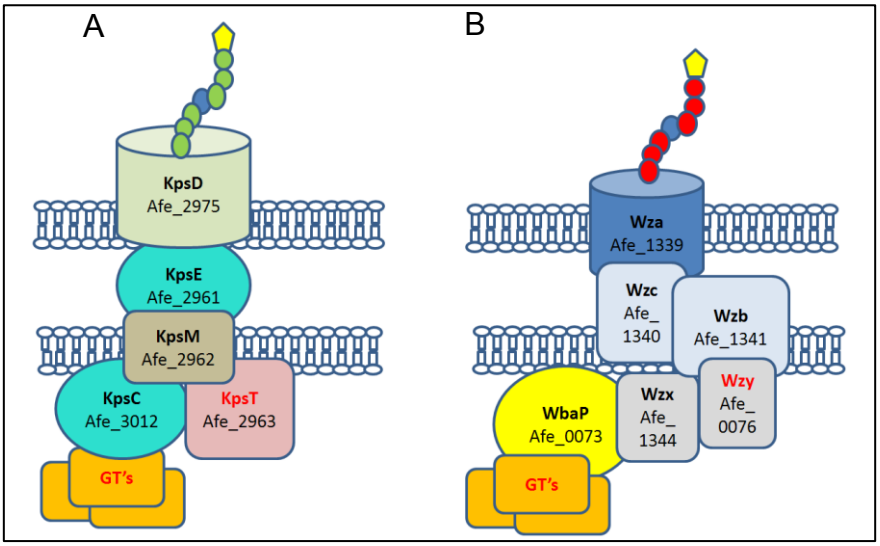

Fig. 25: Schemes for hypothetical capsular polysaccharide biosynthesis and export systems encoded in the *At. ferrooxidans* genome (from Bellenberg 2010).
(A): Kps (capsular polysaccharide biosynthesis) system, (B): Wz (export) system. Abbreviations of protein names were taken from (Whitfield and Roberts 1999): GT's: glycosyltransferases; KpsCand KpsD: capsular polysaccharide export system proteins; KpsT: capsular polysaccharide ABC transporter, ATP-binding protein; KpsM: capsular polysaccharide ABC transporter, permease protein; WbaP: cytoplasmic export system protein; Wzx: Inner membrane (integral) export system protein. Transfers nascent undecaprenyl diphosphate-linked repeat units across the inner membrane. Wzy: Inner membrane (integral) export system protein with periplasmic catalytic site. Putative polymerase; assembles undecaprenyl diphosphate-linked polymers using lipid-linked repeat units exported by Wzx; Wzb: cytoplasmic export system protein tyrosine phosphatase; dephosphorylates Wzc; Wza: outer membrane export system proteins.It forms a multimeric putative translocation channel andinteracts with the periplasmic domain of Wzc. The tail-formation indicate the built polysaccharide chain.

BlastP analyses of these *At. ferrooxidans* proteins in the *At. caldus* genome resulted in genes encoding probably a full set of genes homologues to the ones encoding the Kps-system (KpsE: ACA_2434; KpsM: ACA_2433; KpsT: ACA_2432; KpsD: ACA_2437; KpsC: ACA_1280). However, KpsD ACA_2437 shares also 62 % identity in export periplasmic protein WzA of *At. ferrooxidans*. The Wz- system might be incomplete, because Wzb and Wzc are missing and blastP analysis reveals the same hits for Wzx and Wzy of *At. ferrooxidans* (Wzx/Wzy: ACA_1861), annotated as membrane protein involved in the export of O-antigen and teichoic acids. In the genome of the type strain *At. caldus* several glycosyltransferases (GT's) are encoded. GT's are probably mediate monomer activation and assemblage in the polymer. In *At. caldus* GT's are present in gene clusters of flagella (ACA_0338 and ACA_0854). Additionally, a GT cluster in ACA_1855 till ACA_1860 is also flanked from the potential Wz(xy) protein ACA_1861. However, neither the proteins of this GT cluster nor ACA_1861 were detected in our proteomic studies. The following

Tables 22-25 show only the proteins which could be detected regarding the Kps-System (Table 22), the type IV secretion system (T4SS; Table 23), the formation of flagella (Table 24) and proteins related to chemotaxis, motility and EPS production (Table 25). Abbreviations used in these tables are explained in the Legend page 78.

Table 22: Proteomic data of the proposed Kps-system proteins in *At. caldus*

Product name	short cut	GB	Locus_tag	COG(s)	reg S/TS	t-test
Capsular polysaccharide export system inner membrane protein KpsE	KpsE	ZP_05293224	ACA_2434	COG3524	-0.83	0.312
Capsular polysaccharide ABC transporter, permease protein KpsM	KpsM	ZP_05293223	ACA_2433	COG1682	/	/
Capsular polysaccharide ABC transporter, ATP-binding protein KpsT	KpsT	ZP_05293222	ACA_2432	COG1134	-0.80	0.391
Capsular polysaccharide biosynthesis/export periplasmic protein WcbC	KpsD/ Wza	ZP_05293227	ACA_2437	COG1596	1.50	0.231
Capsule polysaccharide biosynthesis	KpsC	ZP_05293202	ACA_1280	COG3563	/	/

KpsM and KpsC were not detected in any proteome (Table 22).

Apart from these two systems, a type IV secretion system (T4SS) is involved in pili biogenesis controlling phenotypes such as twitching motility and biofilm formation (Filloux 2011). Also in some microorganisms, an analogous system (probably emerged by gene duplication) is involved in DNA transformation (Chen and Dubnau 2004). In the genome of the type strain of *At. caldus* 21 genes are found annotated with the T4SS (ACA_0920 till ACA_0923; ACA_2737; ACA_2738; ACA_2743; ACA_1359 till ACA_1363; ACA_0281 till ACA_0286; ACA_1266; ACA_1574; ACA_0175; ACA_0426; ACA_0427 and ACA_0807). Table 23 shows only the 8 detected proteins associated with the T4SS. All other proteins (13) related to T4SS were not detected in any proteome.

Table 23: Summarized proteomic data of proteins associated with the T4SS in *At. caldus*

Product name	short cut	GB	Locus_tag	COG(s)	reg S/TS	t-test
Type IV fimbrial assembly, ATPase PilB	PilB	ZP_05292252	ACA_0920	COG2804	1.83	0.255
Two-component response regulator PilR	PilR	ZP_05292254	ACA_0922	COG2204	0.81	0.391
Twitching motility protein	PilT	ZP_05292050	ACA_2737	COG2805	0.56	0.106
Probable component of the lipoprotein assembly complex (forms a complex with YaeT, YfgL, and NlpB)	YfiO	ZP_05291879	ACA_0175	COG0457	-1.00	0.046
Type IV pilus biogenesis protein PilQ	PilQ	ZP_05293686	ACA_1363	COG1450	3.32	0.000
Peptidase S49-like protein	ClpP	ZP_05293069	ACA_2743	COG0616	-0.58	0.328
type IV pilus biogenesis/stability protein PilW	PilW	ZP_05293312	ACA_1574	COG3063 COG0457	-0.30	0.600
PilU	PilU	ZP_05294019	ACA_0807	COG2804 COG2805	0.83	0.391

At. caldus is motile and comprises three gene cluster encoding in total 81 proteins for assampling flagella (ACA_0325 till ACA_0365, ACA_0838 till ACA_0862 and ACA_1415 till ACA_1419). Only 11 proteins were detected and are summarized in Table 24.

Table 24: Proteomic data of proteins associated with the formation of flagella in *At. caldus*

Product name	short cut	GB	Locus_tag	COG(s)	reg S/TS	t-test
Glycosyltransferase	GT	ZP_05293411	ACA_0338	COG1216 COG0463	2.86	0.150
Flagellin protein flaB	FlaB	ZP_05293412	ACA_0339	COG1344	2.33	0.076
Hypothetical protein	Hypp	ZP_05293416	ACA_0343	not in COGs	0.83	0.391
Flagellar sensor histidine kinase fleS	FleS	ZP_05293418	ACA_0345	COG0642	-0.93	0.391
Flagellar motor switch protein fliG	FliG_1	ZP_05293422	ACA_0349	COG1536	-1.50	0.182
Flagellar assembly protein fliH	FliH	ZP_05293423	ACA_0350	COG1317	3.00	0.002
RNA polymerase sigma factor for flagellar operon	FliA	ZP_05293437	ACA_0364	COG1191	-0.93	0.391
Flagellar motor switch protein FliN	FliN	ZP_05294058	ACA_0846	COG1886	2.19	0.096
Flagellar motor switch protein fliG	FliG_2	ZP_05294061	ACA_0849	COG1536	0.46	0.726
Glycosyltransferase	GT	ZP_05294066	ACA_0854	COG1216 COG0463	-1.04	0.623
Flagellar biosynthesis protein fliL	FliL	ZP_05293489	ACA_1415	COG1580	2.04	0.113

FlaB (ACA_0339) was found to be up-regulated in S^0 grown cells. Flagellin is the protein subunit that polymerizes to form the flagellae (Kuwajima *et al.* 1986). The Flagellin the subunits are transported through the centre of the filament to the tip, where they polymerize (Nuijten *et al.* 1990).

Furthermore, three flagellar motor switch proteins were detected. In general, a flagellar motor switch protein regulates the direction of flagellar rotation and swimming behaviour in certain bacteria (Brown *et al.* 2002) and probably works in th same way in *At. caldus*. FlhA, FliH, FliI and FliN are also suggested to be involved in the process of flagellum-specific export (Vogler *et al.* 1991).

In Table 25, the proteins related to chemotaxis are summarized. In bacterial chemotaxis, cellular movement is directed in response to chemical gradients. Transmembrane chemoreceptors that sense the stimuli are coupled (via CheW) with a signal transduction histidine kinase (CheA). CheA phosphorylates the response regulators CheB and CheY. The two cytoplasmic proteins, CheW and CheA, contain both homologues SH3-like domains that interact with transmembrane chemoreceptors, or methyl accepting chemotaxis proteins (MCPs). In CheA, a histidine protein kinase domain is fused to the amino-terminus of the SH3 region. CheV is a third type of protein with a CheW-like domain. The *At. caldus* proteins were compared to proteins related to biofilm formation in *Leptosperillum* spp. (Moreno-Paz

et al. 2010). The proteins with were annotated in the genome and could be detected in some proteomes are presented in Table 25.

Table 25: Proteomic data of proteins related to chemotaxis, motility and EPS production in *At. caldus*

Product name	short cut	GB	Locus_tag	COG(s)	reg S/TS	t-test
Osmosensitive K+ channel histidine kinase KdpD	KdpD	ZP_05292562	ACA_0007	COG2205	0.88	0.527
Signal recognition particle, subunit Ffh SRP54	SRP	ZP_05292802	ACA_0101	COG0541	-0.39	0.805
Chemotaxis protein CheV	CheV	ZP_05293385	ACA_0312	COG0835 COG0745 COG0784	2.31	0.188
Signal transduction histidine kinase CheA	CheA	ZP_05293388	ACA_0315	COG0643	3.94	0.071
Chemotaxis regulator - transmits chemoreceptor signals to flagelllar motor components CheY	CheY	ZP_05293390	ACA_0317	COG0745 COG0784	2.96	0.042
Probable methyl-accepting chemotaxis protein	CheW	ZP_05294049	ACA_0837	COG0840	2.46	0.042
Protein-export membrane protein secF	SecF	ZP_05294137	ACA_2041	COG0341	0.67	0.579
Protein-export membrane protein SecD	SecD	ZP_05294138	ACA_2042	COG0342	1.75	0.289
Response regulator receiver modulated diguanylate cyclase/phosphodiesterase	REC	ZP_05293628	ACA_2498	COG0745 COG2200	0.59	0.391

The KdpD sensor kinase proteins regulate the *kdp*FABC operon responsible for potassium transport (Treuner-Lange *et al.* 1997). These genes are also found upstream flanked to *kdpD* gene in the *At. caldus* genome.

Allmost all chemotaxis proteins found in the proteomes are induced or up-regulated in S^0 grown cells.

4.5 Purity test of *At. caldus* S1 and S2

Microscopy of *At. caldus* S1 and S2 showed sporulation randomly during culturing. Since *At. caldus* doesn't form spores, this was the first indication, that the culture *At. caldus* S1 could be contaminated, possibly with *Sulfobacillus*. Nested 16S rDNA PCR with primers for both genera was applied.

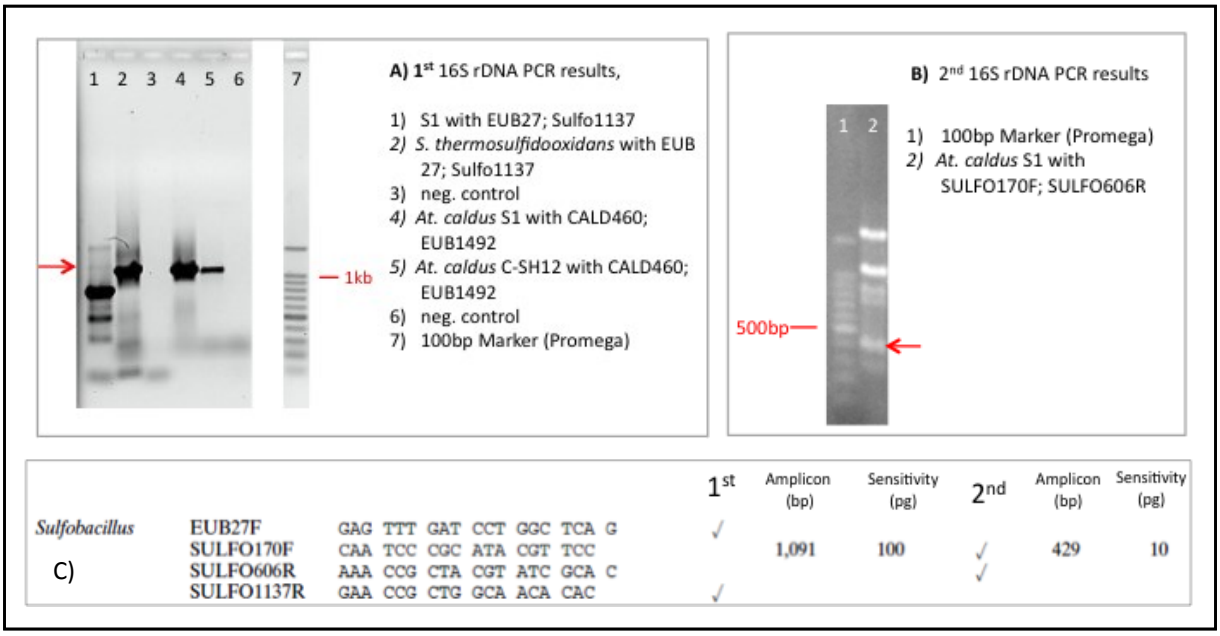

			1st	Amplicon (bp)	Sensitivity (pg)	2nd	Amplicon (bp)	Sensitivity (pg)
Sulfobacillus	EUB27F	GAG TTT GAT CCT GGC TCA G	√					
	SULFO170F	CAA TCC CGC ATA CGT TCC		1,091	100	√	429	10
C)	SULFO606R	AAA CCG CTA CGT ATC GCA C				√		
	SULFO1137R	GAA CCG CTG GCA ACA CAC	√					

Fig. 26: Gels of nested PCR using *Sulfobacilli* and *At. caldus* primers for 16S rDNA with DNA of *At. caldus* S1, according to de Wulf-Durand *et al.* 1997.
For both PCRs the annealing T° was modified (see Table 3A) and a PCR touch-down program was used, starting with 10°C above the actual annealing T° with a decrease of 1°C per cycle to this annealing temperature for further 20 cycles. Electrophoresis was performed using 1.2 % agarose gels, 120V for 45 min. The gels were stained for 20 min by incubation in 0.2 µg/mL ethidium bromide in TAE, washed in water and photographed using a Biorad® GelDoc™ station.
A) Gel of the 1st 16S rDNA PCR, **B)** Gel of the 2nd 16S rDNA PCR. **C)** Shows the used primer and expected amplicons sizes, according to de Wulf-Durand *et al.* 1997.

The first PCR used for amplifying *Sulfobacillus* 16S rDNA, shows a faint band with the expected size. When this PCR product was used as template for the second 16S rDNA PCR, an amplicon with the expected size was clearly observed. Sequence analysis of this amplicon revealed a highest similarity with *Sulfobacillus* L15 (Annex 7.4).

All other PCR tests performed with primers for *At. thiobacillus*, *At. ferrooxidans*, *Leptospirilli* and *Archaea* were negative. The cells of *At. caldus* S2 showed the same results.

4.6 Sor sequences of *Acidithiobacillus caldus*

A *sor* gene is encoded in the type strain of *At. caldus*. Although Sor activity was measured in cells of *At. caldus* SM-1 (sor_{SB}), no *sor* gene was found in the genome of At. caldus SM-1. To answer the question of how conserved is the presence of *sor* in *At. caldus*, PCR with designed degenerated primers was used to screen *sor* in other *At. caldus* strains.

Positive *sor* gene amplicons were detected in almost all *At. caldus* strains, except for *At. caldus* strain 6. The amplicons of approx. 800 bp size were cloned and sequenced (Annex 7.3). A phylogenetic tree was done with the truncated aa sequences, as shown in Fig. 26.

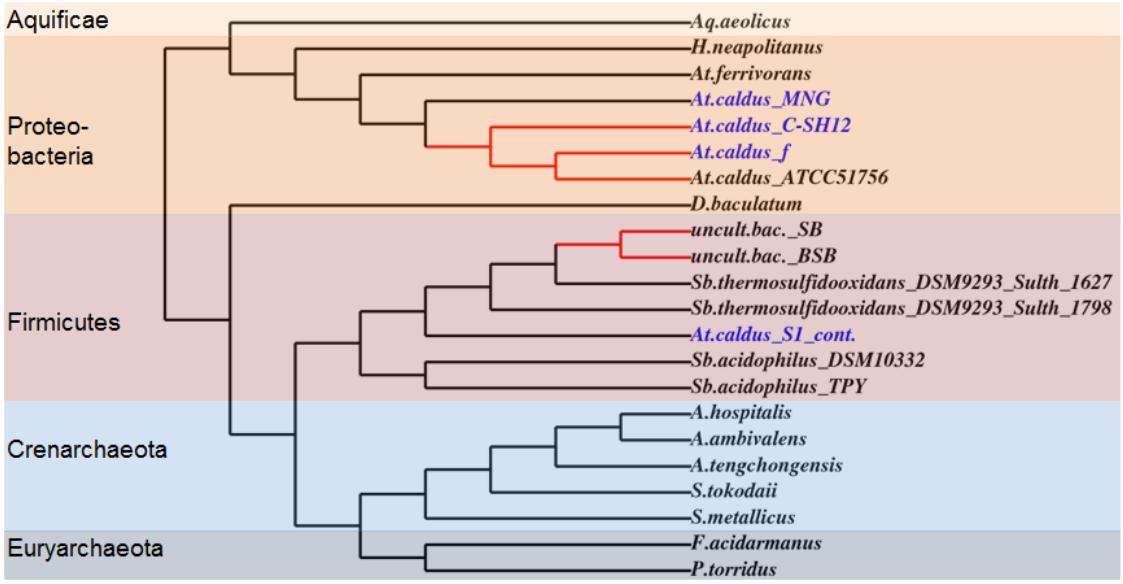

Fig. 27: Tree representation of the phylogenetic relation of Sor proteins from different microorganisms.
The microbial phyla are indicated in colored boxes. Blue lettering indicates sequences obtained in this study, red branches indicate no difference in amino acid sequences.
The Sor aa sequences of *Sb. thermosulfidooxidans* DSM 9293 (obtained from blast analysis using the recent genome sequence). *Aquifex aeolicus* VF5 (NP_21332), *H. neapolitanus* C2 (YP_003263105), *At. ferri*vorans SS3 (YP_004785009), *At. caldus* ATCC 51756 (ZP_05293375), *A. tengchongensis* (AAK58572), *A. ambivalens* (CAA39952), *A. hospitalis* (YP_004457322), *S. tokodaii* (NP_377053), *Picrophilus torridus* (AAT43386), *Ferroplasma acidarman*us fer1 (ZP_01708456), uncultured bacterium SB (ABF2054), uncultured bacterium BSB (ABF20540), *Desulfomicrobium baculatum* DSM 4028 (YP_003157691), *Sb. acidophilus* DSM 10332 (YP_005255611), *Sb. acidophilus* TPY (YP_004718350) and *S. metallicus* (ABN04222). Sor amplicons of *At. caldus* S1 and *At. caldus* S2 showed 100% identical aa sequences.

Sor amplicons of *At. caldus* S1 and *At. caldus* S2 showed 100% identical aa sequences. These sequences cluster in the Sulfobacilli branch, while all other *At. caldus* Sor sequences cluster in the Acidithiobacilli branch.

4.7 Genes involved in sulfur metabolism in *Sb. thermosulfidooxidans*

Sb. thermosulfidooxidans is able to oxidize S^0, thiosulfate and tetrathionate (Krasil´nikova *et al.* 1998). Very recently, the whole genome sequence of the type strain of *Sb. thermosulfidooxidans* was released. This allowed us to search for genes encoding proteins potentially involved in RISC oxidation pathways. The *At. caldus*

aa sequences of relevant proteins involved in this process were used for BlastP analysis in the JGI database and COG analysis were performed for confirmation of these results. Table 26 shows the genes potentially involved in the RISC metabolism of *Sb. thermosulfidooxidans*.

Two homologue genes encoding Sor and one Hdr cluster (Sulth_1021 till Sulth_1026) were found. Also *doxD* and 3 putative *tth* genes were identified. In contrast to the gene locations in *At. caldus, doxD* and *tth* were not found in one cluster in the genome of *Sb. thermosulfidooxidans.* One putative gene cluster of anaerobic dimethyl sulfoxide reductase *dsrABC* and *dsrEFH*-like (Sulth_2366 till Sulth_2369; Sulth_2769; Sulth_1046) were also identified. No genes encoding Sox proteins were found.

Table 26: Genes related to RISC in the type strain of *Sb. thermosulfidooxidans*

Proteins involoved in the RISC metabolism and annotated in the *At. caldus* type strain genome were used for BlastP analyses in the genome of the *Sb. thermosulfidooxidans* type strain.

Annotated protein function	Locus_Tag	max.identity of BlastP	Corresponding gene in *At. caldus*
Protein of unknown function DUF224 cysteine-rich region domain protein	Sulth_1022	59%	HdrB (ACA_2417)
Protein of unknown function DUF224 cysteine-rich region domain protein	Sulth_2771	50%	HdrB (ACA_2417)
FAD-dependent pyridine nucleotide-disulphide oxidoreductase	Sulth_1023	41%	HdrA (ACA_2418)
FAD-dependent pyridine nucleotide-disulphide oxidoreductase	Sulth_2772	40%	HdrA (ACA_2418)
Hypothetical protein	Sulth_1024	30%	Hypp (ACA_2419)
Iron-sulfur cluster-binding protein	Sulth_1025	32%	HdrC (ACA_2420)
Protein of unknown function DUF224 cysteine-rich region domain protein	Sulth_1026	38%	HdrB (ACA_2421)
Nitrate reductase	Sulth_2366	50%	DsrA (ACA_2383)
4Fe-4S ferredoxin iron-sulfur binding domain-containing protein	Sulth_2367	55%	DsrB (ACA_2382)
Hypothetical proteins	Sulth_2368	27%	DsrC (ACA_2381)
Molybdenum cofactor biosynthesis protein A	Sulth_0496	32%	MoaA (ACA_2380)
Rhodanase-like protein	Sulth_2335	35%	Hypp/Rhd (ACA_2379)
Rhodanase-like protein	Sulth_3294	31%	Hypp/Rhd (ACA_2379)
Rhodanase-like protein	Sulth_3040	30%	Hypp/Rhd (ACA_2379)
Rhodanase-like protein	Sulth_1878	29%	Hypp/Rhd (ACA_2379)
SirA-like domain-containing protein	Sulth_1018	52%	Hypp/SirA (ACA_2378)
SirA-like domain-containing protein	Sulth_2781	39%	Hypp/SirA (ACA_2378)
SirA-like domain-containing protein	Sulth_2070	28%	Hypp/SirA (ACA_2378)
Hypothetical protein/ DsrEFH-like	Sulth_2769	36%	Hypp/DsrEFH (ACA_2377)
DsrE family protein	Sulth_1046	31%	Hypp/DsrEFH (ACA_2377)
Hypothetical protein/ HdrC	Sulth_1021	52%	HdrC (ACA_2376)
Hypothetical protein/ HdrC	Sulth_2770	47%	HdrC (ACA_2376)
Sulfur oxygenase reductase	Sulth_1627	48%	Sor (ACA_0302)
Sulfur oxygenase reductase	Sulth_1798	47%	Sor (ACA_0302)
FAD-dependent pyridine nucleotide-disulphide oxidoreductase	Sulth_0548	65%	Sqr_1 (ACA_0303)
FAD-dependent pyridine nucleotide-disulphide oxidoreductase	Sulth_0946	62%	Sqr_1 (ACA_0303)
FAD-dependent pyridine nucleotide-disulphide oxidoreductase	Sulth_0580	58%	Sqr_1 (ACA_0303)
TQO small subunit DoxD domain-containing	Sulth_1689	34%	DoxD (ACA_1632)
Pyrrolo-quinoline quinone repeat-containing protein	Sulth_3251	54%	Tth (ACA_1633)
Pyrrolo-quinoline quinone repeat-containing protein	Sulth_0921	40%	Tth (ACA_1633)
Pyrrolo-quinoline quinone repeat-containing protein	Sulth_1188	31%	Tth (ACA_1633)
Sulfate adenylyltransferase	Sulth_1366	39%	Sat (ACA_2309)
Sulfate adenylyltransferase	Sulth_1433	38%	Sat (ACA_2309)
Adenylyl-sulfate kinase	Sulth_1435	44%	Sat (ACA_2309)
Adenylyl-sulfate kinase	Sulth_1355	40%	Sat (ACA_2309)

4.8 Results of Sor and Sdo enzyme activity tests

Crude extracts of *Sb. thermosulfidooxidans*, *At. ca*ldus type strain, *At. caldus* MNG, *At. caldus* f, *At. caldus* C-SH12 and *S. metallicus* were tested for Sor and Sdo activity. Since the cultures of *At. caldus* S1 and S2 were found to be contaminated with a *Sulfobacillus* strain, the respective enzymatic activity data are not shown.

4.8.1 Enzyme assays with addion of external GSH

As mentioned, after addition of GSH, the activity of thiol group depending sulfur oxygenase like Sdo is measured. It was calculated by the sum of the produced sulfite, sulfate and thiosulfate in the enzyme assays as described (Rohwerder *et al.* 2003). Table 27 show activity values for *Sb. thermosulfidooxidans*, *S. metallicus* and the *At. caldus* type strain. All results were corrected with relation to the internal standard, the phosphate concentration. The contribution of all abiotic factors to the values (assays with BSA) was subtracted.

Table 27: Specific Sdo acitivity (U/mg) in crude ectracts of different acidophiles at different assay temperatures.

Total protein concentrations in the assays were in a range of 50-103 mg/L in 100 mM Tris-buffer/ dialysed sulfur mixture pH 7.5. Mean values are given by n ≥ 3 samples and are corrected by the abiotic reactions, measured in BSA controll assays.

Organism	Temperature			
	30°C	45°C	65°C	70°C
Sb. thermosulfidooxidans	N/A	0.023	0.134	0.327
S. metallicus	0.000	0.000	0.281	N/A
At. caldus	0.008	ND	ND	N/A

U=unit; amount of enzyme required for the formation of 1 µmol of sulfate plus thiosulfate per min
N/A = not analysed
N/D = not detected

Sb. thermosulfidooxidans showed a slight Sdo activity of in crude extracts at 45 °C, while the highest acitivity was measured at 70 °C. Assays at higher temperatures were not performed. Consequently, the temperature optimum could not be concluded. *S. metallicus* showed no Sdo activity at 30 °C and 45 °C, but a slight activity at 65 °C. Also here, assays at higher temperatures were not performed and the temperature optimum could not be concluded. In all assays the enzyme activities of all *At. caldus* strains analyzed were almost zero. The results of the *At. caldus* type strain are representative for all *At. caldus* strains analyzed.

4.8.2 **Enzyme assays without addition of external GSH**

Sor activity is measurable without the addition of external thiol groups. Apart from the produced sulfite, sulfate and thiosulfate (oxygenase activity) also sulfide (reductase activity) is formed during the Sor reaction. Consequently, it was also analysed here (Kletzin 1989). Protein concentrations in the assay ranged between 32-189 mg/L in 100mM Tris-HCl/dialysed S^0 mixtures. At a pH of 7.5 was chosen to determine the optimal Sor activity temperature of *Sb. thermosulfidooxidans* (Fig. 27A). The optimal pH for Sor activity of *Sb. thermosulfidooxidans* was determined at 75 °C (Fig. 27B). Sor assays of *S. metallicus* (determined at pH 8), were used as positive control for the enzyme assays. All results in Table 28 were corrected with relation to the internal standard, phosphate concentration, measured by IC. The abiotic values (assay with BSA) were subtracted.

Neither oxygenase nor reductase activity of Sor were found in any crude extracts of the analysed *At. caldus* strains and in *Sb. thermosulfidooxidans* grown on ferrous iron

Table 28: Specific oxygenase activity (U/mg) of Sor in crude extracts of *Sb. thermosulfidooxidans* and *S. metallicus* at different assay temperatures.

Total protein concentrations in the assays were in a range of 50-103 mg/L in 100 mM Tris-buffer/ dialysed sulfur mixture at pH 7.5. Mean values are given by n ≥ 3 samples and are corrected by the abiotic reactions, measured in BSA controll assays.

Organism	Temperature					
	30°C	45°C	65°C	70°C	75°C	80°C
Sb. thermosulfidooxidans	N/A	0.058	0.023	0.496	1.200	0.908
S. metallicus	0.000	0.015	0.219	N/A	N/A	N/A

U=unit; amount of enzyme required for the formation of 1 µmol of sulfite, sulfate plus thiosulfate per min.

N/A = not analysed

Table 29: Specific reductase activity (U/mg) of Sor in crude extracts of *Sb. thermosulfidooxidans* and *S. metallicus* at different assay temperatures.

Total protein concentrations in the assays were in a range of 50-103 mg/L in 100 mM Tris-buffer/ dialysed sulfur mixture at pH 7.5. Mean values are given by n ≥ 3 samples and are corrected by the abiotic reactions, measured in BSA controll assays.

Organism	Temperature					
	30°C	45°C	65°C	70°C	75°C	80°C
Sb. thermosulfidooxidans	N/A	0.006	0.020	0.042	0.077	0.140
S. metallicus	7.182E-05	0.001	4.983E-04	N/A	N/A	N/A

U=unit; amount of enzyme required for the formation of 1 µmol of sulfide per minute.

N/A = not analysed

.

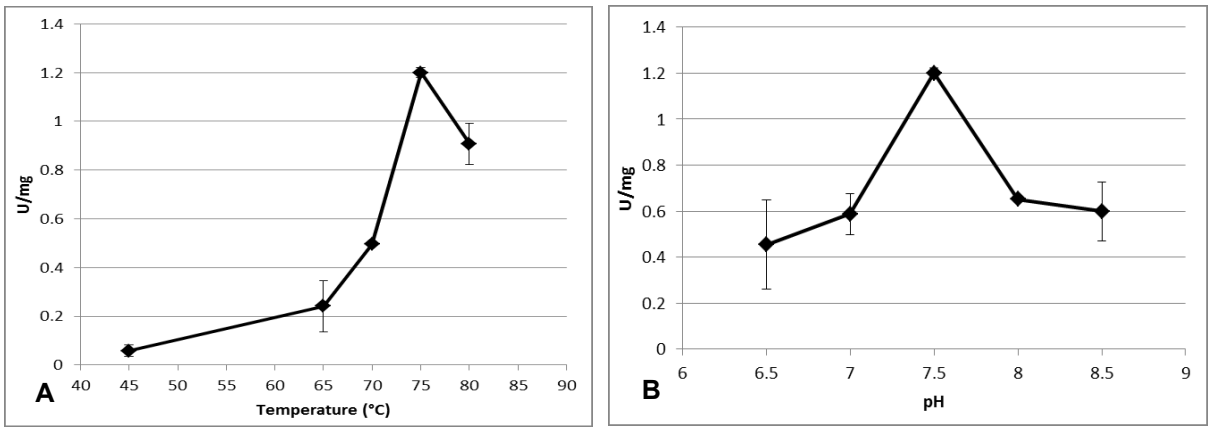

Fig. 28: Graphic presentaition of temperature and pH optimum of *Sb. thermosulfidooxidans* Sor in crude extract.

Total protein concentrations in the assays were in a range of 50-103 mg/L in 100 mM Tris-buffer/ dialysed sulfur mixture. Temperatur optimum was determined at 7.5 assay pH. pH optimum was determined at 75°C assay temperatre. Mean and SD values are given by n ≥ 3 samples and are corrected by the abiotic reactions, measured in BSA controll assays.

A) Determintation of optimal Sor temperature of *Sb. thermosulfidooxidans* at pH 7.5.

B) Determination of optimal Sor pH of *Sb. thermosulfidooxidans* at 75°C.

The Sor enzyme of *Sb. thermosulfidooxidans* showed the best specific oxygenase enzyme activity with 1.2 U/mg at 75 °C and pH 7.5. The corresponding dependence of the reductase acitivity with pH is shown in Table 30. The highest reductase activity of *Sb. thermosulfidooxidans* Sor was also measured at pH 7.5.

Table 30: Specific reductase activity (U/mg) of Sor in crude extracts of *Sb. thermosulfidooxidans* at different pH at 75 °C.

Total protein concentrations in the assays were in a range of 50-103 mg/L in 100 mM Tris-buffer/ dialysed. Mean values are given by n ≥ 3 samples and are corrected by the abiotic reactions, measured in BSA controll assays.

Organism	pH				
	6.5	7.0	7.5	8.0	8.5
Sb. thermosulfidooxidans	0.062	0.006	0.077	0.060	0.020

U=unit; amount of enzyme required for the formation of 1 µmol of sulfide per minute.

5 DISCUSSION

5.1 Growth behaviour of *At. caldus*

At. caldus is capable of chemolithoautotrophic growth with thiosulfate, tetrathionate, sulfide, S^0 and molecular hydrogen (Hallberg and Lindström 1994).

Since the whole genome sequences of two *At. caldus* strains, the type strain *At. caldus* ATCC 51756 and *At. caldus* SM-1, are available, it is known that both strains contain e.g. two *sox* clusters and the type strain contains also a *sor* gene. Sox is mainly discussed to be active during mesophilic growth, wherase Sor is thought to be a thermophilic enzyme. Consequently, the question arose about how *At. caldus* might grow at different temperatures with different RISC's and which enzymatic system might be responsible then for the oxidation.

All growth measuerents were done with cells which were grown at least for one subculture with the respective RISC source to be tested. The same was done considering the growth T°.

At 30 °C the type strain of *At. caldus* grew besth with thiosulfate or S^0. No significant differences in the growth with these two RISCs were detected. However, cells grew poorly with tetrathinonate. ISC concentration measurements of culture supernatant samples showed that in thiosulfate cultures only a concentration of 3.3 mM S^0 was formed, probably due to thiosulfate disproportionation at low pH. This showed, that the main RISC in these cultures was still thiosulfate. No S^0 was detected in tetrathionate grown cultures at this temperature.

Furthermore, these thiosulfate grown cells divided more than 6 times, showing the best growth at 30°C. 21 mM thiosulfate was used as start concentration and an average of 56 mM sulfate was formed (Fig. 15). However, only 42 mM sulfate should have been formed and the cells were washed twice before inoculation. I may be possible that cells used stored RISCs, which would explain these increased sulfate values.

Experimental evidence indicate that an enhanced growth of *At. caldus* under mixotrophic conditions with RISCs and yeast extract or glucose occurs (Hallberg and Lindström 1994). However, my experiments with the type strain of *At. caldus* and strain *At. caldus* C-SH12 did not show siginificant differences in growth behaviour between autotrophic and mixotrophic growth conditions (data not shown). *At. caldus* growth was also tested at 50°C, its max. growth T°. At this temperature, cells showed

a stress response, causing the formation of long filaments and doubled only once with thiosulfate and with tetrathioante. Only cultures with S^0 at this T° showed a slow growth (data not shown). These were used for RT-qPCR analyses.

Interestingely, light-microscopy of *At. caldus* cultures at 30°C with thiosulfate indicated that approx. 10 % of the cells had S^0 globules between day 3 and 4. Between day 5 and 6 these S^0 globules disappeared. The same was observed for tetrathionate cultures (Fig. 9), however the occourence of this S^0 globules shifted. They appeared between day 5 and 6. Also in this case S^0 globules disappeared two days later.
In thiosulfate grown cultures at 45 °C the same formation of S^0 globules occured, starting at day 2. At day 4, S^0 globules disappeared. In tetrathionate cultures grown at 45 °C no S^0 globules were observed at any time. We are the first time to report the presence of S^0 globules in *At. caldus*. These globules might be a result of the missing $Sox(CD)_2$ protein within Sox catalized thiosulfate oxidation pathway. Similar data have been shown for *Al. vinosum* and *Chlorobaculum tepidum* (Sakurai *et al.* 2010; Fig. 3B), which also miss SoxCD. During thiosulfate oxidation, the sulfane sulfur from SoxY cannot be oxidized directly and is most likely transferred to such internal S^0 globules. Other potential candidates for the S^0 globules are proteins like Sqr and Tth. Sqr is responsible for the oxidation of sulfide to S^0, which can be stored as S^0 globules. The production of long-chain polythionates and S^0 in aerated *At. ferrooxidans* cell suspensions incubated with tetrathionate (Steudel *et al.* 1996) and a mechanism of formation and deposition of S^0 globules has been postulated recently (Beard *et al.* 2011). In thiosulfate cultures, under oxygen-sufficient conditions (OSC) *At. ferrooxidans* oxidizes thiosulfate to tetrathionate, which accumulates in the culture medium. Tetrathionate was then oxidized by Tth generating thiosulfate, S^0, and sulfate as final products. However, a massive production of extracellular conspicuous S^0 globules occurred, if thiosulfate-grown *At. ferrooxidans* cultures were shifted to oxygen-limiting conditions (OLC). Concomitantly with the S^0 globule deposition the extracellular concentration of tetrathionate became greatly reduced and sulfite accumulated in the culture supernatant. The intra-cellular activity of the Tth of *At. ferrooxidans* was negligible in OLC-incubated cells indicating that this enzyme was not responsible for tetrathionate disappearance. Another active Tth protein (extracellular) was found in *At. ferrooxidans* culture supernatants. Its activity

was postulated to be related to the observed extracellular S^0 globule production under OLC-conditions.

Analysis of cells of *At. caldus* in thiosulfate cultures under OSC at 30 °C and 45 °C (data not shown), indicated the same occurance of S^0 globules with same frequency as before. OLC-incubated cells have not been analyzed.

Furthermore, the exact location of the S^0 globules is not yet known.

The S^0 globules disapeance might be due to higher activity of S^0 oxidation enzymes, HDR or a reversely working dissimilatory sulfite reductase (DsrAB).

5.2 Expression levels of genes involved in sulfur metabolism of *At. caldus*

In order to investigate, whether there is a differential regulationon according to growth conditions six genes: *sor* (ACA_0302), *soxB* (ACA_2394), *soxX* (ACA_2389), *sqr_I* (ACA_0303), *sqr_II* and *tth* (ACA_1633) were chosen for expression level analyses depending on the substrate (S^0, thiosulfate or tetrathionate) and growth T° (30 °C, 45 °C and 50 °C).

All quantitative RT-PCR calibration curves had a high correlation coefficient and similar amplification efficiencies (Table 5). Cells grown on tetrathionate at 30 °C had the lowest copy number of all analyzed genes. This could be due to reduced amounts of RNA which might be a consequence of a slow cell growth under this condition (Fig. 8). Among these genes, the highest copy number for all samples was noted for *sqr_I*.

Considering every analyzed gene, *sor* was down-regulated on tetrathionate at 45 °C and up-regulated in S^0 grown cells at 30 °C. Since Sor is predicted to be a cytoplasmic enzyme, an enrichment in the cytoplasmic S^0 pool could have stimulated *sor* expression. However, this might have been a result of the growth substate or from products of other RISC oxidizing enzymes within the cytoplasm. Transcriptional analyses for *sor* are known from previous studies (Mangold *et al*. 2011; Chen *et al.* 2012). However, those results are different from my results. No *sor* expression changes between S^0 and tetrathionate grown cells of *At. caldus* type strain were detected with semi quantitative RT-PCR measurements after 30 PCR cycles with S^0 and tetrathionate grown cells of *At. caldus* type strain (Mangold *et al.* 2011). A DNA microarray study showed up-regulation of the *sor* gene in cells of *At. caldus* MTH-04 grown on tetrathionate as compared to cells grown on S^0 (Chen *et al.* 2012). In that study, expression levels of different RISC genes were compared for cells grown in S^0 medium compared with those grown with tetrathionate (wild type).

The Sox system has been investigated in several neutrophilic bacteria, but until now not thoroughly in acidophiles. It is mainly discussed in organisms, which uses thiosulfate as main substrate (Bardischewsky *et al.* 2005; Friedrich *et al.* 2000; Welte *et al.* 2009), e.g. green and purple sulfur bacteria only contain the core of the Sox-system also called thiosulfate oxidizing multi-enzyme system (TOMES). This system seems to also in cells of *At. caldus*. The *soxB_I* and *soxX_I* genes were chosen as example genes of the putative *sox_I* operon. Both genes showed down-regulation in cells grown on S^0 at 45 °C and up-regulation in cells grown in thiosulfate medium. In the genus *Acidithiobacillus sox* genes are present in *At. caldus*, *At. ferrivorans* SS3 and *At. thiooxidans* ATCC 19377, while they are absent in *At. ferrooxidans* strains. No enzyme assays have been done with a Sox system using S^0 until now. Consequently, it is unknown how high the Sox activity is within S^0 grown cells. However, the semi quantitative RT-PCR results indicate that all *sox* genes (both clusters) in *At. caldus* are down-regulated on S^0, when compared to tetrathionate growth (Mangold *et al.* 2011). These results were confirmed with microarray assays for *At. caldus* MTH-04 (Chen *et al.* 2012). In this study no different regulation of Sox enzyme expression between S^0 and thiosulfate grown cells was detected in the proteomes. However, considering the transcription levels, *At. caldus* cells grown with thiosulfate at 30 °C and with tetrathionate at 45°C showed up-regulation of *soxB* and *soxX* as compared to S^0 grown cells. These differences need further investigations.

Both *sqr* genes in the *At. caldus* type strain (ACA_0303 and ACA_2485) show only 20 % identity in amino acid sequences to each other. However, both genes are also found in *At. caldus* SM-1 (Atc_1705 and Atc_1437) sharing 99% identity. The Sqr proteins are members of the disulfide oxidoreductase flavoprotein (DiSR) superfamily, like other well-characterized pyridine nucleotide:disulfide flavoproteins. In general the sequence identity to the other members of the superfamily is low, and even within the Sqr subfamily the sequences are not well-conserved. Based on alignments the Sqr proteins have been classified into at least 2 groups (Marcia *et al.* 2009; Griesbeck *et al.* 2000). Type I Sqr proteins are found in many bacterial species and are involved in the cellular respiration pathway or in anaerobic photosynthesis (Shahak and Hauska 2008). The Sqr proteind of *At. caldus* belong to this type I. In acidophiles Sqr has been found in *Aq. aeolicus* and *At. ferrooxidans* (Marcia *et al.* 2009; Cherney *et al.* 2010). Both are membrane bound enzymes and possess a non-covalently bound FAD cofactor. The high similarity plus the conservation of the gene

observed with *At. ferrooxidans* suggests similar functional properties in *At. caldus* (Mangold *et al.* 2011). The enzymatic reaction includes the oxidation of sulfidic compounds H_2S, HS^- and S^{2-} to (soluble) polysulfides or to S^0 in the form of octasulfur rings. Little is known about the Sqr enzyme in *At. caldus*. In this study, the transcription of *sqr_I* was enhanced in cells grown with S^0 or tetrathionate at 30 °C and down-regulated with all tested RISCs at 45 °C. These results are contradictory to the ones noted for the *sqr_II* gene. Here an enhanced level of expression was found in cells grown on tetrathionate or thiosulfate at 45 °C and down-regulation was measured for S^0 grown cells at 30 °C and at 45 °C. Consequently, it could be speculated that a temperature dependent regulation of *sqr* exists: at 30 °C *sqr_I* is most expressed, while at 45 °C *sqr_II* is dominant. Also in *At. cal*dus strain MTH-04 two *sqr* genes were described (Chen *et al.* 2012). However, only one *sqr* was analyzed for expression level. The expression of this *sqr* is enhanced in cells grown with S^0 compared to tetrathionate. Those cells were grown at 40 °C and no expression studies at different temperatures were done, consequently a temperature relation can not be derived from the data.

Finally, also the gene *tth* was analyzed. It has been investigated several times in *At. caldus* (Bugaytsova *et al.* 2004; Rzhepishevska *et al.* 2007; Mangold *et al.* 2011). Tth is found in an operon, which contains the genes *ISac1*, *rsrR*, *rsrS*, *ttH*, and *doxD*. They code for a transposase, a two-component response regulator (RsrR and RsrS), tetrathionate hydrolase, and DoxD, respectively. The last gene encodes Tqo. As shown by quantitative PCR, the genes *rsrR*, *ttH*, and *doxD* were up-regulated to a different degree in the presence of tetrathionate, as compared to S^0 (Rzhepishevska *et al.* 2007). Western blot analysis also indicated up-regulation of the Tth protein in the presence of tetrathionate, thiosulfate, and pyrite. In this study, the gene expression of *tth* was found to be up-regulated during growth with tetrathionate and thiosulfate showing the highest expression levels in cells grown on thiosulfate at 30 °C (Table 12). Unfortunately, both the former analysis (Rzhepishevska *et al.* 2007) and the analysis of this study showed higher standard deviations. Furthermore, the semi-quantitative RT-PCR analysis in other studies showed no significant differential regulation of this enzyme between tetrathionate and S^0 (Mangold *et al.* 2011). Consequently, the up-regulation needs further studies.

5.3 High throughput proteomic analysis of *At. caldus* grown on sulfur vs thiosulfate

Proteomes from thiosulfate at 45 °C grown *At. caldus* cells were compared with S^0 grown cells. A total number of 1292 proteins was identified corresponding to 45.8 % of the predicted proteome of the *At. caldus* type strain. Of these 1292 proteins, 1215 were detected to be present in S^0 grown samples and 1120 proteins were detected in thiosulfate grown cells (Table 15).

After statistical analysis and exclusion of those proteins found in less than 3 out of the 4 samples for each growth condition, the number of protein decreased to 605. Out of these, 85 proteins were found to be induced and 13 proteins were found to be repressed from S^0 grown cells ($p < 0.05$). After raising the *p*-value from 0.05 to 0.1, additionally 47 proteins were considered to be up-regulated and 11 proteins were found to be down-regulated in cells grown on S^0 (Table 14), bringing the total number to 132 or 24 respectively.

Sulfur metabolism

In the genome of the type strain of *At. caldus* are 7 gene clusters associated with sulfur metabolism. They were closely investigated by proteomic analyses. Hdr (EC: 1.8.98.1) catalyses the reversible reduction of the heterodisulfide (CoM-S-S-CoB) to the thiol-coenzymes coenzyme M (H-S-CoM) and coenzyme B (H-S-CoB). This protein is coupled with energy conservation in methanogenic archaea (Hedderich *et al.* 2005) and sulfate reducing archaea and bacteria (Mander *et al.* 2004). Hdr is composed of three subunits: HdrA, HdrB and HdrC (Madadi-Kahkesh *et al.* 2001). For the Hdr_I cluster, all proteins were detected. However, none of the proteins showed any significant differential regulation between S^0 or thiosulfate grown cells. BlastP results of the hypothetical protein (ACA_2419), within the Hdr cluster, lead only to other hypothetical proteins. However, it has 69% max. identity with a protein found in *At. ferrooxidans* (AFE_2552), which is found in the same genome context of a protein named *orf2* (Fig. 28). Furthermore, in *At. caldus* SM-1 this hypothetical protein is also found in a Hdr complex with 92 % identity (Atc_2349). Consequently, there is a strong evidence that this protein belongs also to the Hdr complex. The *hdr* genes are organized in two clusters in the type strain of At. caldus, while in *At. ferrooxidans* and *At. caldus* SM-1 all genes are organized in one cluster (Fig. 28).

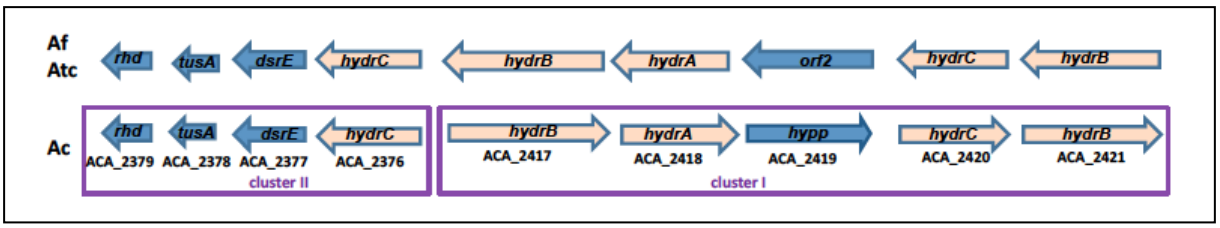

Fig. 29: Comparison of the heterodisulfide reductase *(hdr)* clusters found in the type strains of *At. ferrooxidans* (Af) and *At. caldus* (Ac) and in *At. caldus* SM-1 (Atc).
The graphic is constructed by the gene annotation and gene oriantion given in the NCBI database. The type strain of *At. ferrooxidans* possess one putative *hdr* operon (AFE_2550-AFE_2558). The strain *At. caldus* SM-1 possess also one putative operon (Atc_2348-Atc_2355). In *At. caldus* type strain the *hdr* is organized in two clusters (ACA_2376-ACA_2379; ACA_2417-ACA_2421).

The transcription levels of *hdrBC* genes were analyzed for *At. caldus* MTH-04 (Chen *et al.* 2012). Also in this strain the *hdr* cluster has a similar organization like in the type strain, because *hdrBC* (ACAL_1042; ACAL_1043) is not clustered with the genes *dsrE*, *tusA* and *rhd* (ACAL_2473-ACAL_2475). For *At. caldus* MTH-04, access to the genome sequence was not available. Conseqeuntly, an analysis of a putative *hdrA* gene is not possible. The genes *HdrBC* were significantly induced in S^0 grown cells when compared to tetrathionate cells. Also in the type strain of *At. caldus* the Hdr proteins should be induced in S^0 grown cells. (Extracellular) elemental sulfur (S_8) is activated by thiol groups from special outer-membrane proteins and transported into the periplasmic space as a persulfide sulfur (R-SSH) (Vishniac and Santer 1957; Pronk *et al.* 1990), by a non-enzymatic reaction. Thus, S^0 can be reduced to a nonasulfane derivate (Eq. 3), which can be oxidized subsequently by the postulated Sdo to a sulfinate group. It has been shown that only these thiol-bound sulfane sulfur atoms ($R\text{-}SS_nH$) are reactive enough to be oxidized by Sdo (Rohwerder 2002) and possibly also for Hdr. On the other hand, rhodaneses (EC: 2.8.1.1) could also react transferring a sulfane atom from thiosulfate to sulfur acceptors like cyanide and thiol compounds. Consequently, in an indirect way thiosulfate might be a good RISC source for Hdr. In the *hdr*_II cluster the predicted rhodanese (ACA_2379) was found to be up-regulated (Table 18B) in S^0 grown cells. Additionally, three rhodaneses are annotated in the genome (ACA_0025; ACA_0052; ACA_2527). All were found in the proteomes and ACA_0025 was highly up-regulated in S^0 grown cells. Several studies before pointed out the importance of rhodaneses for sulfur metabolism in leaching bacteria (Ramírez *et al.* 2004; Tabita *et al.* 1969). Nevertheless, in *At. ferrooxidans* the rhodanese activity levels were similar for cells were grown either with ferrous iron with in S^0. However, *At. caldus* is not able to oxidize ferrous iron and, thus, the rhodanese will play a role in other metabolic pathways, e.g. in the sulfur metabolism.

Furthermore, my data indicate that two types of rhodanese may exist. One maybe located in the cytoplasm and the other onr is probably anchored on the periplasmic side of the cytoplasmic membrane in *At. ferrooxidans*. The latter one was induced, when cells were grown with S^0 and not induced with the substrate ferrous iron, thiosulfate, copper sulfide and zinc sulfide (Ramírez *et al.* 2004). However, the potential functions of the rhodaneses annotated in the type strain of *At. caldus* are not clarified yet. Although the ATP sulfurylase (Sat) is not clustered within the hdr cluster, it is connected with the hdr, because it catalyzes the production of ATP and sulfate from APS and pyrophosphate. An enzyme catalyzing the oxidation of sulfite to APS is required and this missing function could be accomplished by *dsrE*, *tusA* or *rhd* embedded in the *hdr* locus of sulfur oxidizers (Quatrini *et al.* 2009). In cells of *At. caldus* Sat (ACA_ 2309) was foundto be up-regulated in S^0 grown cells.

Although *sor* transcripts in *At. caldus* strains were found in thie own and other studies, Sor was not detected in any proteome. Interestingly, instead of M (methionine) in prokaryotes as transcription start codon for *sor* in the *At. caldus* type strain, V (valine) is found. The latter one is more often found as start codon in archaea. Furthermore, no Shine Dalgarno sequence was detectable close to the *At. caldus sor* start codon. Thus, a stable, double-stranded structure that could position the ribosome correctly on the mRNA during translation initiation (Stramer *et al.* 2006) is probably not functional for this gene. This could explain the absence of Sor in the proteomes. The Sor protein was also not reported to be present in the earlier proteomic study of *At. caldus* (Mangold *et al*. 2011). However, in that study only the differently regulated proteins from 2D gels were analysed via MS. All these results indicate that Sor does not have an important role in S^0 oxidation of the *At. caldus* type strain. In contrast, in *At. caldus* MTH-04 the *sor* gene was thoroughly investigated by the creation of a knock-out mutant. In this way changes in RISC metabolism were observed (Chen *et al*. 2012). Consequently, in this mutant the influence of *sor* absence becomes predictable, but enzymatic Sor studies were not done.

Adjacent to the *sor* gene one *sqr* gene is found. Apart from the fact that Sor could deliver sulfide to Sqr, another reaction within the cell can occur. GSH can abiotically react with S^0 to form sulfide, or as product of the catabolism of cysteines sulfide maybe produced (Kimura 2002). H_2S is considered to be a very toxic substance for aerobic organisms hampering oxygen transport and inhibiting oxygen reduction by

heme:copper oxygen reductases (preventing energy production by oxidative phosphorylation). Furthermore, sulfide is a strong nucleophile and may react with disulfide bounds and bind to metal centers of enzymes. Consequently, Sqr might also have a detoxification role for the cells (Shahak and Hauska 2008; Marcia *et al.* 2009). Also a sulfide oxidizing activity has been identified in cells of *At. caldus*, but the enzyme has not been identified (Hallberg *et al.* 1996). Both annotated Sqr proteins detected in the proteomes of my study and showed no significant differential regulation between S^0 and thiosulfate grown cells. Interestingly, in another study both Sqr proteins were found to be up-regulated in tetrathionate grown *At. caldus* cells, when compared to S^0 grown cells (Mangold *et al.* 2011).

Another enzyme reported to be involved in ISC metabolism is Tth. The activity of this enzyme has been detected in several Acidithiobacilli species (Hallberg *et al.* 1996; Brasseur *et al.* 2004). An inspection of the draft genome of *At. caldus* revealed the presence of a candidate *tth* gene upstream of the *doxD* gene. The putative Tth of *At. caldus* shares 71% similarity with the Tth of *At. ferrooxidans.*. It has a conserved pyrrolo-quinoline quinone (PQQ) domain (Pfam: PF01011). Tth has an optimum activity at pH 3.0 and 40 °C and is periplasmically located (Bugaytsova *et al.* 2004). Here I could confirm a down-regulation of Tth in S^0 grown cells as already presented in Mangold *et al.* 2011. Furthermore, I'm able to predict a second Tth (ACA_0092) in the genome of *At. caldus*. A search by BlastP gave a match with a putative tetrathionate hydrolases (53 % identity) from an acid main drainage metagenome sequence (CBH95240.1). This protein was found to be up-regulated in S^0 grown cells. It needs further investigation.

Tetrathionate and thiosulfate can enter the periplasm. They can be hydrolyzed by Tth or DoxD in cycling of thiosulfate oxidation to tetrathionate (DoxD/ Tqo). Quinones are reduced and thiosulfate regenerated by the reduction of tetrathionate. However, for Tqo only the *doxD* gene has been found in all published *At. caldus* genome sequences, while *doxA* is absent. Thiosulfate oxidation by Tqo was analyzed in *A. ambivalens*: DoxD catalyzes the oxidatin of thiosulfate to tetrathionate and gains two electrons. DoxA transfers these electrons to a quinone of the respiratory chain (Mueller *et al.* 2004). Both subunits are thought to be constituents of the terminal oxidase and the function of DoxA is to transfer electrons. It can be hypothesized that another terminal oxidase instead of DoxA interacts with DoxD to perform Tqo ativity in *At. caldus*. In addition, due to the instability of thiosulfate and the stability of

tetrathionate under acidic conditions, the resulting thiosulfate in the periplasm may be rapidly oxidized by the Sox system or enter into the S_4I pathway.
Also the expression levels of *ttH* and *doxD* of the wild type of *At. caldus* MHT-04 in S^0 medium were much higher than in tetrathionate medium (Chen *et al.* 2012). This finding seems to indicate that in this strain a lot of tetrathionate and thiosulfate were produced during S^0 oxidation.

Finally, the *sox* operons were closely analyzed. As mentioned, *At. caldus* has only a truncated Sox pathway, because $Sox(CD)_2$ is missing. From the *sox* cluster 1 all proteins were present in the proteomes and SoxX was found to be up-regulated on S^0. In addition, a protein of unknown function in this cluster (ACA_2393) was also found to be up-regulated in S^0 grown cells. In the Sox cluster 2 the proteins ResB and ResC were not detectable in any proteome. These proteins seems to be essential proteins for system II c-type cytochrome biogenesis (Feissner *et al.* 2005). The hypothetical protein ACA_2313 in cluster 2 was also not found in any proteome. BlastP results suggest this protein is a SoxX homologue, since the protein sequence showed 92 % identity with SoxX of *At. caldus* SM-1 (Atc_2212).
Although Sox reactions of a truncated Sox system were analysed in thiosulfate oxidation (Welte *et al.* 2009), no activity tests considering the preferable RISC source of the truncated Sox system have been performed up to now. In my study reasons for the activity of Sox system in S^0 and in thiosulfate grown cells were described. They confirm that *sox* genes are down-regulated in sulfur grown cells. Consequently, it is unlikely that SoxXY are a transporter proteins. SoxY is presumed to play a role in the activation of S_8, since S_8 bound to a thiol group of SoxY via nonenzymatic conjugation has been reported (Friedrich *et al.* 2000).
A direct sulfite oxidation protein like sulfite:acceptor oxidoreductase (Sar; Zimmermann *et al.* 1999) was not detectable in genome, but the hypothetical protein encoded by ACA_1585 contains a region belonging to SO_family_MoCo Superfamily: Sulfite oxidase (SO) family with a molybdopterin binding domain (Kappler and Bailey 2004). It was found to be induced in S^0 grown cells. Also, this protein needs to be investigated furtheron.

Respiratory complexes

In cells of *At. caldus* the NADH quinone oxidoreductase complex consists of 14 different subunits (*nuoA* to *nuoN*) and two of such complexes are present in the genome. Among the proteins NuoI_1 (ACA_1496) was up-regulated in S^0 grown cells and NuoE_2 (ACA_2703) and NuoI_2 (ACA_2707) were induced in S^0 grown cells. Furthermore, CydA (ACA_2617) belonging to one of the terminal oxidase bd clusters, was induced in S^0 grown cells.

Proteins involved in the respiratory complexes are membrane acossiated. In general, it is worth to mention that membrane proteins are more difficult to detect in proteomes due to the lack of tryptic digestion sites.

Cytochrome bd showed no homology with other heme–copper oxidases (HCOs) like bo_3 and aa_3. It exhibits interesting similarities in case of the catalytic mechanism, but also some characteristic peculiarities (Giuffrè *et al.* 2012). While bo_3 and aa_3 invariantly comprise a high spin heme iron (heme a_3, o_3 or b_3) and a copper metal in the active site, cytochrome bd does not have a copper ion, but three heme centers. Both, bo_3 and aa_3, and cytochrome bd catalyze the complete four electron reduction of O_2 to H_2O. However, cytochrome bd can only use quinols as reducing substrates (Jünemann 1997), whereas the large superfamily of HCOs comprises cytochrome c- and quinoloxidases. HCOs and cytochrome bd are characterized by distinct energetic efficiencies. The overall reaction catalyzed by most cytochromes bd is indeed electrogenic (Jasaitis *et. al.* 2000) leading to proton motive force generation, but contrary to HCOs, is not associated to a proton pumping (Puustinen *et al.* 1991). Thus a reduced efficiency results (Pereira *et al.* 2008).

There is also a strong connection between the expression of the *sox* genes in *At. caldus* MTH-04 and the terminal oxidase genes. The expression of the terminal oxidase genes, especially the cytochrome bo_3 ubiquinol oxidase genes, was found to be up-regulated when *sox* genes had high expression levels (Chen *et al.* 2012). However, only SoxX was detected to be up-regulated with S^0 as substate and only very few proteins of the bo_3 clusters were found in the proteomes. Thus, these findings of transcriptional data could not be confirmed by my study of the *At. caldus* type strain.

Carbon metabolism

At. caldus genomes encode all enzymes for the central metabolism and the assimilation of carbon compounds. Both At. caldus strains (type strain and SM-1) fix CO_2 via the classical CBB cycle, and can operate complete EMP, PPP, and gluconeogenesis. Both strains have a truncated TCA cycle. *At. caldus* SM-1 was able to assimilate carbohydrates This was subsequently confirmed experimentally because addition of 1% glucose or succrose in basic salt medium significantly increased the growth of SM-1 (You *et al.* 2011). In the CBB cluster 1 of the type strain of *At. caldus*, all three proteins were found in all proteomes. No significant differential regulation could be detected here between S^0 and thiosulfate. In CBB cluster 2, the RubisCO activation protein CbbQ (ACA_2016) and CbbO (ACA_2017) belong to a family of proteins which play a role in the post-translational activation of RubisCO (Hayashi *et al.* 1999). Both together with CbbM (ACA_2015) were not detected in any proteome, suggesting that other proteins may replace their functions. One of these proteins is the RubisCO-like protein (ACA_0171), which together with the putative carboxysome peptiede A (ACA_2769) were found to be induced in S^0 grown cells. All other proteins necessary for a functional CBB cycle were found, showing no differential regulation between S^0 and thiosufate grown cells.
To metabolize glucose to pyruvate, *At. caldus* uses the EMP pathway. All proteins involved were detected, exepting two of three annotated pyruvate kinases (ACA_1393 and ACA_2653). The tagatose-6-phosphate kinase (ACA_1396) was found to be induced in proteomes from S^0 samples. In the TCA cycle of *At. caldus*, genes encoding succinate dehydrogenase and the 2-oxoglutarate dehydrogenase (also called α-ketoglutarate dehydrogenase) complex are absent in both the type strain of *At. caldus* and to *At. caldus* SM-1 (You *et al.* 2011). Several hypothetical proteins have not been closely investigated yet. Consequently, hypothetical proteins might have taken the “missing” functions. All enzymes involved in PPP were detected in all proteomes and glucose-6-phosphate 1-dehydrogenase (G6PD; ACA_2792) was found to be up-regulated in S^0 grown cells. All other enzymes showed no significant changes in their levels between S^0 and thiosulfate grown cells.

EPS production and cell motility

At. caldus oxidizes RISCs and sulfur from some MeS like chalcopyrite. In bacterial EPS the saccharidic moiety is synthesized from activated precursors like sugar

nucleotides. The three main mechanisms are called “Wzx/ Wzy dependent,” “ATP-binding cassette (ABC) transporter dependent,” and “synthase dependent,” based on characteristic components (Cuthbertson *et al.* 2010). The Wzx/ Wzy-dependent and ABC transporter-dependent pathways have been analysed for cells of *At. ferrooxidans* (Bellenberg 2010; Krok 2010).

In this study, proteins of the putative CPS biosynthesis and export system in cells of *At. caldus* were investigated. The data indicate that cells of *At. caldus* only possess the ABC transporter (Kps) system (which is similar to the one in cells of *At. ferrooxidans*). BlastP and COG analysis revealed that the Wz-system seems to be incomplete. Two proteins in *At. ferrooxidans* directly involved in the synthesis of CPS of EPS, AFE_2961 and AFE_2975, were found to be induced ($p \leq 0.05$) and up-regulated ($p \leq 0.1$), respectively in biofilm cells: AFE_2961 encodes for a “capsule polysaccharide export” (inner-membrane protein), which shares 23 % identity and 53 % similarity with *E. coli* KpsE protein, a periplasmic protein which couples the ABC transporter, formed by the proteins Wzm and Wzt, to later translocation steps in the pathways in capsule biosynthesis (Whitfield 2006).

The proteins from *At. caldus* cells encoding the Kps- system did not show any differential regulation between S^0 or thiosulfate grown cells, suggesting no different in expression of CPS biosynthesis proteins under our experimental conditions. Considering attachment to MeS surfaces, it may be interesting to investigate the level of protein expression in a mixed culture containing with an iron-oxidizing bacterium. The *At. caldus*-like strain S2 does not attach to pyrite in pure cultures (Noël 2008), but attaches in the presence of cells of *L. ferriphilum*. In such a case the missing proteins may become detectable due to upregulation Furthermore, a type IV secretion system involved in pili biogenesis was investigated in the proteomes. It controls phenotypes, twitching motility and biofilm formation (Filloux 2011). From the 24 T4SS proteins are annotated in the genome of *At. caldus* 8 were found in my study. The PilQ (ACA_1363) was significantly induced in S^0 grown cells. This protein is a structural component of the type IV pilus (Frye *et al.* 2006). Furthermore, three flagellar motor switch proteins were found in the proteomes (ACA_0349, ACA_0846 and ACA_0849). As mentioned before, the flagellar motor switch regulates the direction of flagellar rotation and swimming behaviour in certain bacteria (Brown *et al.* 2002) and most likely also in cells of *At. caldus*.

Considering proteins involved in chemotaxis, allmost all proteins detectable in the proteomes were induced or up-regulated in S^0 grown cells. S^0 is only very little soluble in water (5 µg/L). Consequently, an accumulation of S^0 during rapid growth on various compounds like thiosulfate or tetrathionate and also in the form of a passivation layer (in case of chalcopyrite) in leaching process may occur. Thus, with a positve chemotaxis to S° or RISCs, *At. caldus* could control its movement towards increase substrate concentration.

5.4 Sor and Sdo enzyme activity in *Sb. thermosuldooxidans* and *At. caldus*

Several *At. caldus* strains were screened via PCR for the *sor* presence in their genomes. Apart from *At. cal*dus #6, all other *At. caldus* strains had a *sor* the gene (Fig. 29) with an almost 100% aa identities within the genus. Interestingly, the sequences of *At. caldus* S1 and *At. caldus* S2 matched with the sequences in the Sulfobacilli branch. Later it was demonstrated that these strains were contaminated with Sulfobacilli. Consequentely, the *sor* sequence (as well as enzyme activities) were due to the contamination. After pure cultures of the *At. caldus* strains S1 and S2 were obtained the *sor* sequences were identical with the one of the *At. caldus* type strain (in 800nt). To complicate the situation, the *sor* gene of *At. caldus* SM-1 is branched within the Firmicutes phylum. The *sor* gene, called here sor_{SB}, has been cloned and has been expressed in *E. coli* and the Sor activity was determined. Sor_{SB} exhibited 3.76 U/mg specific oxygenase activity under the determined optimal reaction condition, 75–80 °C and pH 7.5 (Chen *et al.* 2007). Of course, it could be possible that this organism has lost its *sor* gene. However these *sor* sequences pressumably belonging to *At. caldus* SM-1, ($sor_{SA}$and sor_{SB}) were obtained by PCR with degenerated, modified Primer sorC1-F and sorH1-R (Table 3A) designed from metagenomic DNAs (of *Leptospirillum* species, *Sulfobacillus*, *Acidithiobacillus* and *Sphingomonas*) of the bioreactor samples. Furthermore our phylogentic analysis (Fig. 26) shows that the sor_{SB} is more likely coming from a *Sulfobacillus* species than from a *At. caldus* strain. Although Sor activity has been shown in the *At. caldu*s-like strain S1 (Janosch *et al.* 2009), this enzyme activity could later on not be reproducible. Additionaly, after the purity test of this strain it was doubtful, that it was from *At. caldus*, but probably from a Sulfobacilli contaminant. All *At. caldus* strains tested showed no Sor activity in crude extracts. This comes in agreement with the proteomic results of the *At. caldus* type strain, where also no Sor protein was

detected in the proteomes. To analyze the properties of this Sor protein, it was tried to clone this gene in an expression vector. Unfortunately after several attempts for cloning, no positive constructs were obtained.

Sor activity could be measured in this study for type strains of *S. metallicus* and *Sb. thermosulfidooxidans*. Sor enzyme tests of both have not been done before, but transcription levels of *S. metallicus sor* have been analyzed in iron, S^0 and pyrite grown cells (Bathe and Norris 2007). In that study, highest expression levels were found in cells grown in S^0. This was a reason to perform the activity test in this study with S^0 grown *S. metallicus* cells.

It is worth to mention that *S. metallicus* was only used as positive control and comparison for Sor activity. At its optimal growing T° (65 °C), it has a specific Sor oxygenase activity of 0.219 U/mg and a specific Sor reductase activity of 50 nU/mg in crude extracts. These values were smaller than other analyses of native Sors, (values between 0.9 and 10.6 U/mg; Table 1) for Sor oxygenase activity. But, no optimum temperature of the Sor *S. metallicus* was analyzed. Consequently, at higher temperature also a higher activity could be possible. For better comparibility *S. metallicus* Sor was also tetst at 45 °C, the optimum growth temperature of *At. caldus*. At 45 °C the reductase activity was higher with 1 mU/mg. Although, the enzyme test has been performed in closed systems, a ratio of 1 for oxygenase/ reductase activity could not be achieved in any case, which was characterized by Kletzin (1989). One reason for that might that sulfide is volatile and is present in the gas phase over the crude extract in the reaction bottle. The same was true for control experiments to analyze the recovery rate of sulfide (data not shown). These experiments were done in the same buffer and the same concentration of dialysed S^0 and only a recovery rate of approx. 12 % of sulfide at 65 °C could be measured. Consequentely, all specific Sor reductase activities determined, are underestimated under my experimental setup.

For the Sor enzyme of *Sb. thermosulfidooxidans*, some properties were ananlyzed. The optimum conditions for the reductase activity have not been clarified, because enzyme activities at higher temperatures were not analyzed.

Sb. thermosulfidooxidans possess to two homologues of *sor* (Sth_1627 and Sth_1798). Consequently it is difficult to predict whether the enzymatic acitivity is derived from one of these genes or from both together. Expression analyses will be necessary for clarification this question. An up-regulation of *sor* in *Sb.*

thermosulfidooxidans could be suggested, since ferrous iron grown cells didn't show Sor activities (not shown). The optimum Sor oxygenase activity is 15 °C higher than the optimum growing temperature.

Sdo activity test, as performed in this work, were very often not reproducible. Sdo activity may occur in *At. caldus* strains, because this enzyme has been shown to occur in *At. ferrooxidans* R1 and *At. thiooooxidans* DSM 504 and K6 (Rohwerder and Sand 2003). However, neither gene nor gene cluster(s) have been assigned to encode the enzyme(s). *HdrABC* genes may be one possible candidate, but this relation could not be confirmed in this study.

5.5 Sulfur metabolism in *At. caldus* and *Sb. thermosulfidooxidans*

At. caldus and *Sb. thermooxidans* are the main sulfur oxidizers in leaching processes at moderately thermophilic range. Consequentely, an understanding of the sulfur oxidation pathways is of great interest to enhance the leaching process.

In Fig. 29 and 30 the proposed RISC pathways in the type strains of *At. caldus* and *Sb. thermosulfidooxidans* are summarized. The main differences between both strains is the missing Sox system in *Sb. thermosulfidooxidans* and the inactive Sor enzyme in *At. caldus*.

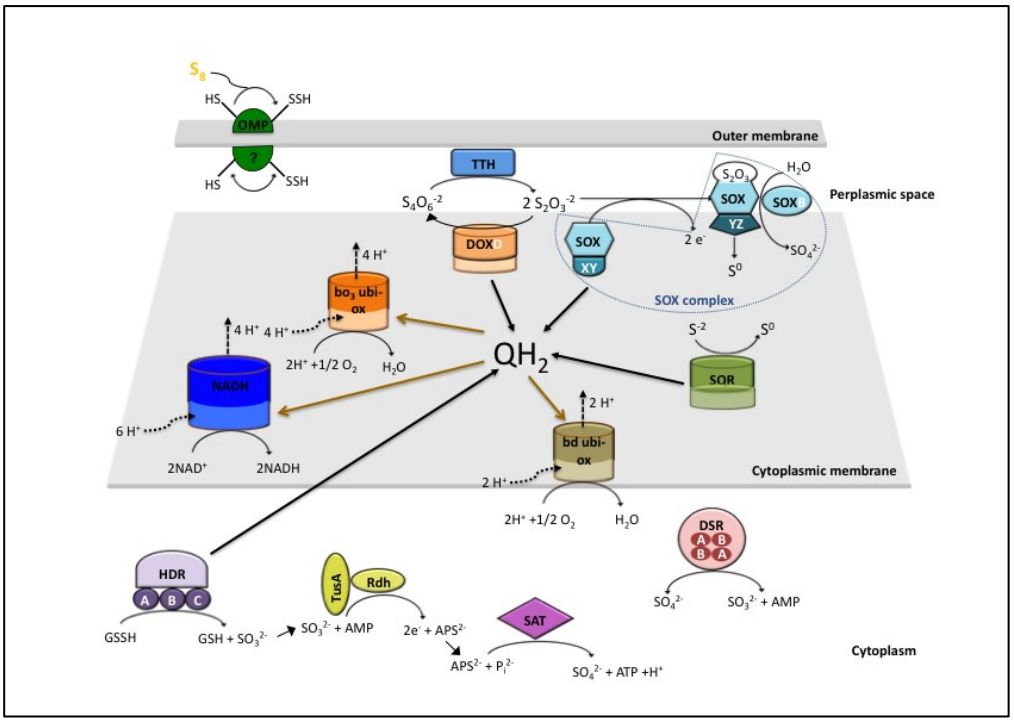

Fig. 30: Model for RISC oxidation pathways in the type strain of *At. caldus*. (Mangold *et al.* 2011 modified by my data)

Abbreviations: HDR: Heterodisulfide Reductase; TusA: Sulfurtransferase; Rdh: Rhodanase; SAT: Sulfate Adenylyltransferase; DSR: Dimethyl Sulfoxide Reductase; SQR: Sulfide:Quinone Oxidoreductase; SOX: Sulfur Oxidizing System; TTH: Tetrathionate Hydrolase; DOXD (TQO): Thiosulfate:Quinone Oxidoreducatase; OMP: Outer Membrane Protein; NADH: NADH Ubiquinone Oxidoreductase; bd and bo_3 ubi-ox: terminal oxidases. For more details see text.

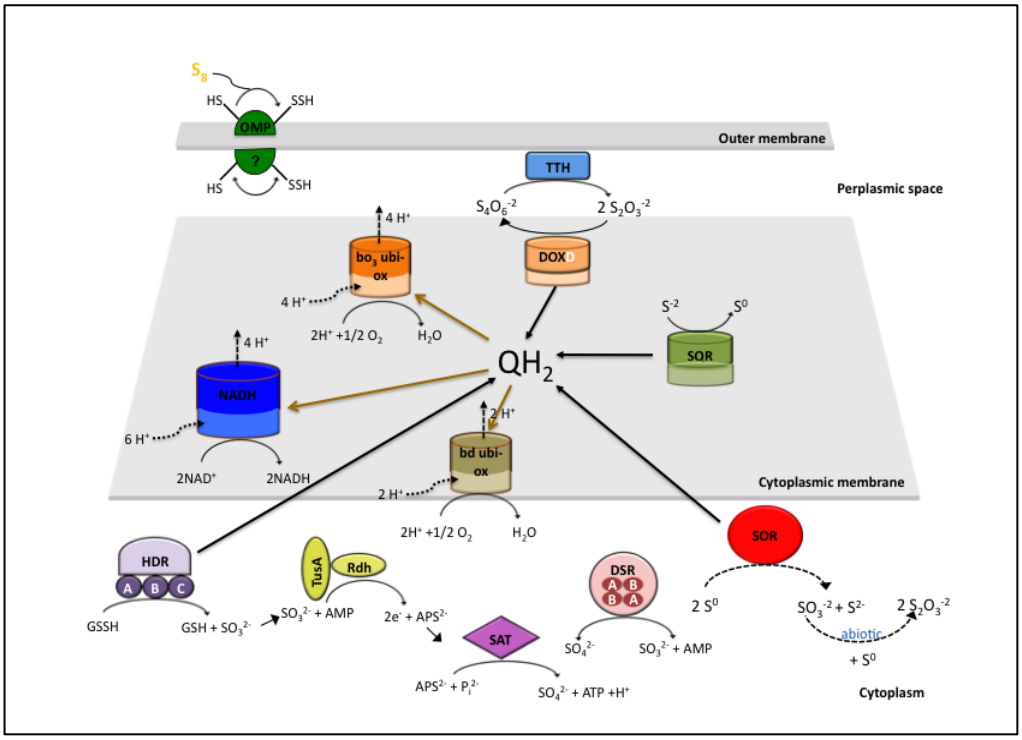

Fig. 31: Model of RISC oxidation pathway in the type strain of *Sb. thermosulfidooxidans*. (Construction by my data analyses)
Abbreviations: HDR: Heterodisulfide Reductase; TusA: Sulfurtransferase; Rdh: Rhodanase; SAT: Sulfate Adenylyltransferase; DSR: Dimethyl Sulfoxide Reductase; SQR: Sulfide:Quinone Oxidoreductase; SOR: Sulfur Oxygenase Reductase; TTH: Tetrathionate Hydrolase; DOXD (TQO): Thiosulfate:Quinone Oxidoreducatase; OMP: Outer Membrane Protein; NADH: NADH Ubiquinone Oxidoreductase; bd and bo_3 ubi-ox: terminal oxidases. For more details see text.

In both organsims, the model starts with extracellular elemental sulfur (S_8). This sulfur is activated and transported into the periplasmic space as persulfide sulfur (R-SH). S^0 transport pathways may be different considering the intrinsic differences between Gram-positive and Gram-negative bacteria. The exact reaction pathway for both organisms is not fully known yet, but an OMP is hypothesized to be involved in this reaction. HDR catalyzes sulfane sulfide (RSSH) to produce sulfite and regenerate RSH. In *Sb. thermosulfidooxidans* S^0 oxidantion may possibly occur via the Sor pathway. As educt S_n is used and sulfite and sulfide are formed. Two homologous *sor* genes were found in the genome of *Sb. thermosulfidooxidans*. Sulfite produced e.g. via Hdr can enter into the Sox pathway in *At. caldus* or combine with elemental sulfur to form thiosulfate via a nonenzymatic reaction. This thiosulfate can either enter the Sox pathway in *At. caldus*, or be oxidized to tetrathionate catalyzed by Tqo. Two *sox* gene clusters exist in *At. caldus*. One cluster is organized in an poeron, as shown by my data. Interestingly SoxX of cluster 1 showed transcriptional up-

regulation in thiosulfate grown cells, while comparison using proteomic data, SoxX was found to be down-regulated in thiosulfate grown cells. Consequently, this protein/ gene needs further investigation. Tqo (DoxD) oxidizes thiosulfate to tetrathionate, which is then hydrolyzed by Tth producing thiosulfate, sulfate and S^0. Tth and Tqo are found encoded in the type strain of *At. caldus* and the type strain of *Sb. thermosulfidooxidans* genomes. In *At. caldus* one *tth* (ACA_1633) could already be confirmed to function, a second gene (ACA_0092) is predicted. The first one (ACA_1633) was found to be down-regulated in S^0 grown cells in the proteome analysis as well as in the transcription level analysis. In contrast, ACA_0092 was found to be induced in S^0 grown *At. caldus* cells. In *Sb. thermosulfidooxidans* at least three possible genes encoding Tth are present.
S^0 produced from hydrolysis of tetrathionate, oxidation of H_2S (by Sqr) or from a truncated oxidation of thiosulfate by the SOX pathway can accumulate in the form of polymeric elemental sulfur (S_n) in the periplasm, from which it may be transferred into the cytoplasm. There it can be oxidized via Hdr (or via Sor in case of *Sb. thermosulfidooxidans)*. In *At. caldus* at least two putative *sqr* are found to be encoded in the genome. Both showed no differential regulation in the proteomes from thiosulfate or S^0 grown cells. However, at the transciption level a down-regulation for S^0 grown cells was measured for *sqr_II.* In *Sb. thermosulfidooxidans* three putative *sqr* candidates are present. Electrons from Sqr, Tqo, Hdr and SoxAX are transferred to the quinole pool at the cytoplasmic membrane. There, they are utilized by terminal oxidases bd or bo_3 to produce a proton gradient (to generate ATP) or by the NADH complex to generate reducing power.

All these findings are important for optimization of bioleaching process in the moderately thermophilic range. Due to the fact that *At. caldus* is a strict sulfur-oxidizer, RISC oxidation need tobe analyzed also in mixed cultures as well as in cells grown in the presence of MeS. *Sb. thermosulfidooxidans* is able to oxidize both, iron(II)-ions and RISCs. How active these proteins are in case of leaching e.g. pyrite, is an interesting question is one pathway preferentially used and which one?
What it is happening, if both organisms *Sb. thermosulfidooxidans* and *At. caldus* grow together in leaching processes? Are iron and sulfur oxidation pathways simultaneously active in cells of *Sb. thermosulfidooxidans* as compared to pure culture of this bacterium, or is the iron oxidation more active, because *At. caldus*

competes for the RISCs? Proteome analyses of *Sb. thermosulfidooxidans* in pure and in mixed cultures might be one way to solve these questions.

6 REFERENCES

Achenbach L and Woese C (1995): 16S and 23S rRNA-like primers. In Archaea. A Laboratory Manual (K. R. Sowers and H. J. Schreier, eds), pp. 521–523. Cold Spring Harbor Laboratory Press, Cold Spring Harbor.

Alahuhta M, Salin M, Casteleijn M G, Kemmer C, El-Sayed I, Augustyns K, Neubauer P and Wierenga R K (2008): Structure-based protein engineering efforts with a monomeric TIM variant: the importance of a single point mutation for generating an active site with suitable binding properties. *Protein Eng. Des. Sel.* **21**, 257-266.

Aljanabi S M and Martinez I (1997): Universal and rapid salt-extraction of high quality genomic DNA for PCR-based techniques, *Nucl. Acids Res*. **25**, 4692-4693.

Amend J P and Shock E L (2001). Energetics of overall metabolic reactions in thermophilic and hyperthermophilic Archaea and Bacteria, *FEMS Microbiol.Rev*. **25**, 175–243.

Aravind L and Koonin E V (1999): Novel predicted RNA-binding domains associated with the translation machinery. *J Mol Evol.* **48**, 291-302.

Bardischewsky F, Quentmeier A, Rother D, Hellwig P, Kostka S and Friedrich C G (2005): Sulfur Dehydrogenase of *Paracoccus pantotrophus*: The Heme-2 Domain of the Molybdoprotein Cytochrome *c* Complex Is Dispensable for Catalytic Activity. *Biochemistry* **44***,* 7024-7034.

Bathe S and Norris P (2007): Ferrous Iron- and Sulfur-Induced Genes in *Sulfolobus metallicus, Appl Environ Microbiol* **73**, 2491–2497.

Batty J D and Rorke G V (2006): Development of commercial demonstration of BioCOP™ thermophile process. *Hydromeetallurgy* **83**, 83-89.

Beard S, Paradela A, Albar J P and Jerez C A (2011): Growth of *Acidithiobacillus ferrooxidans* ATCC 23270 in thiosulfate under oxygen-limiting conditions generates extracellular sulfur globules by means of a secreted tetrathionate hydrolase. *Front Microbio* **2** doi: 10.3389/fmicb.2011.00079.

Begley T P, Downs D M, Ealick S E, McLafferty F W, Van Loon A P, Taylor S, Campobasso N, Chiu H J, Kinsland C, Reddick J J and Xi J (1999): Thiamin biosynthesis in prokaryotes. *Arch. Microbiol.* **171,** 293-300.

Bellenberg S (2010): Transcriptomic and microscopic analysis of capsular polysaccharide production by *Acidithiobacillus ferrooxidans*. M.Sc. thesis, Unversität Duisburg-Essen.

Berg I A (2011): MINIREVIEW: Ecological aspects of the distribution of different autotrophic CO_2 fixation pathways. *Appl. Environ. Microbiol.* **77**, 1925–1936.

Berg A and de Kok A (1997): 2-Oxo acid dehydrogenase multienzyme complexes. The central role of the lipoyl domain. *Biol. Chem.* **378**, 617-34.

Biarrotte-Sorin S, Hugonnet J E, Delfosse V, Mainardi J L, Gutmann L, Arthur M and Mayer C (2006): Crystal structure of a novel beta-lactam-insensitive peptidoglycan transpeptidase. *J. Mol. Biol.* **359**, 533-538.

Bogdanova T I, Tsaplina I A, Kondrat'eva T F, Duda V I, Suzina N E, Melamud V S, Tourova T P and Karavaiko G I (2006): *Sulfobacillus thermotolerans* sp. nov., a thermotolerant, chemolithotrophic bacterium. *Int. J. Syst. Evol. Microbiol.* **56**, 1039-1042.

Bordo D and Bork P (2002): The rhodanese/Cdc25 phosphatase superfamily. Sequence-structure-function relations. *EMBO Rep.* **3**, 741-746.

Bosecker B (1997): Bioleaching: Metal solubilisation by microorganisms; *FEMS Microbiological Reviews* **20**, 591-604.

Bonnefoy V and Homes D (2011): Genomic insights into microbial iron oxidation and iron uptake strategies in extremely acidic environments. *Environ Microbiol.* doi: 10.1111/j.1462-2920.2011.02626.x.

Boulegue J (1978): Solublity of elemental sulfur in water at 298 K. *Phosphorus Sulfur* **5**, 127-128.

Bowman A B, Patel-King R S, Benashski S E, McCaffery J M, Goldstein L S and King S M (1999): Drosophila roadblock and Chlamydomonas LC7: a conserved family of dynein-associated proteins involved in axonal transport, flagellar motility, and mitosis. *J. Cell Biol.* **146**, 165-180.

Bradford M M (1976): A rapid and sensitive method for the quantitation of microgram quantities of protein utilizing the principle of protein-dye binding. *Anal. Biochem.* **72**, 248-254.

Brasseur G, Levican G, Bonnefoy V, Holmes D, Jedlicki E and Lemesle-Meunier D (2004): Apparent redundancy of electron transfer pathways via bc1 complexes and terminal oxidases in the extremophilic chemolithoautotrophic *Acidithiobacillus ferrooxidans*. *Biochim Biophys Acta* **1656**, 114-126.

Bridge T A M, Johnson D B (1998): Reduction of soluble iron and reductive dissolution of ferric iron-containing minerals by moderately thermophilic iron-oxidizing bacteria. *Appl Environ Microbiol.* **64**, 2181-2186.

Brierley C L (1978): Bacterial leaching. *Crit. Rev. Microbiol.* 6207-6262.

Brierley J A (1990): Acidophilic Thermophilic archaebacteria: potential application for metal recovery. FEMS *Microbiology Reviews* **75**, 287-292.

Brierley J A and Brierley C L (2001): Present and future commercial application of biohydrometallurgy. *Hydrometallurgy* **59**, 233-239.

Brito J A, Sousa F L, Stelter M, Bandeiras T M, Vonrhein C, Teixeira M, Pereira M M and Archer M (2009): Structural and functional insights into sulfide:quinone oxidoreductase. *Biochemistry* **48**, 5613-5622.

Brosius J, Palmer J L, Kennedy H P, Noller H F (1978): Complete nucleotide sequence of a 16S ribosomal RNA gene from *Escherichia coli*. *Proc Natl Acad Sci*; **75**, 4801–4805.

Brown P N, Hill C P and Blair D F (2002): Crystal structure of the middle and C-terminal domains of the flagellar rotor protein FliG. *EMBO J.* **21**, 3225-3234.**Bugaytsova Z and Lindström E B (2004):** Localization, purification and properties of a tetrathionate hydrolase from *Acidithiobacillus caldus*. *Eur J Biochem* **271**, 272-280.

Busenlehner L S, Pennella M A and Giedroc D P (2003): The SmtB/ArsR family of metalloregulatory transcriptional repressors: structural insights into prokaryotic metal resistance. *FEMS Microbiology Reviews* **27**, 131-143.

Cammack R, Fernandez V M and Hatchikian E C (1994): Nickel-iron hydrogenase. *Meth. Enzymol.* **243**, 43-68.

Chahal B S (1986): A further study on the purification of the sulfur-oxidising enzyme from *Thiobacillus thiooxidans.* M.Sc. thesis, University of Manitoba, Winnipeg.

Chaney M, Grande R, Wigneshweraraj S R, Cannon W, Casaz P, Gallegos M-T, Schumacher J, Jones S, Elderkin S, Dago A E, Morett E and Buck M (2001): Binding of transcriptional activators to sigma 54 in the presence of the transition state analog ADP–aluminum fluoride: insights into activator mechanochemical action. *Genes Dev.* **15**, 2282–2294.

Chen I and Dubnau D (2004): DNA uptake during bacterial transformation. *Nat Rev Microbiol* **2**, 241-249.

Chen L, Ren Y, Lin J, Liu X, Peng X and Lin J (2012): *Acidithiobacillus caldus* sulfur oxidation model based on transcriptome analysis between wild type and sulfur oxygenase reductase defective mutant. *PLOS ONE* **7**; e39470.

Chen Z-W, Liu Y-Y, Wu J-F She Q, Jiang C-Y and Liu S-J (2007): Novel bacterial sulfur oxygenase reductases from bioreactors treating gold-bearing concentrates. *Appl Microbiol Biotechnol* **74**, 688-689.

Cherney M M, Zhang Y, Solomonson M, Weiner J H and James M N G (2010): Crystal structure of sulfide:quinone oxidoreductase from *Acidithiobacillus ferrooxidans*: Insights into sulfidotrophic respiration and detoxification. *J. Mol. Biol.* **398**, 292-305.

Costerton J W, Lewandowski Z, Caldwell D E, Korber D R and Lappin-Scott H M (1995): Microbial biofilms. *Ann Rev Microbiol* **49**, 711-745.

Compton S J and Jones C G (1985): Mechanism of dye response and interference in the Bradford protein assay. *Anal.Biochem.* **151**, 369-374.

Conrad C and Rauhut R (2002): Ribonuclease III: new sense from nuisance. *Int J Biochem Cell Biol.* **34**,116-129.

Cort J R, Selan U, Schulte A, Grimm F, Kennedy M A and Dahl C (2008): *Allochromatium vinosum* DsrC: solution-state NMR structure, redox properties, and interaction with DsrEFH, a protein essential for purple sulfur bacterial sulfur oxidation. *J Mol Biol* **382**, 692–707.

Cox R J, Sherwin W A, Lam L K P and Vederas J C (1996): Synthesis and evaluation of novel substrates and inhibitors of N-succinyl-LL-diaminopimelate aminotransferase (DAP-AT) from *Escherichia coli*. *J. Am. Chem. Soc.* **118**, 7449-7460.

Creighton T E and Yanofsky C (1970): Chorismate to tryptophan (*Escherichia coli*) - anthranilate synthetase, PR transferase, PRA isomerase, InGP synthetase, tryptophan synthetase. *Methods Enzymol.* **17A**, 365-380.

Croitoru V, Semrad K, Prenninger S, Rajkowitsch L, Vejen M, Laursen BS, Sperling-Petersen HU and Isaksson L A (2006): RNA chaperone activity of translation initiation factor IF1. *Biochimie* **88**(12):1875-1882.

Dahl C, Engels S, Pott-Sperling A S, Schulte A, Sander J, Lubbe Y, Deuster O and Brune D C (2005): Novel Genes of the *dsr* Gene Cluster and Evidence for Close Interaction of Dsr Proteins during Sulfur Oxidation in the Phototrophic Sulfur Bacterium *Allochromatium vinosum*. *J Bacteriol* **187**: 1392-1404.

Davies G and Henrissat B (1995): Structures and mechanisms of glycosyl hydrolases. *Structure* **3**, 853-859.

Delarue M and Moras D (1993): The aminoacyl-tRNA synthetase family: modules at work. *Bioessays* **15**, 675-687.

Delgado-Nixon V M, Gonzalez G and Gilles-Gonzalez M A (2000): Dos, a heme-binding PAS protein from Escherichia coli, is a direct oxygen sensor. *Biochemistry* **39**, 2685-2691.

Derr P, Boder E and Goulian M (2006): Changing the specificity of a bacterial chemoreceptor. *J. Mol. Biol.* **355**, 923-932.

DEV, DIN 38 406 (1989): Deutsche Einheitsverfahren zur Wasser-, Abwasser- und Schlammuntersuchung; Anionen (Gruppe D), Teil 26 photometrische Bestimmung des gelösten Sulfids (D26), Normenausschluß Wasserwesen im DIN Deutsches institut für Normierung e.V: **22**. Lieferung 1989.

De Wulf-Durand P, Bryant L J and Sly L I (1997): PCR-mediated detection of acidophilic, bioleaching-associated bacteria. *Appl Environ Microbiol*. **63**(7), 2944-2948.

Dold B (2008): Sustainability in metal mining: from exploration, over processing to mine waste management. *Rev Environ Sci Biotechnol* **7**, 275–285.

Dopson M and Lindström E B (2004): Analysis of community composition during moderately thermophilic bioleaching of pyrite, arsenical pyrite and chalcopyrite. *Microb Ecol* **48**, 19-28.

Edelbro R, Sandström A and Paul J (2003): Full potential calculations on the electron bandstructures of spalerite, pyrite and chalcopyrite. *Appl Surf Sci***206**: 300-313.

Ehrich 2002

Eicken C, Pennella M A, Chen X, Koshlap K M, VanZile M L, Sacchettini J C and Giedroc D P (2003): A metal-ligand-mediated intersubunit allosteric switch in related SmtB/ArsR zinc sensor proteins. *J. Mol. Biol.* **333**, 683-695.

Eikmanns B J, Follettie M T, Griot M U and Sinskey A J (1989): The phosphoenolpyruvate carboxylase gene of Corynebacterium glutamicum: molecular cloning, nucleotide sequence, and expression. *Mol. Gen. Genet.* **218**, 330-339.

Emmel T, Sand W, König W A and Bock E (1986): Evidence for the existence of a sulphur oxygenase in *Sulfolobus brierleyi*. *J. Gen. Microbiol*. **132**,3415-3420.

Esparza M, Cardenas J P, Bowien B, Jedlicki E and Holmes D S (2010): Genes and pathways for CO_2 fixation in the obligate, chemolithoautotrophic acidophile, *Acidithiobacillus ferrooxidans*, carbon fixation in *A. ferrooxidans*. *BMC Microbiol.* **10**, 229-244.

Fauque G, Peck H D Jr, Moura J J, Huynh B H, Berlier Y, Der Vartanian D V, Teixeira M, Przybyla A E, Lespinat PA and Moura I (1988): The three classes of hydrogenases from sulfate-reducing bacteria of the genus *Desulfovibrio*. *FEMS Microbiol. Rev.* **4**, 299-344.

Fillinger S, Boschi-Muller S, Azza S, Dervyn E, Branlant G and Aymerich S (2000): Two glyceraldehyde-3-phosphate dehydrogenases with opposite physiological roles in a nonphotosynthetic bacterium. *J. Biol. Chem.* **275**, 14031-14037.

Filloux A (2011): Protein secretion systems in *Pseudomonas aeruginosa*: anessay on diversity, evolution, and function. *Front Microbiol.* **2**, art. 155.

Flemming H C, Neu T R and Wozniak D J (2007): The EPS Matrix: The “House of Biofilm Cells”. *J Bacteriol* **189,** 7945-7947.

Fletcher T S, Kwee I L, Nakada T, Largman C and Martin B M (1992): DNA sequence of the yeast transketolase gene. *Biochemistry* **31**, 1892-1896.

Franz B, Lichtenberg H, Hormes J, Dahl C and Prange A (2009): The speciation of soluble sulphur compounds in bacterial culture fluids by X-ray absorption near edge structure spectroscopy. *Environ Technol* **30**: 1281-1289.

Friedrich C G, Quentmeier A, Bardischewsky F, Rother D, Kraft R, Kostka S and Prinz H (2000): Novel genes coding for lithotrophic sulfur oxidation of *Paracoccuspantotrophus* GB17.*J Bacteriol* **182**, 4677-4687.

Friedrich C G, Rother D, Bardischewsky F, Quentmeier A Fischer J (2001): Oxidation of reduced inorganic sulfur compounds by bacteria: emergence of a common mechanism? *Appl. Environ. Microbiol.***67**, 2873-2882.

Friedrich C G, Bradischewsky F, Rother D, Quentmeier A, Fischer J (2005): Prokaryotic sulfur oxidation, *Curr. Opin. Microbiol.* **8**, 253-259.

Friedrich C G, Quentmeier A, Bardischewsky F, Rother D, Orawski G, Hellwig P and Fischer J (2008): Redox Control of Chemotrophic Sulfur Oxidation of *Paracoccuspantotrophus*. In: Microbial Sulfur Metabolism (Dahl, C. and Friedrich, C.G., [eds.]). Springer, Berlin, Germany, 139-150.

Frigaard N U and Dahl C (2009): Sulfur Metabolism in Phototrophic Sulfur Bacteria. In: *Advances in Microbial Physiology,* Vol 54. (Hell, R.; Dahl, C.; Knaff, D. B.; Leustek, T. [eds.]). Academic Press Ltd, London, UK, pp. 103-200.

Frølund B, Palmgren R, Keiding K and Nielsen P H (1996): Extraction of extracellular polymers from activated sludge using a cation exchange resin. *Water Res* **30**, 1749-1758.

Frye S A, Assalkhou R, Collins R F, Ford R C, Petersson C, Derrick J P, Tønjum T (2006): Topology of the outer-membrane secretin PilQ from Neisseria meningitidis*. Microbiology.* **152,** 3751-3764.

Fukuyama K, Ueki N, Nakamura H, Tsukihara T and Matsubara H (1995): Tertiary structure of [2Fe-2S] ferredoxin from *Spirulina platensis* refined at 2.5 A resolution: structural comparisons of plant-type ferredoxins and an electrostatic potential analysis*. J. Biochem.* **117**, 1017-1023.

Garcia-Horsman J A, Puustinen A, Gennis R B and Wikström M (1995): Proton transfer in cytochrome bo3 ubiquinol oxidase of *Escherichia coli*: Second-site mutations in subunit I that restore proton pumping in the mutant Asp135.fwdarw.Asn. *Biochemistry*, 34, pp 4428–4433.

Garcia-Pino A, Balasubramanian S, Wyns L, Gazit E, De Greve H, Magnuson R D, Charlier D, van Nuland N A and Loris R (2010): Allostery and intrinsic disorder mediate transcription regulation by conditional cooperativity. *Cell* **142** 101-111.

Gehrke T and Sand W (2006): Extracellular polymeric substances mediate bioleaching/biocorrosion via interfacial processes involving iron(III)-ions and acidophilic bacteria. *Res Microbiol* **157**, 49-56.

Gericke M, Pinches A and van Rooyen J V (2001): Bioleaching of chalcopyrite concentrate using extreme thermophiles. *Int. J. Min. Process.* **62**, 243-255.

Ghrist A C and Stauffer G V (1995): Characterization of the *Escherichia coli* gcvR gene encoding a negative regulator of gcv expression. *J Bacteriol* **177**, 4980–4984.

Giuffrè A, Borisov V B, Mastronicola D, Sarti P and Forte E (2012): Cytochrome bd oxidase and nitric oxide: From reaction mechanisms. *FEBS Letters* **586**, 622–629.

Goebel B M and Stackebrandt E (1994): Cultural and phylogenetic analysis of mixed microbial populations found in natural and commercial bioleaching environments. *Appl.Environ.Microbiol.* **60**, 1614-1621.

Golovacheva and Karavaiko (1978): *Sulfobacillus*, a new genus of thermophilic sporeforming bacteria. *Mikrobiologiya* **47**, 815-822.

González-Toril E, Liorbet-Brossa E, Casamayor E O, Amann R and Amils R (2003): Microbial Ecology of an extreme acidic environment, the Tinto river; Applied and *Environmental Microbiology* **69**, 4853-4865.

Griesbeck C, Hauska G and Schütz M (2000): Biological Sulfide Oxidation: Sulfide-Quinone Reductase (SQR), the Primary Reaction. In: Pandalai, S.G. (ed): Recent Research Developments in Microbiology, Vol. 4, 179-203. Research Signpost, Trivadrum, India.

Grisolia S (1962): Phosphoglyceric acid mutase. *Methods Enzymol.* **5**, 236-242.

Hallberg K B, Dopson M and Lindström E B (1996): Reduced sulfur compound oxidation in *Thiobacillus caldus*. *Journal of Bacteriology* 178, 6-11.

Hallberg K B and Lindström E B (1994): Characterization of *Thiobacillus caldus* sp. nov., a moderately thermophilic acidophile. *Microbiology* **140**, 3451-3456.

Hamann N, Mander G J, Shokes J E, Scott R A, Bennati M and Hedderich R (2007): A cysteine-rich CCG domain contains a novel [4Fe-4S] clusterbinding motif as deduced from studies with subunit B of heterodisulfide reductase from *Methanothermobacter marburgensis*. *Biochemistry* **46**, 12875-12885.

Hashimoto T, Otaka E and Mizuta K (1993): The ribosomal proteins I. An introduction to a compilation of the protein species equivalents from various organisms by a universal code system. *Protein Seq. Data Anal.* **5**, 285-300.

Hawkins C F, Borges A and Perham R N (1990): Cloning and sequence analysis of the genes encoding the alpha and beta subunits of the E1 component of the pyruvate

dehydrogenase multienzyme complex of *Bacillus stearothermophilus*. *Eur. J. Biochem.* **191,** 337-346.

Hayashi N R, Arai H, Kodama T and Igarashi Y (1999): The *cbbQ* genes, located downstream of the form I and form II RubisCO genes, affect the activity of both RubisCOs. *Biochem. Biophys. Res. Commun.* **265** 177-183.

He Z, Li Y, Zhou P and Liu S (2000): Cloning and heterologous expression of a sulfur oxygenase/reductase gene from the thermoacidophilic archaeon *Acidianus* sp. S5 in *Escherichia coli*. *FEMS Microbiol Lett* **193**, 217-221.

He Z G, Zhong H and Li Y (2004): *Acidianus tengchongensis* sp. nov., a new species of acidothermophilic archaeon isolated from an acidothermal spring. *Curr Microbiol*. **48**(2), 159-163.

Hedderich R, Hamann N and Bennati M (2005): Heterodisulfide reductase from methanogenic archaea: a new catalytic role for an ironsulfur cluster. *Biol Chem* **386**, 961-970.

Helmann J D and Chamberlin M J (1988): Structure and function of bacterial sigma factors. *Annu. Rev. Biochem.* **57**, 839-872.

Helmann J D, Wang Y, Mahler I and Walsh C T (1989): Homologous metalloregulatory proteins from both Gram-positive and Gram-negative bacteria control transcription of mercury resistance operons. *J. Bacteriol.* **171**, 222-229.

Hensen D, Sperling D, Trüper H G, Brune D C and Dahl C (2006): Thiosulfate oxidation in the phototrophic sulfur bacterium *Allochromatium vinosum*. *Mol. Microbiol.***62**, 794-810.

Hershko A (1991): The ubiquitin pathway for protein degradation. *Trends Biochem. Sci.* **16,** 265-268.

Higgins D, Thompson J, Gibson T, Thompson J D, Higgins D G and Gibson T J (1994): Clustal W analysis: CLUSTAL W: improving the sensitivity of progressive multiple sequence alignment through sequence weighting, position-specific gap penalties and weight matrix choice. *Nucleic Acids Res*. **22**, 4673-4680.

Huber G and Stetter K O (1991): *Sulfolobusmetallicus*, sp. nov., a novel strictly chemolithotrophic thermophilic archaeal species of metal-mobilizers. *Syst. Appl. Microbiol.***14**, 372-378.

Huber G, Spinnler C, Gambacorta A and Stetter K O (1989): *Metallosphaera sedula* gen. and nov. represents a new genus of aerobic, metal-mobilizing, thermophilic achaebacteria, *Systematic and Applied Microbiology* **12**, 38-47.

Husten E J and Eipper B A (1991): The membrane-bound bifunctional peptidylglycine alpha-amidating monooxygenase protein. Exploration of its domain structure through limited proteolysis. *J. Biol. Chem.* **266** 17004-17010.

Ito K, Arai R, Fusatomi E, Kamo-Uchikubo T, Kawaguchi S, Akasaka R, Terada T, Kuramitsu S, Shirouzu M and Yokoyama S (2006): Crystal structure of the conserved protein TTHA0727 from *Thermus thermophilus* HB8 at 1.9 A resolution: A CMD family member distinct from carboxymuconolactone decarboxylase (CMD) and AhpD. *Protein Sci.* **15**, 1187-92.

Janner A (2008a): Comparative architecture of octahedral protein cages. I. Indexed enclosing forms. *Acta Crystallogr* A **64**: 494-502.

Janner A (2008b): Comparative architecture of octahedral protein cages. II. Interplay between structural elements. *Acta Crystallogr* A **64**: 503-512.

Janosch C, Thyssen C, Vera M, Bonnefoy V, Rohwerder T and Sand W (2009): Sulfur oxygenase reductase in different *Acidithiobacillus caldus*-like strains. *Adv Materials Res* 71-73: 239-242.

Jasaitis A, Borisov V B, Belevich N P, Morgan J E, Konstantinov A A and Verkhovsky M I (2000): Electrogenic reactions of cytochrome bd. *Biochemistry* **39**, 13800–13809.

Johnson D B (2003): Chemical and microbiological characteristics of mineral spoils and drainage water at aboned coal and metal mines; Water, Air and Soil Pollution 3: 47-66.

Johnson D B and Hallberg K B (2003): Acid mine drainage remediation options: A review; Science of the Total Environment 338: 3-14. *Arch. Microbiol.* **185**, 212-221.

Jordan H, Sanhueza A, Gautier V, Escobar B and Vargas T (2006): Electrochemical study of the catalytic influence of *Sulfolobus metallicus* in the bioleaching of chalcopyrite at 70°C; *Hydrometallurgy* 83: 55-62.

Jünemann S (1997): Cytochrome bd terminal oxidase. *Biochim. Biophys. Acta.***1321**, 107–127.

Kanao T, Kamimura K and Sugio T (2007): Identification of a gene encoding a tetrathionate hydrolase in *Acidithiobacillus ferrooxidans*. *J Biotechnol***132**: 16-22.

Kappler U and Bailey S (2004): Crystallization and preliminary X-ray analysis of sulfite dehydrogenase from *Starkeya novella*. *Acta Crystallogr D Biol Crystallogr.* **60**, 2070-2072.

Karavaiko G I, Zakharchuk L M, Bogdanova T I, Egorova M A, Tsaplina I A, and Krasil'nikova E N (2001): The enzymes of carbon metabolism in the thermotolerant bacillar strain K1. *Micorbiology* **71**, 651-656.

Karuppiah V and Derrick JP (2011): Structure of the PilM-PilN inner membrane type IV pilus biogenesis complex from *Thermus thermophilus*. *J Biol Chem* **286**, 24434-24442.

Kelly D P and Harrison A P (1989): Genus *Thiobacillus* Beijerinck. in *Bergey.s Manual of Systematic Bacteriology* Vol **3**, pp.1842-1858. (Staley, J.T., M.P. Bryant, N. Pfennig and J.G. Holt, Eds.), Springer-Verlag, New York.

Kelly D P and Wood A P (2000): Reclassification of some species of *Thiobacillus* to the newly designated genera *Acidithiobacillus* gen. nov., *Halothiobacillus* gen. nov. and *Thermithiobacillus* gen. nov. *Int. J. Syst. Evol. Microbiol.* **50**, 511-516.

Kim N S, Umezawa Y, Ohmura S and Kato S (1993): Human glyoxalase I. cDNA cloning, expression, and sequence similarity to glyoxalase I from *Pseudomonas putida*. *J. Biol. Chem.* **268**, 11217-11221.

Kinney J N, Axen S D and Kerfeld C A (2011): Comparative analysis of carboxysome shell proteins. *Photosynth Res.* **109**, 21–32.

Kinzler K, Gehrke T, Telegdi J and Sand W (2003): Bioleaching – A result of interfacial processes caused by extracellular polymeric substances (EPS). *Hydrometallurgy* **71**, 83-88.

Kletzin A (1989): Coupled enzymatic production of sulfite, thiosulfate, and hydrogen sulfide from sulfur: purification and properties of a sulfur oxygenase reductase from the facultatively anaerobic archaebacterium *Desulfurolobus ambivalens*. *J. Bacteriol*. **171**, 1638-1643.

Kletzin A (1992): Molecular characterization of the sor gene, which encodes the sulfur oxygenase/reductase of the thermophilic archaeum *Desulfurolobus ambivalens. J Bacteriol* **174**: 5854-5859.

Kletzin A (2006): Metabolism of inorganic sulfur compounds in archaea, *Archaea: Evolution, Physiology and Molecular Biology* (Ed: Garrett R. A., Klenk H.-P.) Blackwell Publishing, Oxford, pp. 261-274.

Kletzin A (2008): Oxidation of Sulfur and Inorganic Sulfur Compounds in *Acidianus ambivalens*. In: *Microbial Sulfur Metabolism* (Dahl, C. and Friedrich, C.G., [eds.]). Springer, Berlin, Germany, pp. 184-201.

Krasil'nikova E N, Tsaplina I A, Zakharchuk L M and Bogdanova T I (2001): Effects of exogenous factors on the activity of enzymes involved in carbon metabolism in thermoacidophilic bacteria of the genus Sulfobacillus. *Prikl Biokhim Mikrobiol.* **37**, 418-423.

Kimura H (2002): Hydrogen sulfide as a neuromodulator. *Mol Neurobiol* **26**, 13-19.

Krell K and Eisenberg M A (1970): The purification and properties of dethiobiotin synthetase. *J. Biol. Chem.* **245,** 6558-6566**.**

Krok B A (2010): Microscopical and High Throughput Proteomic studies of the Biofilm Formation process in *Acidithiobacillus ferrooxidans*. Master thesis, Unversität Duisburg-Essen.

Kuwajima G, Asaka J, Fujiwara T, Fujiwara T, Node K and Kondo E (1986): Nucleotide sequence of the hag gene encoding flagellin of *Escherichia coli*. *J. Bacteriol.* **168**, 1479-1483.

Lacey D T and Lawson F (1970): Kinetics of the liquid-phase oxidation od acid ferrous sulphate by the bacterium *Thiobacillus ferrooxidans*. *Biotechnology and Bioengineering*. **12**, 29-50.

Laemmli U K (1970): Cleavage of Structural Proteins during the Assembly of the Head of Bacteriophage T4. *Nature* 227: 680-685.

Lamb J R, Tugendreich S and Hieter P (1995): Tetratrico peptide repeat interactions: to TPR or not to TPR? *Trends Biochem. Sci.* **20**, 257-259.

Lane D J (1991): 16S/23S rRNA sequencing. *In: Stackebrandt E, Goodfellow M, editors; Stackebrandt E, Goodfellow M, editors. Nucleic acid techniques in bacterial systematics.*Chichester, United Kingdom: John Wiley & Sons; 115–175.

Laspidou C S and Rittman B E (2002): A unified theory for extracellular polymeric substances, soluble microbial products, and active and inert biomass. *Wat Res* **36**, 2711-2720.

Li B, Chen Y, Liu Q, Hu S and Chen X (2011): Complete genome analysis of *Sulfobacillus acidophilus* strain TPY, isolated from a hydrothermal vent in the Pacific Ocean. *J. Bacteriol.* **193**, 5555-5556.

Li M, Chen Z, Zhang P, Pan X, Jiang C, An X, Liu S and Chang W (2008): Crystal structure studies on sulfur oxygenase reductase from *Acidianus tengchongensis*. *Biochem Biophys Res Commun* **369**: 919-923.

Lolis E, Alber T, Davenport R C, Rose D, Hartman F C and Petsko G A (1990): Structure of yeast triosephosphate isomerase at 1.9-A resolution. *Biochemistry* **29** 6609-6618.

Loschi L, Brokx S J, Hills TL, Zhang G, Bertero M G, Lovering A L, Weiner J H and Strynadka NC (2004): Structural and biochemical identification of a novel bacterial oxidoreductase. *J Biol Chem.* **279**, 50391-50400.

Luther G W III (1987): Pyrite oxidation and reduction: molecular orbital theora considerations. *Geochim Cosmochim Acta* **51**, 3193-3199.

Mackintosh M E (1978): Nitrogen fixation by *Thiobacillus ferrooxidans*. *J. Gen. Microbiol.* **105***,* 215-218.

Madadi-Kahkesh S, Duin E C, Heim S, Albracht S P, Johnson M K and Hedderich R (2001): A paramagnetic species with unique EPR characteristics in the active site of heterodisulfide reductase from methanogenic archaea. *Eur. J. Biochem.* **268,** 2566-2577.

Maddocks S E and Oyston P C (2008): Structure and function of the LysR-type transcriptional regulator (LTTR) family proteins. *Microbiology*. **154**, 3609-3623.

Melamud V S, Pivovarova T A, Tourova T P, Kalganova T V, Osipov G A, Lysenko A M, Kondrat'eva T F and Karavaiko G I (2003): *Sulfobacillus sibiricus* sp. nov., a novel moderately thermophilic bacterium. *Microbiology* (engl. translation of Mikrobiologiya) **22**, 605-612.

Mander G J, Pierik A J, Huber H and Hedderich R (2004): Two distinct heterodisulfidereductase-like enzymes in the sulfate-reducingarchaeon *Archaeoglobus profundus*. *Eur J Biochem* **271**, 1106-1116.

Mangold S, Valdés J, Holmes D and Dopson M (2011): Sulfur metabolism in the extreme acidophile *Acidithiobacillus caldus*. *Front Microbio* **2:**17 doi: 10.3389/fmicb.2011.00017

Marcia M, Ermler U, Peng G and Michel H (2009): The structure of *Aquifex aeolicus* sulfide:quinone oxidoreductase, a basis to understand sulfide detoxification and respiration. *Proc Natl Acad Sci U S A.* **106**, 9625-9630.

Martin H H, Maskos C and Burger R (1975): D-alanyl-D-alanine carboxypeptidase in the bacterial form and L-form of *Proteus mirabilis*. *Eur J Biochem.* **55**, 465-473.

Meganathan R (2001): Ubiquinone biosynthesis in microorganisms.
FEMS Microbiol. Lett. **203**, 131-139**.**

Mehta P K, Hale T I and Christen P (1993): Aminotransferases: demonstration of homology and division into evolutionary subgroups. *Eur. J. Biochem.* **214**:549–561.

Merrick M J (1993): In a class of its own--the RNA polymerase sigma factor sigma 54 (sigma N). *Mol. Microbiol.* **10**, 903-909.

Miallau L, Alphey M S, Kemp L E, Leonard G A, McSweeney S M, Hecht S, Bacher A, Eisenreich W, Rohdich F and Hunter W N (2003): Biosynthesis of isoprenoids: crystal structure of 4-diphosphocytidyl-2C-methyl-D-erythritol kinase. *Proc. Natl. Acad. Sci. U.S.A.* **100**, 9173-9178.

Minic Z and Hervé G (2004): Biochemical and enzymological aspects of the symbiosis between the deep-sea tubeworm *Riftia pachyptila* and its bacterial endosymbiont. *Eur J Biochem*, **271**: 3093-3102.

Mio T, Yamada-Okabe T, Arisawa M and Yamada-Okabe H (2000): Functional cloning and mutational analysis of the human cDNA for phosphoacetylglucosamine mutase: identification of the amino acid residues essential for the catalysis. *Biochim. Biophys. Acta* **1492**, 369-376.

Moreno-Paz M, Gómez MJ, Arcas A, Parro V (2010): Environmental transcriptome analysis reveals physiological differences between biofilm and planktonic modes of life of the iron oxidizing bacteria *Leptospirillum* spp. in their natural microbial community. BMC Genomics **11**:404. doi: 10.1186/1471-2164-11-404.

Morishita R, Kawagoshi A, Sawasaki T, Madin K, Ogasawara T, Oka T and Endo Y (1999): Ribonuclease activity of rat liver perchloric acid-soluble protein, a potent inhibitor of protein synthesis. *J. Biol. Chem.* **274** 20688-20692.

Mouilleron S, Badet-Denisot M A and Golinelli-Pimpaneau B (2006): Glutamine binding opens the ammonia channel and activates glucosamine-6P synthase. *J. Biol. Chem.* **281**, 4404-4412.

Müller F H, Bandeiras T M, Urich T, Teixeira M, Gomes C M and Kletzin A (2004): Coupling of the pathway of sulphur oxidation to dioxygen reduction: characterization of a novel membrane-bound thiosulphate:quinone oxidoreductase. *Mol Microbiol* **53**, 1147-1160.

Noël N (2008): Comparative study of planktonic and sessile cells in cultures of *Leptospirillum ferriphilum* and *Acidithiobacillus caldus* on pyrite. Master thesis. Universität Duisburg-Essen, Germany.

Norris P R, Burton N P and Foulis N A M (2000): Acidophiles in bioreactor mineral processing. *Extremophiles* **4**, 71-76.

Norris P R, Clark D A, Owen J P and Waterhouse S (1996): Characteristics of *Sulfobacillus acidophilus* sp. nov. and other moderate thermophilic mineral-sulphide-oxidising bacteria. *Microbiology* **142**, 775-783.

Nuijten P J, van Asten F J, Gaastra W and van der Zeijst B A (1990): Structural and functional analysis of two *Campylobacter jejuni* flagellin genes. *J. Biol. Chem.* **265**, 17798-17804.

Obmolova G, Teplyakov A, Bonander N, Eisenstein E, Howard A J and Gilliland G L (2001): Crystal structure of dephospho-coenzyme A kinase from *Haemophilus influenzae*. *J. Struct. Biol.* **136**, 119-125.

Olsen L R, Vetting M W and Roderick S L (2007): Structure of the *E. coli* bifunctional GlmU acetyltransferase active site with substrates and products. *Protein Sci.* **16**, 1230-1235.

Olson G J, Brierley J A and Brierley C L (2003): Bioleaching review part B: Progeress in bioleaching: applications of microbial process by the mineral industries. *Appl Microbiol Biotechnol* **63**, 3094-3101.

Omi R, Mizuguchi H, Goto M, Miyahara I, Hayashi H, Kagamiyama H and Hirotsu K (2002): Structure of imidazole glycerol phosphate synthase from *Thermus thermophilus* HB8: open-closed conformational change and ammonia tunneling. *J. Biochem.* **132**, 759-765.

Pao G M and Saier M H Jr (1995): Response regulators of bacterial signal transduction systems: selective domain shuffling during evolution. *J. Mol. Evol.* **40**, 136-154.

Papagianni M (2012): REVIEW: Recent advances in engineering the central carbon metabolism of industrially important bacteria. *Microbial Cell Factories*, **11**:50. doi:10.1186/1475-2859-11-50.

Paschos A, Bauer A, Zimmermann A, Zehelein E and Bock A (2002): HypF, a carbamoyl phosphate-converting enzyme involved in [NiFe] hydrogenase maturation.
J. Biol. Chem. **277**:49945-49951.

Pereira M M , Sousa F L, Verissimo A F and Teixeira M (2008): Looking for the minimumcommondenominator in haem-copper oxygen reductases: towards a unified catalytic mechanism. *Biochim. Biophys. Acta* **1777**: 929–934.

Perham R N (1990): The fructose-1,6-bisphosphate aldolases: same reaction, different enzymes. *Biochem. Soc. Trans.* **18**, 185-187.

Pfaffl M W (2001): A new mathematical model for relative quantification in real-time RT PCR. *Nucleic Acids Res.* **29**. 2002-2007.

Pfaffl M W, Horgan G W and Dempfle L. (2002): Relative expression software tool (REST) for groupwise comparison and statistical analysis of relative expression results in real-time PCR. *Nucleic Acids Res*.**30**, E36.

Pott A S and Dahl C (1998): Sirohaem sulfite reductase and other proteins encoded by genes at the dsr locus of *Chromatium vinosum* are involved in the oxidation of intracellular sulfur. *Microbiol-Sgm* **144**: 1881-1894.

Poretsky R S, Sun S, Mou X and Moran M A (2010): Transporter genes expressed by coastal bacterioplankton in response to dissolved organic carbon. *Environ Microbiol.* **12**, 616–627.

Pronk J T, Meulenberg R, Hazeu W, Bos P, Kuenen J G (1990): Oxidation of reduced inorganic sulphur compounds by acidophilic thiobacilli. *FEMS Microbiol. Rev*. **75**, 293-306.

Protze J, Müller F H, Lauber K, Naß B, Mentele R, Lottspeich F and Kletzin A (2011): An extracellular tetrathionate hydrolase from the thermoacidophilic archaeon *Acidianus*

ambivalens with an activity optimum at pH 1. *Front Microbio.* **2**:68 doi: 10.3389/fmicb.2011.00068.

Prunetti L, Infossi P, Brugna M, Ebel C, Giudici-Orticoni M-T and Guiral M (2010): New Functional Sulfide Oxidase-Oxygen Reductase Supercomplex in the Membrane of the Hyperthermophilic Bacterium *Aquifex aeolicus*, *JBC* **285**, 41815–41826.

Qiu G Z, Fu B, Zhou H B, Lui X, Gao J, Lui F F and Chen X H (2007): Isolation of a strain of *Acidithiobacillus caldus* and its role in bioleaching of chalcopyrite. *World J Microbiol Biotechnol*, **23**, 1217-1225.

Quatrini R, Appia-Ayme C, Denis Y, Jedlicki E, Holmes D S and Bonnefoy V (2009): Extending the models for iron and sulfur oxidation in the extreme Acidophile *Acidithiobacillus ferrooxidans*. *BMC Genomics* **10:**394. doi:10.1186/1471-2164-10-394.

Ramírez P, Guiliani N, Valenzuela L, Beard S and Jerez C A (2004): Differential protein expression during growth of *Acidithiobacillus ferrooxidans* on ferrous iron, sulfur compounds, or metal sulfides. *Appl Environ Microbiol* **70**: 4491-4498.

Rappas M, Niwa H and Zhang X (2004): Mechanisms of ATPases--a multi-disciplinary approach. *Curr. Protein Pept. Sci.* **5,** 89-105.

Rawlings N D and Barrett A J (1995): Evolutionary families of metallopeptidases. *Meth. Enzymol.* **248**, 183-228.

Rawlings D E, TributschH and Hansford G S (1999a): Reasons why '*Leptospirillum*' -like species rather than *Thiobacillus ferrooxidans* are the dominant iron-oxidising bacteria in many commercial processes for the biooxidation of pyrite and related ores, *Microbiology* **145**, 5–13.

Rawlings D E, Coram N J, Gardner M N and Deane S M (1999b): *Thiobacillus caldus* and *Leptospirillum ferrooxidans* are widely distributed in continuous- flow biooxidation tanks used to treat a variety of metal-containing ores and concentrates. In *Biohydrometallurgy* and the environment toward the mining of the 21st century. Part A. Edited by: Amils R, Ballester A. Elsevier Press, Amsterdam, 777-786.

Rawlings D E (2002): Heavy metal mining using microbes; Annual Review in Microbiology **56**, 65-91.

Rawlings D E and Johnson D B (2007): The microbiology of biomining: development and optimization of mineral-oxidising microbial consortia. *Microbiology*. **153**, 315-24.

Rao C V, Kirby J R and Arkin A P (2005): Phosphatase localization in bacterial chemotaxis: divergent mechanisms, convergent principles. *Phys. Biol.* **2** 148, doi:10.1088/1478-3975/2/3/002.

Roca J (1995): The mechanisms of DNA topoisomerases. *Trends Biochem. Sci.* **20** 156-160.

Rohwerder T (2002): Untersuchungen zur enzymatischen Oxidation von Elementarschwefel bei acidophilen Laugungsbakterien, Dissertation, Universität Hamburg, Fachbereich Biologie, Hamburg.

Rohwerder T and Sand W (2003): The sulfane sulfur of persulfides is the actual substrate of the sulphur oxidising enzymes from *Acidithiobacillus* and *Acidiphilium* spp. *Microbiology* **149:** 1699-1709.

Rohwerder T, Gehrke T, Kinzler K and Sand W (2003): Bioleaching review part A: progress in bioleaching: fundamentals and mechanisms of bacterial metal sulfide oxidation. *Appl Microbiol Biotechnol.* **63**(3), 239-248.

Rohwerder T and Sand W (2007): Review: Oxidation of inorganic sulfur compounds in acidophilic prokaryotes, *Eng. Life Sci.* **7**, 301-309.

Romano A H and Conway T (1996): Evolution of carbohydrate metabolic pathways. *Res Microbiol.* **147**, 448-455.

Ronimus R S and Morgan H W (2003): Distribution and phylogenies of enzymes of the Embden-Meyerhof-Parnas pathway from Archaea and hyperthermophilic bacteria support a gluconeogenic origin of metabolism. *Archaea* **1**, 199–221.

Rosenthal E and Leustek T (1995): A multifunctional Urechis caupo protein, PAPS synthetase, has both ATP sulfurylase and APS kinase activities. *Gene* **165**, 243-248.

Rubio R F (2012): Mining: The Challenge Knocks on our Door. *Mine Water Environ* DOI 10.1007/s10230-012-0169-5.

Rzhepishevska O I, Valdes J, Marcinkeviciene L, Gallardo C A, Meskys R, Bonnefoy V, Holmes D S and Dopson M (2007): Regulation of a novel *Acidithiobacillus caldus* gene cluster involved in metabolism of reduced inorganic sulfur compounds. *Appl Environ Microb* **73**, 7367-7372.

Sakurai H, Ogawa T, Shiga M, Inoue K (2010): Inorganic sulfur oxidizing system in green sulfur bacteria. *Photosyn. Res.* **104**, 163–176.

Sand W, Gehrke T, Hallmann R and Schippers A (1995): Sulfur chemistry, biofilm, and the (in)direct attack mechanism – A critical evaluation of bacterial leaching; *Applied Microbiology & Biotechnology* **43**, 961-966.

Sand W, Gehrke T, Jozsa P-G and Schippers A (2001): (Bio)chemistry of bacterial leaching – direct vs indirect bioleaching. *Hydrometallurgy* **59**,159-175.

Schippers A (2004): Biogeochemistry of metal sulfide oxidation in mining environments, sediments and soils. In: Amed J P, Edwards K J, Lyons TW, eds. Sulfur biogeochemistry –

Past and present. Special Paper 379, Geological Society of America, Boulder, Colorado, 49-62.

Schippers A and Sand W (1999): Bacterial Leaching of Metal Sulfides Proceeds by Two Indirect Mechanisms via Thiosulfate or via Polysulfides and Sulfur. *Appl. Environ. Microbiol* **65**, 319-321.

Schippers A and Jørgensen B B (2002): Biogeochemistry of pyrite and iron sulfide oxidation in marine sediments. *Geochimica et Cosmochimica Acta*. **66**, 85–92

Schippers A, Jozsa P-G and Sand W (1996): Sulfur chemistry in bacterial leaching of pyrite. *Appl Environ Microbiol* **63**, 3424-3431.

Schulein R, Gentschev I, Mollenkopf H J and Goebel W (1992): A topological model for the haemolysin translocator protein HlyD. *Mol. Gen. Genet.* **234**: 155-163.

Segerer A, Stetter K O and Klink F (1985): Two contrary modes of chemolithotrophy in the same archaebacterium, *Nature* **313**, 787-789.

Segerer A, Neuner A, Kristjansson J K and Stetter K O (1986): *Acidianus infernus* gen. Nov., sp. Nov., and *Acidianus brierleyi* comb. Nov.: Facultatively aerobic, extremely acidophilic Thermophilic sulfur-metabolizinh archaeabacteria; *International Journal of Systematic Bacteriology* **36**: 559-564.

Sekowska A, Denervaud V, Ashida H, Michoud K, Haas D, Yokota A and Danchin A. (2004): Bacterial variations on the methionine salvage pathway. *BMC Microbiol*. **4**, 9.

Shahak Y and Hauska G. (2008): Sulfide oxidation from cyanobacteria to humans: sulfide–quinone oxidoreductase (SQR). In Advances in Photosynthesis and Respiration (Hell R, Dahl C, Knaff D and Leustek T, eds), (Springer, Netherlands), **27**, 319–335.

Shimokawa N and Yamaguchi M (1992): Calcium administration stimulates the expression of calcium-binding protein regucalcin mRNA in rat liver. *FEBS Lett.* **305** 151-154.

Shimokawa N and Yamaguchi M (1993): Molecular cloning and sequencing of the cDNA coding for a calcium-binding protein regucalcin from rat liver. *FEBS Lett.* **327** 251-255.

Sofia H J, Chen G, Hetzler B G, Reyes-Spindola J F and Miller N E (2001): Radical SAM, a novel protein superfamily linking unresolved steps in familiar biosynthetic pathways with radical mechanisms: functional characterization using new analysis and information visualization methods. *Nucleic Acids Res*. **29**, 1097-1106.

Ståhlberg A, Åman P, Ridell B, Mostad P and Kubista M (2003): Quantitative real-time pcr method for detection of B-lymphocyte monoclonality by comparison of k and l immunoglobulin light chain expression. *Clin. Chem*. **49**, 51‑59.

Ståhlberg A, Håkansson J, Xian X, Semb H and Kubista M (2004): Properties of the reverse transcription reaction in mRNA quantification. *Clin. Chem.* **50**, 509‑515.

Ståhlberg A, Zoric N, Åman P and Kubista M (2005): Quantitative real-time PCR for cancer detection: the lymphoma case. *Expert Rev. Mol. Diagn*. **5**, 221‑230.

Stephens K, Hartzell P and Kaiser D (1989): Gliding motility in *Myxococcus xanthus*: mgl locus, RNA, and predicted protein products. *J. Bacteriol.* **171**, 819-830.

Steudel R (1996): Mechanism for the formation of elemental sulfur from aqueous sulfide in chemical and microbiological desulfurization processes. *Ind. Eng. Chem. Res*. **35**:1417-1423.

Steudel R (2000): The chemical sulfur cycle. In: Lens, P. N. L. & Hulshof Pol, L. *Environmental technologies to treat sulfur pollution, Chap. 1, IWA Publishing, London,* 1-31.

Stramer J, Stomp A, Vouk M and Bitzer D (2006): Predicting Shine–Dalgarno sequence locations exposes genome annotation errors*. PLoS Comput Biol* **2**, e57. DOI: 10. 1371/journal.pcbi.0020057.

Sturr M G, Krulwich T A and Hicks D B (1996): Purification of a cytochrome bd terminal oxidase encoded by the *Escherichia coli* app locus from a delta cyo delta cyd strain complemented by genes from *Bacillus firmus* OF4. *J. Bacteriol.* **178**,1742-1749.

Sun C W, Chen Z W, He Z G, Zhou P J and Liu S J (2003): Purification and properties of the sulfur oxygenase/reductase from the acidothermophilic archaeon, *Acidianus* strain S5. *Extremophiles* **7**, 131-134

Suzuki I (1965): Incorporation of atmospheric oxygen-18 into thiosulfate by sulfur-oxidising enzyme of *Thiobacillus thiooxidans, Biochim. Biophys. Acta* **110**, 97-101.

Suzuki I (1974): Mechanisms of inorganic oxidation and energy coupling. *Annu. Rev. Microbiol*. **28**, 85-101.

Suzuki I (1994): Sulfur-oxidising enzymes. *Methods Enzymol.* **243**, 455-462.

Szurmant H, Bunn M W, Cannistraro V J and Ordal G W (2003): *Bacillus subtilis* Hydrolyzes CheY-P at the Location of Its Action, the Flagellar Switch*. *J Biol Chem* **278**, 48611–48616.

Tabita F R, Hanson T E, Satagopan S, Witte B H and Kreel N E (2008): Phylogenetic and evolutionary relationships of RubisCO and the RubisCO-like proteins and the functional lessons provided by diverse molecular forms. *Philos Trans R Soc Lond B Biol Sci.* **363**, 2629-2640.

Takagi T and Cox J A (1991): Primary structure of myohemerythrin from the annelid Nereis diversicolor. *FEBS Lett.* **285,** 25-27.

Tanaka S, Kerfeld C A, Sawaya M R, Cai F, Heinhorst S, Cannon G C and Yeates T O (2008): Atomic-level models of the bacterial carboxysome shell. *Science* **319**, 1083-1086.

Tano T and Imai K (1968): Physiological studies on thiobacilli. Part II: The metabolism of colloidal sulfur by the cell-free enzyme system of *Thiobacillus thiooxidans*. *Agric Biol Chem* **32**, 51-54.

Tatusov R L, Natale D A, Garkavtsev I V, Tatusova T A, Shankavaram U T, Rao B S, Kiryutin B, Galperin M Y, Fedorova N D and Koonin E V (2000): The COG database: new developments in phylogenetic classification of proteins from complete genomes. *Nucleic Acids Res.* **29**, 22-28.

Taylor P L, Blakely K M, de Leon G P, Walker J R, McArthur F, Evdokimova E, Zhang K, Valvano M A, Wright GD and Junop M S (2008): Structure and function of sedoheptulose-7-phosphate isomerase, a critical enzyme for lipopolysaccharide biosynthesis and a target for antibiotic adjuvants. *J. Biol. Chem.* **283**, 2835-2845.

Titz B, Rajagopala SV, Ester C, Häuser R and Uetz P (2006): Novel conserved assembly factor of the bacterial flagellum. *J Bacteriol.* **188**, 7700-7706.

Tourova T P, Kovaleva O L, Sorokin D Y and Muyzer G (2010): Ribulose-1,5-bisphosphate carboxylase/oxygenase genes as a functional marker for chemolithoautotrophic halophilic sulfur-oxidizing bacteria in hypersaline habitats. *Microbiology*. **156**, 2016-2025.

Treuner-Lange A, Kuhn A and Durre P (1997): The kdp system of *Clostridium acetobutylicum*: cloning, sequencing, and transcriptional regulation in response to potassium concentration. *J. Bacteriol.* **179** 4501-4512.

Tsaplina I A, Osipov G A, Bogdanova T I, Nedorezova T P and Karavaiko G I (1994): Fatty acid composition of lipids in thermoacidophilic bacteria of the genus *Sulfobacillus*. *Microbioogy.***63**, 459-464.

Urich T (2005): The sulfur oxygenase reductase from *Acidianus ambivalens*; function and structural characterization of a sulfur disproportional enzyme. Dissertation; Fachbereich Biologie der Technischen Universität Darmstadt.

Urich T, Gomes C M, Kletzin A and Frazao C (2006):X-ray structure of a self-compartmentalizing sulfur cycle metalloenzyme*. Science* **311**, 996-1000.

Valdes J, Quatrini R, Hallberg K, Dopson M, Valenzuela P D and Holmes D S (2009): Draft genome sequence of the extremely acidophilic bacterium *Acidithiobacillus caldus* ATCC 51756 reveals metabolic versatility in the genus Acidithiobacillus.*J Bacteriol.***191**, 5877-5878.

Vásquez M and Espejo R T (1997): Chemolithotrophic bacteria in copper ores leached at high sulfuric acid concentration*; Applied Environmental Microbiology* 63: 332-334.

Veith A, Klingl A, Zolghadr B, Lauber K, Mentele R, Lottspeich F, Rachel R, Albers S V and Kletzin A (2009): *Acidianus*, *Sulfolobus* and *Metallosphaera* surface layers: structure, composition and gene expression. *Mol Microbiol* **73**, 58-72.

Veith A, Urich T, Seyfarth K, Protze J, Frazão C and Kletzin A (2011a): Substrate pathways and mechanisms of inhibition in the sulfur oxygenase reductase of *Acidianus ambivalens*. *Front Microbio* **2,** 37. doi: 0.3389/fmicb.2011.00037.

Veith A, Botelho H M, Gomes C M and Kletzin A (2011b): The Sulfur Oxygenase Reductase from the Mesophilic Bacterium *Halothiobacillus neapolitanus* is a Highly Active Thermozyme. *J Bacteriol*.doi: 10.1128/JB.06531-1.

Vishniac W and Santer M (1957): The thiobacilli. *Bacteriol. Rev*. **21**, 195-213.

Vera M, Krok B, Bellenberg S, Sand W and Poetsch A (2013): Shotgun proteomics study of early biofilm formation process of *Acidithiobacillus ferrooxidans* ATCC 23270 on pyrite. *Proteomics* **13**, 1133-1144.

Vera M, Pagliai F, Guiliani N and Jerez J A (2008): The chemolithoautotroph *Acidithiobacillus ferrooxidans* can survive under phosphate limiting conditions by the expression of a C-P lyase operon that allows it to grow on phosphonates. *Appl. Environ. Microbiol.* doi:10.1128/AEM.02101-07.

Vogler A P, Homma M, Irikura V M and Macnab R M (1991): *Salmonella typhimurium* mutants defective in flagellar filament regrowth and sequence similarity of FliI to F0F1, vacuolar, and archaebacterial ATPase subunits. *J. Bacteriol.* **173**, 3564-3572.

von Delft F, Inoue T, Saldanha S A, Ottenhof H H, Schmitzberger F, Birch L M, Dhanaraj V, Witty M, Smith A G, Blundell T L and Abell C (2003): Structure of E. coli ketopantoate hydroxymethyl transferase complexed with ketopantoate and Mg^{2+}, solved by locating 160 selenomethionine sites. *Structure* **11**, 985-996.

Wakai S, Kikumuto M, Kanao T and Kamimura K (2004): Involvement of sulfide:quinone oxidoreductase in sulfur oxidation of an acidophilic iron-oxidising bacterium, *Acidithiobacillus ferrooxidans* NASF-1, *Biochim. Biophys. Acta* **1656**, 114-126.

Walker J E (1992): The NADH:ubiquinone oxidoreductase (complex I) of respiratory chains. *Q. Rev. Biophys*. **25**, 253-324.

Wang A-Y, Grogan D W and Cronan J E Jr. (1992): Cyclopropane fatty acid synthase of Escherichia coli: deduced amino acid sequence, purification, and studies of the enzyme active site. *Biochemistry* **31**, 11020-11028.

Watanabe S, Matsumi R, Arai T, Atomi H, Imanaka T and Miki K (2007): Crystal structures of [NiFe] hydrogenase maturation proteins HypC, HypD, and HypE: insights into cyanation reaction by thiol redox signaling. *Mol. Cell* **27**: 29-40.

Watling H R (2006): The bioleaching of sulphide minerals with emphasis on copper sulfides – A review; *Hydrometallurgy* 84: 81-108.

Weiß J (1991): *Ionenchromatographie*. VCH. Weinheim.

Welte C, Hafner S, Krätzer C, Quentmeier A T, Friedrich C G and Dahl C (2009): Interaction between Sox proteins of two physiologically distinct bacteria and a new protein involved in thiosulfate oxidation. *FEBS Lett.* **583**, 1281–1286.

Whitfield C and Roberts I S (1999): Structure, assembly and regulation of expression of capsules in *Escherichia coli*. *Mol Microbiol* **31**, 1307–1319.

Whitfield C (2006): Biosynthesis and Assembly of Capsular Polysaccharides in *Escherichia coli*. *Annu Rev Biochem* **75**, 39-68.

Yeats C, Rawlings N D and Bateman A (2004): The PepSY domain: a regulator of peptidase activity in the microbial environment? *Trends Biochem. Sci.* **29**, 169-172.

Yon J M, Desmadril M, Betton J M, Minard P, Ballery N, Missiakas D, Gaillard-Miran S, Perahia D and Mouawad L (1990): Flexibility and folding of phosphoglycerate kinase. *Biochimie* **72**, 417-429.

You X Y, Guo X, Zheng H J, Zhang M J, Liu L J, Zhu Y Q, Zhu B, Wang S Y, Zhao G P, Poetsch A, Jiang C Y and Liu S J (2011): Unraveling the *Acidithiobacillus caldus* complete genome and its central metabolisms for carbon assimilation. *J Genet Genomics* **38**, 243-252.

Zhang R, Andersson C E, Savchenko A, Skarina T, Evdokimova E, Beasley S, Arrowsmith C H, Edwards A M, Joachimiak A and Mowbray S L (2003): Structure of *Escherichia coli* ribose-5-phosphate isomerase: a ubiquitous enzyme of the pentose phosphate pathway and the Calvin cycle. *Structure* **11**, 31-42.

Zhou H B, Lui X, Fu B, Qui G-Z, Huo Q, Zeng W-M, Liu J-S and Chen X-H (2007): Isolation and characterization of *Acidithiobacillus caldus* from several typical environments in China. *J. Cent. South Univ. Technol.* **14**, 163-169.

Zhuravleva A E, Ismailov A D, Zakharchuk L M, Krasil'nikova E N andTsaplina I A (2008): Energy supply processes in moderately thermophilic bacteria of the genus *Sulfobacillus*. Mikrobiologiia. **77**, 708-712.

Zimmermann P, Laska S and Kletzin A (1999): Two modes of sulfite oxidation in the extremely thermophilic and acidophilic archaeon Acidianus ambivalens. *Arch Microbiol* **172**, 76-82.

Curriculum vitae

Claudia Janosch

“For privacy protection the CV is not included in the online version of this dissertation!”

Hiermit versichere ich, dass ich die vorliegende Arbeit mit dem Titel:

“Sulfur oxidation in moderately thermophilic leaching bacteria”

selbst verfasst und keine außer den angegebenen Hilfsmitteln und Quellen benutzt habe, und dass die Arbeit in dieser oder ähnlicher Form noch bei keiner anderen Universität eingereicht wurde.

Essen, im April 2013